HUMBOLDT-UNIVERSITÄT ZU BERLIN

Lebenswissenschaftliche Fakultät
Institut für Biologie

Bachelorarbeit

Zum Erwerb des akademischen Grades Bachelor of Science

Physiologically-Based Pharmacokinetic/Pharmacodynamic Modeling of Dapagliflozin: Exploring the Impact of Dosing, Hepatorenal Impairment and Food Intake

Physiologisch basierte pharmakokinetische/pharmakodynamische Modellierung von Dapagliflozin: Untersuchung der Auswirkungen von Dosierung, hepatorenale Beeinträchtigung und Nahrungsaufnahme

vorgelegt von

Nike Nemitz

Matrikelnummer: 618434

E-Mail: nike.philine.elise.nemitz@student.hu-berlin.de

Geburtsdatum und -ort: 14.11.2000 in Berlin

Arbeitsgruppe: Systems Medicine of the Liver

Berlin, 11.06.2025

Erstprüfer: Dr. Matthias König
Zweitprüfer: Prof. Dr. Hanspeter Herzel

Contents

Abstract

English

Dapagliflozin is a SGLT2 inhibitor used in the management of type 2 diabetes. Its effect is based on the reduction of plasma glucose levels by promoting glucose excretion in the urine. The pharmacokinetics and pharmacodynamics of dapagliflozin exhibit considerable interindividual variability, which is influenced by patient-specific factors and potentially affects therapeutic outcomes. In this study, a physiologically based pharmacokinetic/ pharmacodynamic (PBPK/PD) model was developed to systematically assess how these factors influence dapagliflozin disposition. Using curated data from 27 clinical trials, a modular SBML-based model with sub-models for intestinal absorption, hepatic metabolism and renal excretion was developed. Parameter optimization resulted in good agreement between simulations and observed clinical PK/PD profiles. The validated model accurately reproduced dose-dependent kinetics within the therapeutic range, captured the effects of physiological variability and functional impairments, and simulated food-drug interactions. In addition, the model enabled direct comparison of urinary glucose excretion (UGE) under renal and hepatic impairment. Results showed that renal dysfunction substantially reduces UGE, while hepatic impairment has only a minor effect. Furthermore, the simulations revealed that food intake, although not altering total systemic exposure (AUC), significantly affects peak concentrations ($C_{\max}$), which in turn influences pharmacodynamic outcomes such as UGE. This suggests a clinically relevant food effect that is often underestimated. Despite some limitations, the model offers mechanistic insight into the sources of PK/PD variability and supports individualized dosing strategies, contributing to predictive tools for personalized diabetes management and pharmacotherapy optimization.

Deutsch

Dapagliflozin ist ein SGLT2-Hemmer, der bei der Behandlung von Typ-2-Diabetes eingesetzt wird. Seine Wirkung beruht auf der Senkung des Plasmaglukosespiegels durch Förderung der Glukoseausscheidung über den Urin. Die Pharmakokinetik und Pharmakodynamik von Dapagliflozin weisen eine beträchtliche interindividuelle Variabilität auf, die von patientenspezifischen Faktoren beeinflusst wird und sich potenziell auf die therapeutischen Ergebnisse auswirkt. In dieser Studie wurde ein physiologisch basiertes pharmakokinetisches/pharmakodynamisches (PBPK/PD) Modell entwickelt, um systematisch zu bewerten, wie diese Faktoren die Dapagliflozin-Disposition beeinflussen. Unter Verwendung kuratierter Daten aus 27 klinischen Studien wurde ein modulares SBML-basiertes Modell mit Untermodellen für die intestinale Absorption, den hepatischen Stoffwechsel und die renale Ausscheidung entwickelt. Die Optimierung der Parameter führte zu einer guten Übereinstimmung zwischen den Simulationen und den beobachteten klinischen PK/PD-Profilen. Das validierte Modell gab die dosisabhängige Kinetik innerhalb des therapeutischen Bereichs genau wieder, erfasste die Auswirkungen physiologischer Variabilität und funktioneller Beeinträchtigungen und simulierte Wechselwirkungen zwischen Nahrungsmitteln und Arzneimitteln. Darüber hinaus ermöglichte das Modell einen direkten Vergleich der Glukoseausscheidung im Urin (UGE) bei Nieren- und Leberfunktionsstörungen. Die Ergebnisse zeigten, dass eine Nierenfunktionsstörung die UGE erheblich reduziert, während eine Leberfunktionsstörung nur einen geringen Einfluss hat. Darüber hinaus zeigten die Simulationen, dass die Nahrungsaufnahme zwar die systemische Gesamtexposition (AUC) nicht verändert, aber die Spitzenkonzentrationen ($C_{\max}$) erheblich beeinflusst, was wiederum pharmakodynamische Ergebnisse wie die UGE beeinflusst. Dies deutet auf einen klinisch relevanten Nahrungsmitteleffekt hin, der häufig unterschätzt wird. Trotz einiger Einschränkungen bietet das Modell mechanistische Einblicke in die Quellen der PK/PD-Variabilität und unterstützt individualisierte Dosierungsstrategien, was zu prädiktiven Instrumenten für ein personalisiertes Diabetesmanagement und die Optimierung der Pharmakotherapie beiträgt.

1 Introduction

Diabetes mellitus, commonly known as diabetes, is a chronic metabolic disorder characterized by elevated blood glucose (hyperglycemia). This condition arises when the body is unable to produce sufficient insulin, a hormone essential for regulating blood sugar, or cannot effectively utilize the insulin it produces. Insulin, secreted by the pancreas, facilitates the transport of glucose from the bloodstream into tissues such as muscle, adipose tissue and liver, where it is either converted into energy or stored. Without adequate insulin function, glucose accumulates in the blood, leading to the hallmark of diabetes: persistent hyperglycemia [52].
The two most common forms of diabetes are Type 1 diabetes (T1DM) and Type 2 diabetes (T2DM). T1DM is an autoimmune condition in which the body's immune system destroys the beta cells that produce insulin in the pancreas, resulting in little or no insulin production. It typically develops in children or young adults and requires lifelong insulin therapy. In contrast, T2DM, which accounts for approximately 90% of all diabetes cases, is primarily characterized by insulin resistance, where the body's cells do not respond effectively to insulin, and a relative insulin deficiency due to progressive beta cell dysfunction [2]. It is often associated with factors such as obesity, age, and family history and may remain undiagnosed for years due to subtle or absent symptoms. Both types, if left untreated, can lead to serious complications such as cardiovascular disease, kidney damage (nephropathy), nerve damage (neuropathy), lower-limb amputation, and vision loss due to retinal damage [21, 52]. In 2021, an estimated 537 million people were living with diabetes, with projections suggesting this number will rise to 643 million by 2030 and 783 million by 2045 [52]. Improved prevention, diagnosis, and management strategies are urgently needed.

1.1 Blood glucose regulation

The regulation of blood glucose levels is a complex process involving many organs. After carbohydrates are ingested with food, they are digested into glucose in the gastrointestinal tract with the help of enzymes. In the small intestine glucose is actively absorbed by enterocytes via specific membrane proteins, because glucose cannot pass through the lipid bilayer on its own due to its polar properties [1]. The glucose transporters can be divided into two structurally and functionally different groups: the Na^+-independent glucose transporter (GLUT) and the Na^+-dependent glucose cotransporter (SGLT) [72]. Once absorbed, glucose enters the bloodstream, where insulin, secreted by the pancreas, plays a critical role in regulating its distribution and use. Insulin facilitates the uptake of glucose into insulin-sensitive tissues such as muscle and adipose tissue, where it is used as an energy source or stored as glycogen. In addition, insulin suppresses glucose production in the liver, contributing to overall blood glucose homeostasis [45].
In individuals with normal glucose tolerance, almost all glucose is completely reabsorbed in the proximal renal tubule. This reabsorption is mainly facilitated by the SGLT2 transporter (90%) and the SGLT1 transporter (10%) [60, 56], see Fig. 1. Once transported into the proximal tubule cells of the kidney by the SGLT2 transporter, glucose exits the basolateral cell membrane through the GLUT2 transporter [1]. When glucose becomes very high in untreated diabetes, glucose can be excreted via the kidneys, a process called glucosuria. This effect was already observed in 1674 by the British physician Thomas Willis, who described the urine of diabetic patients as sweet-tasting. Consequently, the condition was given the scientific name "diabetes mellitus," with mellitus derived from the Latin word meaning "honey-sweet."

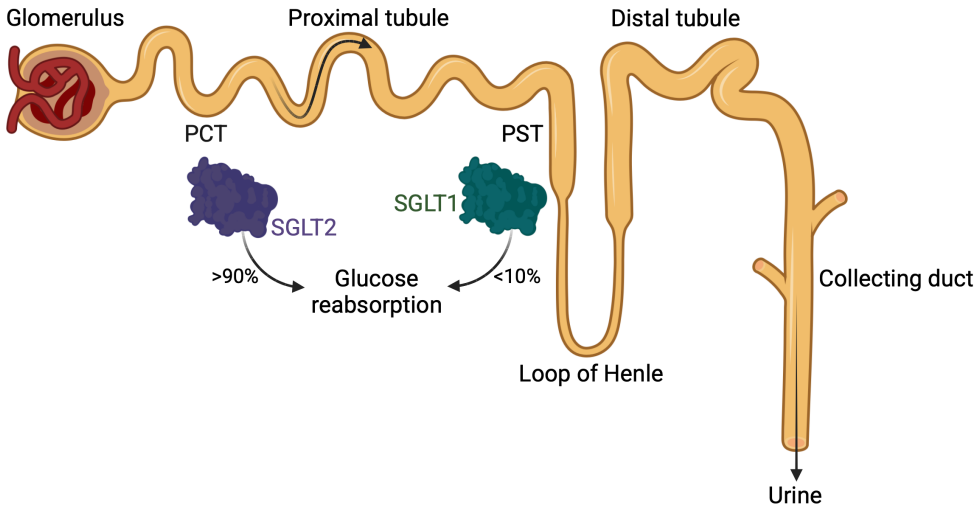

Figure 1: **Glucose reabsorption in the kidney.** Glucose is filtered at the glomerulus and then reabsorbed in the proximal tubule. The reabsorption is primarily (90%) facilitated by the sodium-glucose cotransporter 2 (SGLT2), located in segment 1 of the proximal convoluted tubule (PCT), and 10% by the sodium-glucose cotransporter 1 (SGLT1), located in segment 3 of the proximal straight tubule (PST). The process is completed before reaching the distal tubule, loop of Henle, and collecting duct, where no further glucose reabsorption occurs [60, 56, 3].

1.2 SGLT2 inhibitors

In 2012, the kidney emerged as a promising target for blood glucose-lowering therapies due to its critical role in glucose homeostasis through glomerular filtration and reabsorption of glucose in the proximal convoluted tubule of the nephron via sodium-glucose cotransporters (SGLTs) [73]. Blocking the SGLT2 transporter, which is responsible for most of glucose reabsorption in the kidney, prevents glucose from being reabsorbed into the bloodstream. This mechanism facilitates glucose excretion via urine, thus lowering blood glucose levels.
This process is used by a novel class of drugs known as SGLT2 inhibitors (also known as gliflozines or flozines), developed specifically for the treatment of T2DM. Beyond their primary effect of reducing blood glucose levels, SGLT2 inhibitors offer additional benefits, including the prevention of hypoglycemia, modest weight loss, and improved cardiovascular outcomes [60]. These advantages make SGLT2 inhibitors an attractive option for addressing the multifaceted challenges of managing T2DM.

1.3 Dapagliflozin

An important representative of SGLT2 inhibitors is dapagliflozin, the first SGLT2 inhibitor to be approved. Farxiga, a tablet form of dapagliflozin, was approved in 2014 to improve blood glucose control in adults with T2DM in combination with diet and exercise, and seven years later also to reduce the risk of worsening kidney function, kidney failure, cardiovascular death and hospitalization for heart failure in adults with chronic kidney disease. Dapagliflozin is popular due to its pharmacokinetic and pharmacodynamic properties such as oral efficacy and high selectivity [6, 5]. Dapagliflozin has demonstrated HbA1c-lowering efficacy in both the short and long term [18, 51].

1.4 Dapagliflozin pharmacokinetics

Pharmacokinetics, which describes the movement of a drug within the body (including its absorption, distribution, metabolism, and excretion (ADME)) plays a crucial role in understanding how medications achieve their therapeutic effects. For dapagliflozin, this process is well-characterized. Orally administered dapagliflozin is rapidly absorbed and generally reaches

peak plasma concentrations within 2 hours with a half-life of approximately 13 hours. It shows a dose-proportional systemic exposure over a wide dose range (0.1-500 mg) and has an oral bioavailability of about 78%. Metabolization occurs predominantly in the liver and kidneys through Uridine 5'-diphospho-glucuronosyltransferase 1A9 (UGT1A9), which leads to the formation of the main metabolite dapagliflozin-3-O-glucuronide (D3G). Approximately 60% of the administered dose is metabolized via glucuronidation and excreted in the urine as dapagliflozin-3-O-glucuronide, while less than 2% of the dose is recovered in the urine as the parent compound [5, 54], see Fig. 2.

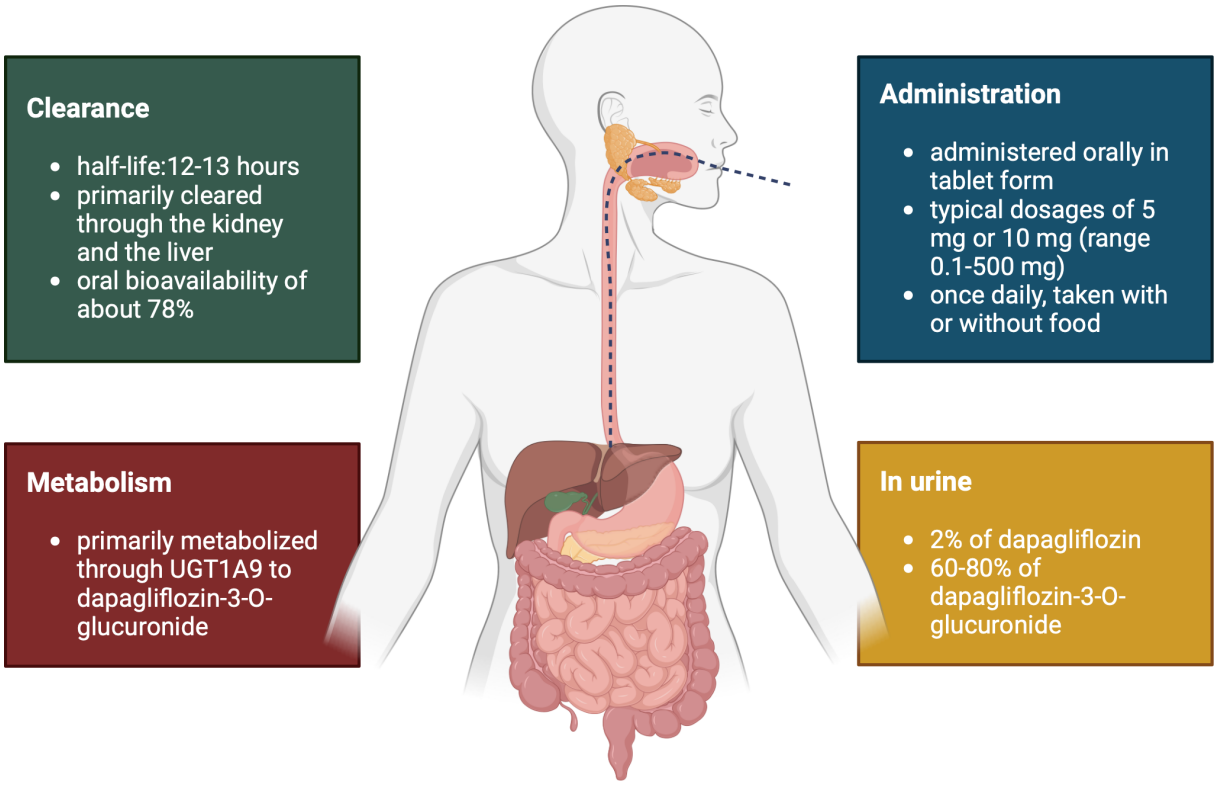

Figure 2: **Summary of administration, clearance, metabolism and elimination.** After administration, dapagliflozin, with an oral bioavailability of 78% and a half-life of 12–13 hours, is taken up by the liver and metabolized primarily (85%) by Uridine 5'-diphospho-glucuronosyltransferase 1A9 (UGT1A9) to dapagliflozin-3-O-glucuronide (D3G). Excretion occurs via the intestines and kidneys, with urinary excretion comprising approximately 2% unchanged dapagliflozin and 60–80% as dapagliflozin-3-O-glucuronide [5, 54].

1.5 Dapagliflozin pharmacodynamics

Pharmacodynamics refers to the study of the effects of drugs on the body, including how they interact with receptors, enzymes, or other molecular targets to produce therapeutic effects. It involves understanding drug potency, efficacy, and the dose-response relationship, which guide the appropriate dosing and prediction of side effects.

SGLT2 inhibitors, such as dapagliflozin, improve glycemic control in patients with T2DM by lowering plasma glucose levels through SGLT2 inhibition, resulting in a decrease in the renal threshold for glucose excretion (RTG) due to reduced renal glucose reabsorption, thus promoting urinary glucose excretion (UGE) [34, 61]. Treatment with dapagliflozin leads to a reduction in the maximum renal glucose reabsorptive capacity (TmG) in both diabetic and non-diabetic subjects and to an increase in the splay — mechanisms that promote glucosuria by lowering the threshold for the excretion of glucose in the urine [11].

1.6 Hepatic and renal impairment

People with diabetes, particularly T2DM, are at increased risk of developing comorbidities such as chronic kidney disease (CKD) and metabolic dysfunction-associated fatty liver disease (MAFLD). These conditions can result in changes in key physiological parameters such as hepatic blood flow, plasma protein binding, and biliary excretion, all of which can affect the pharmacokinetics of a drug [34]. Such changes can affect the efficacy and safety of a drug and may require dose adjustments.
Clinical markers such as the Child-Turcotte-Pugh (CTP) score for liver function and the glomerular filtration rate (GFR) for kidney function are commonly used to assess the degree of functional impairment in these organs, guiding dose adjustments for drugs processed by the liver and kidneys (see Fig. 3). The CTP score combines serum bilirubin, serum albumin, ascites, and hepatic encephalopathy and prothrombin time to estimate the severity of cirrhosis and prognosis of chronic liver disease [7, 57]. The glomerular filtration rate (GFR) is a measure of kidney function that quantifies the amount of blood filtered by the glomeruli.

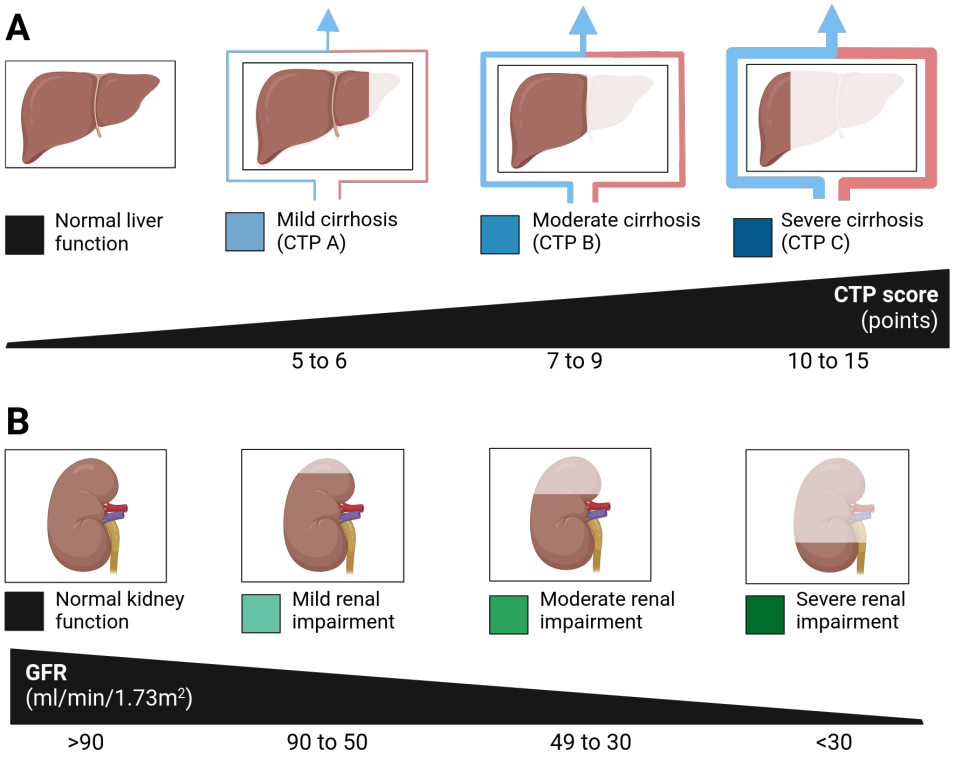

Figure 3: **Impairment strength in liver-kidney dysfunction.** Impairments in liver and kidney function significantly affect drug metabolism and excretion. Hepatic impairment is commonly evaluated using the Child-Turcotte-Pugh (CTP) score, which classifies liver function based on clinical and laboratory markers. Renal impairment is assessed by the glomerular filtration rate (GFR), with reduced GFR indicating diminished kidney function and lower drug clearance. Both the CTP score and GFR are essential for adjusting medication dosing to ensure safe and effective treatment in patients with liver or kidney dysfunction [67, 50].

Both the kidneys and the liver play an important role in the metabolism of dapagliflozin. Renal functional impairment has a major effect of dapagliflozin pharmacokinetics and pharmacodynamics. With decreasing renal function, the plasma concentrations of dapagliflozin and dapagliflozin-3-O-glucuronide increase and the cumulative amount of glucose excreted in the urine decreases, resulting in reduced efficacy [33]. In patients with impaired liver function, as measured by a higher CTP score, increased exposure to dapagliflozin may pose safety risks [67, 34]. It is recommended to assess renal function before starting dapagliflozin therapy.

1.7 Food-drug interaction

Another important factor for the safety of pharmacotherapy is the simultaneous examination of food and drugs, as this can have a strong influence on the release, absorption, distribution, metabolism, and / or excretion of drugs.
Drug absorption typically begins in the proximal region of the small intestine, which is close connection to the splanchnic circulation. After absorption, the substances are transported via the portal system to the liver, where they may undergo metabolism. From there they are carried into the systemic circulation through the hepatic artery, allowing them to exert their therapeutic effects throughout the body [70].
Each ingestion of food or drink alters the physiological conditions of the human gastrointestinal (GI) tract, affecting factors such as GI motility, splanchnic blood flow, and secretion [70]. Welling categorized food-drug interactions into five types: reduced, delayed, increased, accelerated absorption, or no effect. The most commonly observed outcome is delayed drug absorption, often due to slower gastric emptying and/or increased gastric pH (Fig. 4). As a result, delayed gastric emptying usually leads to a lower maximum plasma concentration (C_{max}) and a longer time to reach it (t_{max}), although the overall bioavailability of the drug is usually not affected [64, 49].
Food–drug interactions can be further divided into specific and unspecific interactions. A typical example of specific food-drug interactions includes substances such as alcohol or grapefruit juice, which can have a direct impact on drug effectiveness. In contrast, nonspecific interactions arise from general physiological changes in the GI tract and may affect any orally administered drug. Studies on orally administered dapagliflozin have focused on nonspecific interactions, examining how variables such as luminal conditions, absorption, metabolism, and elimination are influenced by food intake. The clinical relevance of these effects depends largely on the drug's physicochemical properties and formulation [47].
Multiple studies have examined the effect of food on the pharmacokinetics and bioequivalence of dapagliflozin in healthy volunteers. While a high-fat meal consistently delayed the time to reach maximum plasma concentration (t_{max}) for dapagliflozin and by approximately 1–2.5 hours and its metabolite dapagliflozin-3-O-glucuronide reduced C_{max} by 30–50%, the area under the curve (AUC) and half-life ($t_{1/2}$) remained largely unchanged. These changes were considered minor and clinically insignificant, indicating no relevant food effect on overall systemic exposure [31, 62, 48, 41].

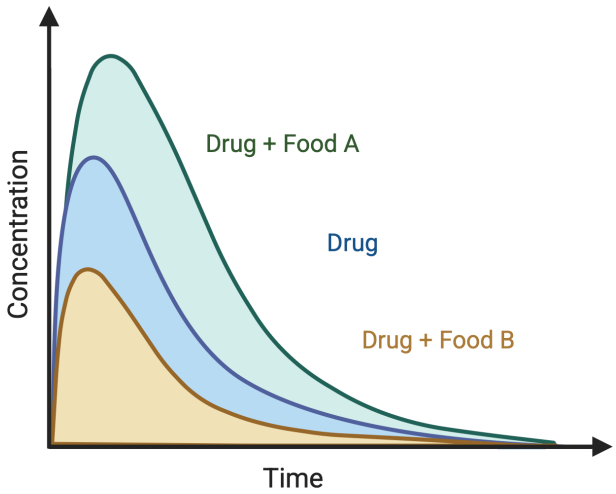

Figure 4: **Food can influence medication effectiveness.** The pharmacological effect of a drug may be influenced by food intake, which may increase (Drug + Food A), accelerate, decrease (Drug + Food B) or delay absorption and overall effect.

1.8 Physiologically based pharmacokinetic/ pharmacodynamic model

A physiologically based pharmacokinetic model (PBPK) is a computational model that enables the simulation of absorption, distribution, metabolism and excretion (ADME) of a drug and its metabolites. In combination with a pharmacodynamic model (PD), the effect profile and optimal dosage of new drugs can be predicted in order to achieve the desired exposure. Such a PBPK/PD model consists of a larger number of compartments corresponding to different organs or tissues in the body. These compartments are connected by flow rates corresponding to the circulatory system. Based on a set of differential equations parameterized with physiological variables, the model integrates detailed physiological, biochemical and anatomical data to predict the behavior of a drug in the organism as realistically as possible [26].

1.9 Question, scope and hypotheses

This project aims to address several important questions about the pharmacokinetics and pharmacodynamics of dapagliflozin, in particular, how these are influenced by a variety of patient-specific factors. Key questions include: How do individual characteristics such as liver impairment, renal impairment, and food intake affect the pharmacokinetics and pharmacodynamics of dapagliflozin?
The primary objective is to develop a physiologically based pharmacokinetic/pharmacodynamic (PBPK/PD) model for dapagliflozin using existing clinical data from healthy volunteers, patients with T2DM, and those with renal or hepatic dysfunction to investigate these questions.
The hypotheses driving this research are as follows:

- Impairment in renal or hepatic function lead to reduced metabolism and excretion of dapagliflozin and its primary metabolite dapagliflozin-3-O-glucuronide.
- Administration of dapagliflozin in a fed state leads to a slower absorption compared to the fasted state, thereby affecting pharmacokinetics and pharmacodynamics.

The developed model should accurately simulate the pharmacokinetics and pharmacodynamics of dapagliflozin in different patient populations, providing information that could lead to more personalized treatment strategies and improve the efficacy and safety of dapagliflozin treatment.

2 Methods

A systematic approach was followed for this work, which includes the following steps: systematic literature search for dapagliflozin (Sec. 2.1), data curation of clinical studies (Sec. 2.2), PBPK/PD model development (Sec. 2.3), simulation of study data (Sec. 2.4), analysis of food-drug interaction (Sec. 2.5), parameter optimisation of model parameters using clinical data (Sec. 2.6), parameter scans for renal function, liver function and food effect (Sec. 2.7) and calculation of pharmacokinetic parameters (Sec. 2.8).

2.1 Systematic literature research

A systematic literature search was conducted to select studies that included data on the pharmacokinetics or pharmacodynamics of dapagliflozin. The search was performed on 2024-04-23, in PubMed, using the keywords `dapagliflozin AND pharmacokinetics` and using `dapagliflozin` in PKPDAI [19]. Based on the search an initial literature corpus on the pharmacokinetics of dapagliflozin was generated. From this collection, available PDF files of selected studies were retrieved, and clinical studies were screened according to predefined inclusion criteria. In addition to healthy subjects, trials in patients with diabetes type 1 and type 2, renal and hepatic impairment were included. Studies in paediatric patients and animal studies were excluded. In addition, the literature was also reviewed for relevant pharmacodynamic data. Fig. 5 provides an overview of the literature review process.

2.2 Data curation

Data from the selected literature were curated and uploaded to the open pharmacokinetics database PK-DB [20]. The articles were screened for patient information such as age, sex, specific diseases and drugs, dapagliflozin dosing protocol and dapagliflozin pharmacokinetic profiles. These data were then curated using standard protocols for pharmacokinetic information [20]. Data from figures were digitised using WebPlotDigitizer [58]. Data from tables and textual descriptions were also curated in a specific format as described in [20].
Data were systematically curated according to the following structure: (i) Groups: Patient groups were entered into the database with relevant group characteristics such as age, height, weight, sex and ethnicity. Information on diabetes status, renal or hepatic impairment and other diseases was coded. (ii) Individuals: For some trials, individual patient characteristics were reported. Information on individual subject characteristics was recorded in the same way as for the groups. (iii) Interventions: In each trial, dapagliflozin was given to patients either as an oral dose in the form of a tablet or capsule, or as an intravenous dose in the form of a solution. Information on dose, time of administration (if multiple doses were administered), and route of administration were recorded. (iv) Time course data: In each study, the authors reported a number of different parameters. The main data of interest were the time courses of concentrations and amounts of dapagliflozin or its metabolite dapagliflozin 3-o-glucuronide in plasma and urine and urinary glucose excretion (UGE). (v) Pharmacokinetic/pharmacodynamic parameters: In addition, many studies reported pharmacokinetic parameters such as C_{max}, t_{max} and $t_{1/2}$ and pharmacodynamic parameters such as fasting plasma glucose (FPG), UGE, and renal threshold for glucose (RTG).
The extensive heterogeneous data set provided the database for model development and validation. All data are available in PK-DB (`https://pk-db.com`) [20] with an overview of the curated studies in Tab. 2.

2.3 PBPK/PD model

The PBPK/PD and tissue models were developed in the Systems Biology Markup Language (SBML) [22, 35]. The libraries sbmlutils [44] and cy3sbml [46, 42] were used for the programmatic manipulation and visualisation of the models. The models are ordinary differential equation (ODE) models solved numerically using sbmlsim [43] based on the high performance SBML simulator libroadrunner [65, 71]. The model is made available in SBML under a CC-BY 4.0 licence with all model equations from `https://github.com/matthiaskoenig/dapagliflozin-model`. The version of the model used in this thesis is 0.9.5 [55].
The PBPK/PD model developed consists of a whole-body model linking different organs via the systemic circulation (Fig. 6). The model follows a hierarchical structure, with the whole-body model linking sub-models for the intestine, kidney and liver.

Hepatic functional impairment Liver functional impairment was modelled as a gradual increase in cirrhosis by scaling liver function with the parameter `f_cirrhosis` [-] from 0.0 (no cirrhosis) to 0.95 (critical cirrhosis). The cirrhosis implementation is based on an indocyanine green model of cirrhosis [40, 39] with parameters for mild (0.40), moderate (0.70) and severe cirrhosis (0.81) corresponding to the Child-Pugh-Turette classes CPT A, CPT B and CPT C, respectively [7, 57]. Cirrhosis is modelled as a combination of a reduction in functional liver volume and shunting of blood around the liver, both of which lead to a reduction in blood flow. With increasing `f_cirrhosis` both liver functional volume and blood shunted around the liver are increased resulting in a reduction in liver function.

Renal functional impairment Renal impairment was modelled as a progressive decline in renal function by scaling all renal processes with the factor `f_renal_function` [-], where 1.0 represents normal function and <1.0: reduced renal function. The cut-offs for the different stages of renal impairment were based on the international KDIGO guidelines [66] with mild renal impairment (0.69), moderate renal impairment (0.32) and severe renal impairment (0.19) [53].

Dose dependency The dose dependency was studied by changing the parameters corresponding to intravenous and oral dose of dapagliflozin, `IVDOSE_dap` [mg] and `PODOSE_dap` [mg], respectively. Doses were changed in the typical dosing regime of dapagliflozin between 0 and 100 mg.

Food effect The food effect was modelled by adjusting the absorption scaling parameter `f_absorption` for dapagliflozin in the intestine. Fasted simulations were simulation with 1.0, where as food (fed) was implemented with a reduced absorption of 0.3. These changes result in a change in absorption rate as

$$absorption = f_{absorption} \cdot DAPABS_k \cdot Vgu \cdot dap_{lumen}$$

2.4 Simulations

For all curated clinical trials (Tab. 2), *in silico* simulation experiments were created. For the simulations, the parameters corresponding to the pathophysiology (`KI__f_renal_function` and `f_cirrhosis`), for the food effect (`GU__f_absorption`), and the dosing (`PODOSE_dap`, `IVDOSE_dap`) were modified according to the study.
Bodyweights were set according to the information in the studies via the parameter `BW`.
Because UGE depends on the plasma concentration the fasting plasma glucose (FPG) concentrations were set for the respective simulations via the parameter `KI__glc_ext`.
In the case of multiple dosing, the appropriate doses were administered at the specified times.

2.5 Analysis of food-drug interaction

Table 1: **Types of effects based on the calculated ratios**

Ratio	Effect
ratio ≥ 5.0	strong induction ($\uparrow\uparrow\uparrow$)
$5.0 >$ ratio ≥ 2.0	moderate induction ($\uparrow\uparrow$)
$2.0 >$ ratio ≥ 1.25	weak induction ($\uparrow$)
$1.25 >$ ratio ≥ 0.8	no effect ($\varnothing$)
$0.8 >$ ratio ≥ 0.5	weak inhibition ($\downarrow$)
$0.5 >$ ratio ≥ 0.2	moderate inhibition ($\downarrow\downarrow$)
$0.2 >$ ratio	strong inhibition ($\downarrow\downarrow\downarrow$)

To determine the effect of food, the ratios between the mean values of AUC and C_{max} between the fasted and fed states were calculated. These values were obtained from tables in the respective studies. Depending on the ratio between the mean values, a rough statement can be made about the effect. If $ratio$ is > 1, it means that there was an increase in a certain mean value and $ratio < 1$ indicates a corresponding reduction in the mean values after food intake. The following equation was used for the calculation of the ratios for AUC and C_{max}, where the "fasted" condition refers to dapagliflozin administered on an empty stomach, and the "fed" condition represents dapagliflozin intake after food consumption:

$$ratio = \frac{\mu_{fed}}{\mu_{fasted}}$$

The standard deviation of the ratios (σ_{ratio}) can be approximated using the ratio itself, the mean values (μ) for the fasted and fed states, and their respective standard deviations (σ):

$$\sigma_{ratio} \approx ratio \cdot \sqrt{(\frac{\sigma_{fasted}}{\mu_{fasted}})^2 + (\frac{\sigma_{fed}}{\mu_{fed}})^2}$$

The calculated ratios and the conditions listed in Tab. 1 can be used to determine the type and the strength of the effect on the AUC [9]. The symbols in parentheses were used to represent the varying effects of the drugs.
A two-sided t-test was conducted to compare the mean values of dapagliflozin intake under fasting and fed conditions and to determine statistical significance based on the test results.
The value of the test statistic t was calculated using the following equation, where μ_1 and μ_2 represent the mean values of the intake of dapagliflozin in the fasting and fed states, respectively. Likewise, σ_1 and σ_2 denote the corresponding standard deviations, while n_1 and n_2 are the sample sizes for each condition:

$$t = \frac{\mu_1 - \mu_2}{\sigma_{pooled} \times \sqrt{\frac{1}{n_1} + \frac{1}{n_2}}}$$

With the following definition for the pooled standard deviation σ_{pooled}:

$$\sigma_{pooled} = \sqrt{\frac{(n_1 - 1) \cdot \sigma_1^2 + (n_2 - 1) \cdot \sigma_2^2}{n_1 + n_2 - 2}}$$

The degrees of freedom df can be calculated from the sample sizes n_1 and n_2 using the following equation:

$$df = n_1 + n_2 - 2$$

The p-values, which provide insights into the relationship between the two groups, are determined using the t-statistic t and the degrees of freedom df. Once calculated, the p-values can be used to assess the significance level α: $p \leq 0.05$ (*), $p \leq 0.01$ (**), $p \leq 0.001$ (***).

2.6 Parameter optimization

Parameter fitting was used to minimise the distance between experimental data and model predictions by optimising a subset of ten parameters of the model. For this purpose, a subset of curated time curves from healthy subjects, as well as subjects with diabetes or renal impairment after single dose application was used, as listed in Tab. 2. Parameters were optimised in a multistep process based on the route of administration. First, parameters relevant to intravenous dapagliflozin were optimised using the subset of intravenous data. Next, parameters for oral administration of dapagliflozin were optimised using a subset of the oral dapagliflozin data. Finally, the parameters related to the hepatic metabolism of dapagliflozin and its conversion to dapagliflozin-3-O-glucuronide were optimized. This strategy allowed the parameters of dapagliflozin and dapagliflozin-3-O-glucuronide to be determined separately with subsequent optimisation of the coupling step.
The cost function, which depends on the parameter $\vec{p}$, minimised the sum of the quadratic weighted residuals $r_{i,k}$ for all time courses k and data points i. Time courses were weighted by the number of participants in each study n_k and individual time points with the standard deviation $\sigma_{i,k}$ associated with the measurement, resulting in weights $w_{i,k} = n_k/\sigma_{i,k}$.

$$F(\vec{p}) = 0.5 \sum_{i,k} (w_{i,k} \cdot r_{i,k}(\vec{p}))^2$$

Multiple optimisation runs were performed with different initial parameters based on a local optimiser, with the optimal parameters used in the final model. The fitted parameters are shown in Tab. 3 and Tab. 4. For validation, data from multiple administrations, disease states, different doses, and food conditions were used.

2.7 Parameter scans

Parameter scans were conducted to evaluate the effects of liver impairment, kidney impairment, and absorption activity on dapagliflozin pharmacokinetics. The parameters were scanned in the following ranges: `f_cirrhosis` in `linspace(0, 0.9, num=10)` with normal liver function corresponding to 0.0; `f_renal_function` in `logspace(-1, 1, num=10)` with normal kidney function corresponding to 1. 0; `GU__f_absorption` in `logspace(-1, 1, num=10)` with 1.0 representing absorption in the fed state and values below 1.0 corresponding to the fasted state. Simulations were performed for a typically given single oral dose of 5 mg dapagliflozin.

2.8 Pharmacokinetic parameters

Pharmacokinetic parameters of dapagliflozin and dapagliflozin-3-O-glucuronide were calculated from plasma concentration time curves and urinary excretion using standard non-compartmental methods. The elimination rate k_{el}[1/min] was calculated by linear regression in logarithmic space in the decay phase. The area under the curve AUC [mmole·min/L] was calculated using the trapezoidal rule and extrapolated to infinity by linear interpolation. Apparent clearance Cl [ml/min] was calculated as $Cl/F = k_{\mathrm{el}} \cdot V_{\mathrm{d}}$ with apparent volume of distribution $V_{\mathrm{d}}/F = D/(AUC_{\infty} \cdot k_{el})$. D is the applied dose of dapagliflozin.
Pharmacodynamic parameters of dapagliflozin are described separately in Sec. 3.2.5.

3 Results

3.1 Data

In this work, an extensive database of dapagliflozin pharmacokinetics and pharmacodynamics was established and used to develop and validate a physiologically based pharmacokinetic and pharmacodynamic (PBPK/PD) model of dapagliflozin.
A comprehensive literature search was conducted using the PKPDAI and PubMed databases to identify relevant clinical studies. Of more than 200 trials initially screened, 89 were prioritized according to the following inclusion criteria: (1) the study was conducted in humans; (2) subjects were adults; (3) the study was performed in vivo; and (4) time-course data on plasma or urine concentrations of dapagliflozin and/or its primary metabolite, dapagliflozin-3-O-glucuronide, were reported. Special emphasis was placed on studies involving participants with renal or hepatic impairment, as well as those assessing the effects of food on dapagliflozin pharmacokinetics. Based on these criteria, 27 studies were selected for detailed data curation, forming the core dataset used to develop and evaluate the PBPK/PD model. An overview of the study selection process is shown in Fig. 5.
The curated dataset has been made publicly available as open data to support transparency and reproducibility. A summary of the selected studies, including participant characteristics and dosing protocols, is presented in Tab. 2.

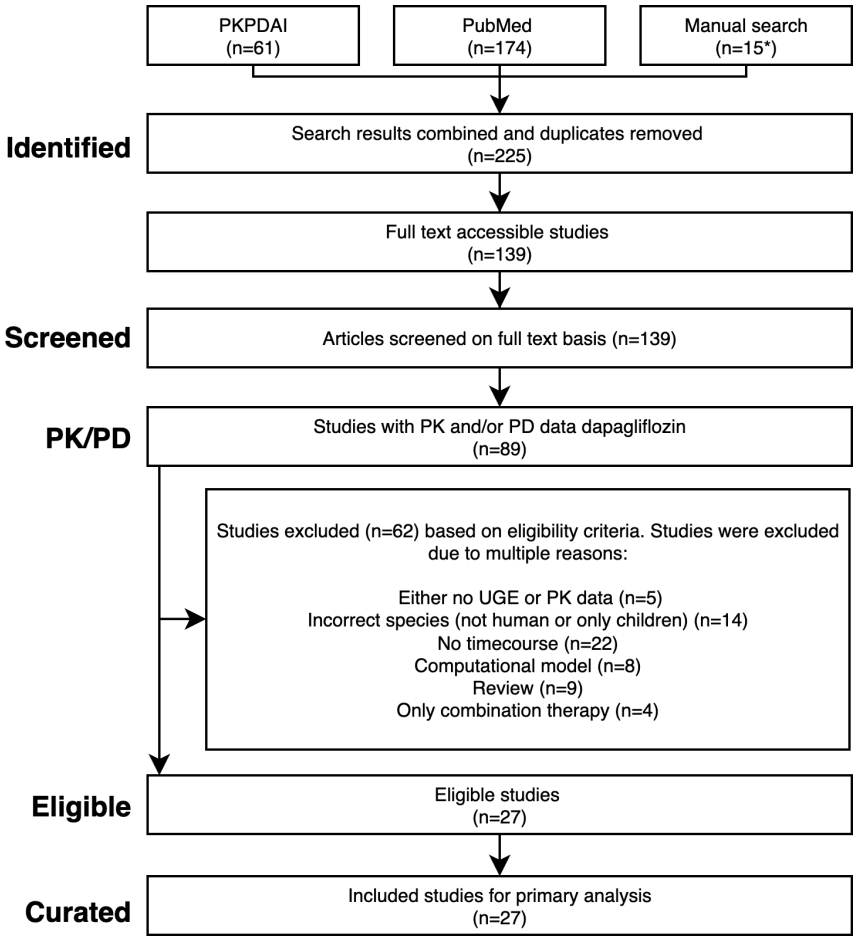

Figure 5: **Overview of the literature search and selection of studies for data curation.** Publications related to dapagliflozin pharmacokinetics were retrieved using PKPDAI and PubMed searches. Studies with full text available in PDF format were screened (* one publication [17] contained multiple clinical studies). Eligible studies included in vivo pharmacokinetic data in adult humans. Studies with missing data or with focus on coadministration of other drugs were excluded from data curation.

Table 2: **Summary of studies for modeling.** Overview of study identifiers, PK-DB IDs, administered substance, route, dosing, and subject characteristics, including health status (H), renal impairment (RI), hepatic impairment (HI), fasting status and urinary glucose excretion (UGE) and renal treshold for glucose (RTG). $DAP\ P$ = dapagliflozin plasma, $DAP\ U$ = dapagliflozin urine, $DAP\ F$ = dapagliflozin feces, $D3G\ P$ = dapagliflozin-3-O-glucuronide plasma, $D3G\ U$ = dapagliflozin-3-O-glucuronide urine.

Study	PK-DB	Substance	Route	Dosing	Dose [mg]	H	RI	HI	T1	T2	DAP P	DAP U	DAP F	D3G P	D3G U	Fed	Fast	UGE	RTG
Boulton2013 [4]	PKDB00838	dap, [14C]dap	oral, iv	single	10, 0.080	✓					✓								
Cho2021 [8]	PKDB00839	dap	oral	single	10	✓					✓								
FDAMB102002 [13]	PKDB00959	dap	oral	multi	2.5, 10, 20, 50, 100	✓					✓							✓	
FDAMB102003 [14]	PKDB00960	dap	oral	single, multi	5, 25, 100					✓	✓							✓	
FDAMB102006 [15]	PKDB00970	[14C]dap	oral	single	50	✓					✓	✓	✓		✓				
FDAMB102007 [16]	PKDB00971	dap	oral	single, multi	20, 50	✓	✓			✓	✓	✓							
Hwang2022a [23]	PKDB00923	dap	oral	single	10	✓					✓			✓					
Imamura2013 [24]	PKDB00893	dap	oral	single	10					✓	✓								
Jang2020 [25]	PKDB00913	dap	oral	multi	10	✓					✓								
Kasichayanula2011 [34]	PKDB00841	dap	oral	single	10	✓		✓			✓			✓					
Kasichayanula2011a [28]	PKDB00842	dap	oral	single, multi	2.5, 10, 20, 50	✓				✓	✓			✓	✓			✓	
Kasichayanula2011b [31]	PKDB00843	dap	oral	single	10	✓					✓			✓		✓	✓		
Kasichayanula2011c [30]	PKDB00924	dap	oral	single	20, 50	✓					✓								
Kasichayanula2012 [32]	PKDB00925	dap	oral	single	20	✓					✓								
Kasichayanula2013 [33]	PKDB00844	dap	oral	single, multi	20, 50	✓	✓			✓	✓	✓		✓	✓		✓		
Kasichayanula2013a [29]	PKDB00845	dap	oral	single	10	✓					✓	✓		✓			✓	✓	
Khomitskaya2018 [36]	PKDB00926	dap	oral	single	10	✓					✓								
Kim2023 [37]	PKDB00927	dap	oral	multi	10	✓					✓								
Kim2023a [38]	PKDB00928	dap	oral	single	10	✓					✓								
Komoroski2009 [41]	PKDB00846	dap	oral	single, multi	2.5, 10, 20, 50, 100, 250, 500	✓					✓	✓			✓	✓	✓	✓	
LaCreta2016 [48]	PKDB00847	dap	oral	single	2.5, 10	✓					✓					✓	✓		
Obermeier2010 [56]	PKDB00848	dap, [14C]dap	oral	single	50	✓					✓								
Sha2015 [61]	PKDB00891	dap	oral	single	10	✓					✓						✓	✓	✓
Shah2019a [62]	PKDB00849	dap	oral	single	5	✓					✓					✓	✓		
vanderAart-vanderBeek2020 [68]	PKDB00929	dap	oral	multi	10		✓				✓								
Watada2019 [69]	PKDB00850	dap	oral	multi	5, 10				✓		✓			✓				✓	
Yang2013 [73]	PKDB00851	dap	oral	single, multi	5, 10	✓					✓	✓		✓	✓		✓	✓	

3.2 Computational model

3.2.1 PBPK/PD model

Using the curated data set, a physiologically based pharmacokinetic/ pharmacodynamic (PBPK/ PD) model was developed to simulate the absorption, distribution, metabolization, and elimination of dapagliflozin and its primary metabolite, dapagliflozin-3-O-glucuronide, in the body, see Fig. 6 and their effect on UGE. Dapagliflozin is typically given orally in the form of a tablet (e.g. Forxiga/ Farxiga), but can also be administered as a capsule or intravenously as a solution. Depending on the study, dapagliflozin was administered as a single dose or as multiple doses at regular intervals, for example, every morning for several days.

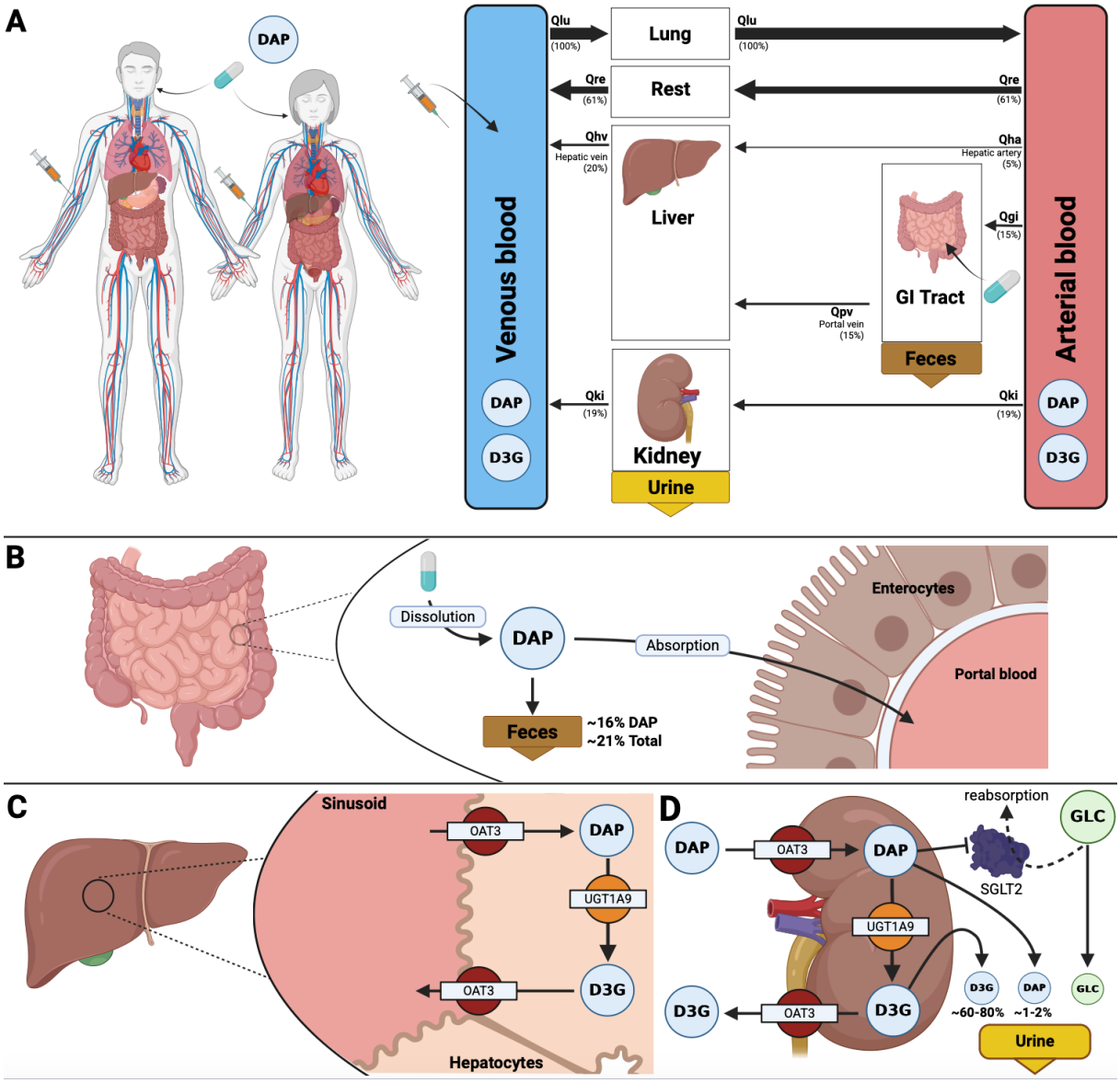

Figure 6: **Overview of the PBPK/PD model of dapagliflozin.** A) Whole body model responsible for dapagliflozin (DAP) and dapagliflozin-3-O-glucuronide (D3G) systemic circulation via the blood. Dapagliflozin can be administred either orally or intravenously. B) Intestine model describing the absorption of dapagliflozin by enterocytes. Dapagliflozin has a high bioavailability with $\tilde{1}6\%$ excreted in feces. C) Hepatic model depicting the uptake of dapagliflozin by hepatocytes and its conversion by uridine diphosphate glucuronosyltransferase 1A9 (UGT1A9) to dapagliflozin-3-O-glucuronide. D) Renal model showing the uptake and excretion of dapagliflozin and dapagliflozin-3-O-glucuronide in the urine and metabolic conversion of dapagliflozin to dapagliflozin-3-O-glucuronide. Dapagliflozin in the kidneys inhibits SGLT2 resulting in reduced reabsorption and increased urinary excretion of glucose.

3.2.2 Intestine model

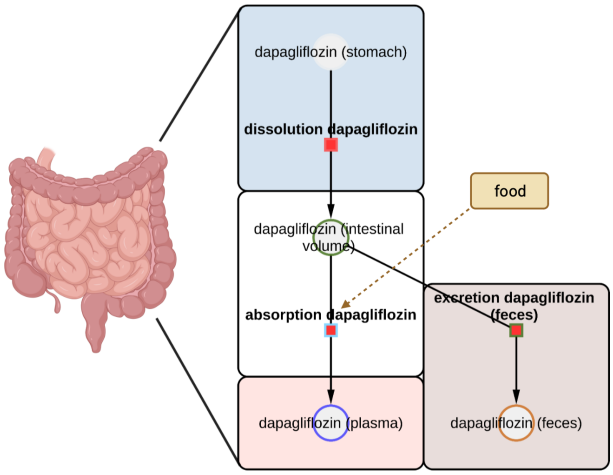

Figure 7: **SBML graph of intestine model of dapagliflozin.** After ingestion, dapagliflozin is dissolved in the stomach and enters the intestine. A large fraction of the dose (84%) is absorbed and enters the plasma, the remainder (16%) is excreted in the feces. Food can change the absorption rate in the model.

After oral administration, the tablet dissolves in the stomach and the drug is released into the intestine. Dapagliflozin is absorbed into the intestinal blood via the enterocytes (see Fig. 7). The dissolution process, which determines how quickly the drug enters the intestine, is described via:

$$\text{dissolution}_{\text{dap}} = \frac{Ka_{\text{dis,dap}}}{60\ \frac{min}{hr}} \cdot \frac{\text{PODOSE}_{\text{dap}}}{M_r^{\text{dap}}}$$

Once in solution, the drug can be absorbed from the gut lumen. The rate of absorption depends on the scaling factor absorption, which is altered with food, the rate constant of absorption DAPABS_k, the volume of the intestine V_{gu}, and the local drug concentration dap:

$$\text{DAPABS} = f_{\text{absorption}} \cdot \text{DAPABS}_k \cdot V_{\text{gu}} \cdot \text{dap}_{\text{lumen}} \quad [\text{mmol/min}]$$

However, only a fraction of the drug $F_{\text{dap,abs}}$ is absorbed and reaches the portal vein:

$$\text{absorption} = F_{\text{dap,abs}} \cdot \text{absorption}$$

The remainder which is not absorbed is excreted via the feces. This unabsorbed fraction is determined via:

$$\text{DAPABS} = (1 - F_{\text{dap,abs}}) \cdot \text{absorption}$$

The resulting differential equations are:

$$\frac{d\,\text{PODOSE}_{\text{dap}}}{dt} = -\text{dissolution}_{\text{dap}} \cdot M_r^{\text{dap}}$$

$$\frac{d\,\text{dap}_{\text{ext}}}{dt} = \frac{\text{DAPABS}}{V_{\text{ext}}}$$

$$\frac{d\,\text{dap}_{\text{feces}}}{dt} = \text{DAPEXC}$$

$$\frac{d\,\text{dap}_{\text{lumen}}}{dt} = -\frac{\text{DAPABS}}{V_{\text{lumen}}} - \frac{\text{DAPEXC}}{V_{\text{lumen}}} + \frac{\text{dissolution}_{\text{dap}}}{V_{\text{lumen}}}$$

3.2.3 Liver model

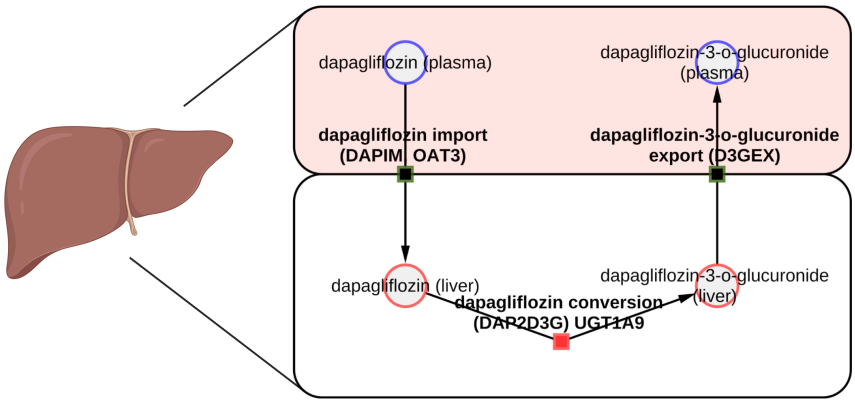

Figure 8: **SBML graph of liver model of dapagliflozin.** Dapagliflozin in the plasma of the liver is imported into hepatic tissue via organic anion transporter 3 (OAT3). Within the liver, it undergoes conversion to dapagliflozin-3-O-glucuronide (D3G) via uridine diphosphate glucuronosyltransferase 1A9 (UGT1A9). The resulting dapagliflozin-3-O-glucuronide is then exported (D3GEX) into plasma.

Dapagliflozin is taken up by the liver (see Fig. 8), with the help of transport proteins, possibly by OAT3 and modelled as reversible Michaelis-Menten kinetics with Km=33µM FDA [17].

$$\text{DAPIM} = \frac{\text{DAPIM}_{\text{Vmax}}}{\text{DAPIM}_{\text{Km,dap}}} \cdot V_{\text{li}} \cdot \frac{\text{dap}_{\text{ext}} - \text{dap}}{1 + \frac{\text{dap}_{\text{ext}}}{\text{DAPIM}_{\text{Km,dap}}} + \frac{\text{dap}}{\text{DAPIM}_{\text{Km,dap}}}}$$

The metabolism of dapagliflozin to dapagliflozin-3-O-glucuronide is catalysed by the enzyme uridine diphosphate glucuronosyltransferase 1A9 (UGT1A9) and modelled as irreversible Michaelis-Menten kinetics.

$$\text{DAP2D3G} = f_{\text{ugt1a9}} \cdot \text{DAP2D3G}_{\text{Vmax}} \cdot V_{\text{li}} \cdot \frac{\text{dap}}{\text{dap} + \text{DAP2D3G}_{\text{Km,dap}}}$$

After dapagliflozin has been converted to dapagliflozin-3-O-glucuronide, it is exported. This is possibly catalyzed by OAT3 with Km=115µM FDA [17] and modelled via reversible Michaelis-Menten kinetics.

$$\text{D3GEX} = \frac{\text{D3GEX}_{\text{Vmax}}}{\text{D3GEX}_{\text{Km,d3g}}} \cdot V_{\text{li}} \cdot \frac{\text{d3g} - \text{d3g}_{\text{ext}}}{1 + \frac{\text{d3g}}{\text{D3GEX}_{\text{Km,d3g}}} + \frac{\text{d3g}_{\text{ext}}}{\text{D3GEX}_{\text{Km,d3g}}}}$$

The resulting differential equations are:

$$\frac{d\,\text{d3g}}{dt} = \frac{\text{DAP2D3G}}{V_{\text{li}}} - \frac{\text{D3GEX}}{V_{\text{li}}}$$

$$\frac{d\,\text{d3g}_{\text{ext}}}{dt} = \frac{\text{D3GEX}}{V_{\text{ext}}}$$

$$\frac{d\,\text{dap}}{dt} = \frac{\text{DAPIM}}{V_{\text{li}}} - \frac{\text{DAP2D3G}}{V_{\text{li}}}$$

$$\frac{d\,\text{dap}_{\text{ext}}}{dt} = -\frac{\text{DAPIM}}{V_{\text{ext}}}$$

3.2.4 Kidney model

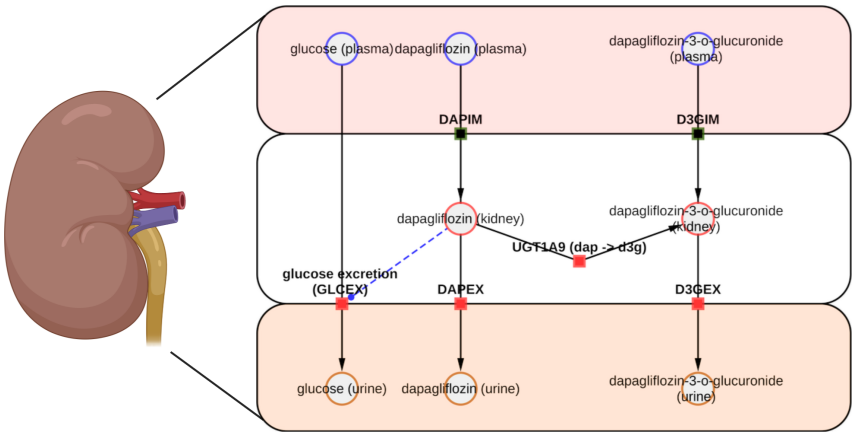

Figure 9: **SBML graph of kidney model of dapagliflozin.** Plasma glucose is filtered in the kidney and partly reabsorbed, with the remaining fraction excreted into the urine (GLCEX). Dapagliflozin appears in plasma after administration and is imported (DAPIM) into renal tissue, where a portion is excreted (DAPEX) unchanged into the urine. In the kidney, dapagliflozin is also metabolized to dapagliflozin-3-O-glucuronide (D3G) via uridine diphosphate glucuronosyltransferase 1A9 (UGT1A9). Dapagliflozin-3-O-glucuronide in plasma is imported (D3GIM) into renal tissue and subsequently excreted (D3GEX) in the urine.

Dapagliflozin is imported into renal tissue (DAPIM), where it is partially excreted unchanged (DAPEX) and metabolized to dapagliflozin-3-O-glucuronide, which is also excreted in the urine (D3GEX).
For the import of dapagliflozin into the kidney, carrier-mediated transport processes were implemented in the model (see Fig. 9). The transport of dapagliflozin across the renal membrane is described by a reversible Michaelis-Menten equation:

$$\mathrm{DAPIM} = \frac{\mathrm{DAPIM}_{\mathrm{Vmax}}}{\mathrm{DAPIM}_{\mathrm{Km,dap}}} \cdot V_{\mathrm{ki}} \cdot \frac{\mathrm{dap}_{\mathrm{ext}} - \mathrm{dap}}{1 + \frac{\mathrm{dap}_{\mathrm{ext}}}{\mathrm{DAPIM}_{\mathrm{Km,dap}}} + \frac{\mathrm{dap}}{\mathrm{DAPIM}_{\mathrm{Km,dap}}}}$$

Similarly, the import of its primary metabolite, dapagliflozin-3-O-glucuronide, into kidney cells is described by the equation:

$$\mathrm{D3GIM} = \frac{\mathrm{D3GIM}_{\mathrm{Vmax}}}{\mathrm{D3GIM}_{\mathrm{Km,d3g}}} \cdot V_{\mathrm{ki}} \cdot \frac{\mathrm{d3g}_{\mathrm{ext}} - \mathrm{d3g}}{1 + \frac{\mathrm{d3g}_{\mathrm{ext}}}{\mathrm{D3GIM}_{\mathrm{Km,d3g}}} + \frac{\mathrm{d3g}}{\mathrm{D3GIM}_{\mathrm{Km,d3g}}}}$$

Within the kidney, dapagliflozin is further metabolized to dapagliflozin-3-O-glucuronide through the enzymatic action of UGT1A9, a process referred to as DAP2D3G. The corresponding irreversible Michaelis-Menten equation is:

$$\mathrm{DAP2D3G} = f_{\mathrm{ugt1a9}} \cdot \mathrm{DAP2D3G}_{\mathrm{Vmax}} \cdot V_{\mathrm{ki}} \cdot \frac{\mathrm{dap}}{\mathrm{dap} + \mathrm{DAP2D3G}_{\mathrm{Km,dap}}}$$

The transport of dapagliflozin and dapagliflozin-3-O-glucuronide were assumed to be fast compared to the metabolic conversion.
Both dapagliflozin and dapagliflozin-3-O-glucuronide are excreted via the kidney in the urine. Their renal excretion rates are given by:

$$\mathrm{DAPEX} = f_{\text{renal function}} \cdot \mathrm{D3GEX}_k \cdot V_{\mathrm{ki}} \cdot \mathrm{d3g}_{\mathrm{ext}}$$

$$\mathrm{D3GEX} = f_{\text{renal function}} \cdot \mathrm{DAPEX}_k \cdot V_{\mathrm{ki}} \cdot \mathrm{dap}_{\mathrm{ext}}$$

For this purpose, the parameter $f_{\text{renal\_function}}$ was introduced as a scaling factor to simulate varying degrees of renal function. A value of ($= 1$) corresponds to normal renal function, whereas values (< 1) represent reduced renal function, as observed in patients with renal impairment. This parameter uniformly scales the renal excretion rates of both dapagliflozin and dapagliflozin-3-O-glucuronide.
The kidney volume V_{ki} was set to 0.44% of total body weight. This volume is used to scale concentration-dependent processes, such as renal transport and metabolism, ensuring physiological relevance of the calculated rates.
The resulting differential equations are:

$$\frac{d\,\text{d3g}}{dt} = \frac{\text{D3GIM}}{V_{\text{ki}}} + \frac{\text{DAP2D3G}}{V_{\text{ki}}}$$

$$\frac{d\,\text{d3g}_{\text{ext}}}{dt} = -\frac{\text{D3GIM}}{V_{\text{ext}}} - \frac{\text{D3GEX}}{V_{\text{ext}}}$$

$$\frac{d\,\text{d3g}_{\text{urine}}}{dt} = \text{D3GEX}$$

$$\frac{d\,\text{dap}}{dt} = \frac{\text{DAPIM}}{V_{\text{ki}}} - \frac{\text{DAP2D3G}}{V_{\text{ki}}}$$

$$\frac{d\,\text{dap}_{\text{ext}}}{dt} = -\frac{\text{DAPIM}}{V_{\text{ext}}} - \frac{\text{DAPEX}}{V_{\text{ext}}}$$

$$\frac{d\,\text{dap}_{\text{urine}}}{dt} = \text{DAPEX}$$

3.2.5 Pharmacodynamics model

The pharmacodynamics models describes how the UGE is affected by dapagliflozin. The UGE depends on the renal threshold for glucose (RTG), the plasma glucose concentration at which glucose reabsorption by the kidneys begins to saturate [12]. RTG is calculated as a basal RTG depending on fasting plasma glucose (fpg) which is reduced via dapagliflozin:

$$\text{RTG}_{\text{fpg}} = \text{RTG}_{\text{base}} + \text{RTG}_{\text{m, fpg}} \cdot (\text{glc}_{\text{ext}} - fpg_{\text{healthy}})$$

$$\text{RTG}_{\text{delta}} = \text{RTG}_{\text{fpg}} \cdot \text{RTG}_{\text{max inhibition}}$$

$$\text{RTG} = \text{RTG}_{\text{fpg}} - \text{RTG}_{\text{delta}} \cdot \frac{\text{dap}_{\text{ext}}^{\text{RTG}_\gamma}}{\text{RTG}_{\text{E50}}^{\text{RTG}_\gamma} + \text{dap}^{\text{RTG}_\gamma}}$$

Above RTG, excess glucose that cannot be reabsorbed is excreted in the urine, leading to an increase in UGE. Above RTG, glucose excretion (GLCEX) depends on glomerular filtration rate (GFR), which plays a decisive role in the filtration of plasma glucose through the kidneys and plasma glucose. Below the RTG no glucose is excreted in the urine.
The GFR depends on the status of the kidneys. $f_{\text{renal\_function}}$ is a scaling factor reflecting normal ($= 1$) or reduced (< 1) renal function

$$\text{GFR} = f_{\text{renal\_function}} \cdot \text{GFR}_{\text{healthy}}$$

$$\text{GLCEX} = \begin{cases} \frac{\text{GFR}}{\text{cf}_{\text{ml/l}}} \cdot (\text{glc}_{\text{ext}} - \text{RTG}) & \text{if } \text{glc}_{\text{ext}} > RTG \\ 0 \text{ mmole/min} & \text{if } \text{glc}_{\text{ext}} \leq RTG \end{cases}$$

The glucose concentration in plasma $\mathrm{glc}_{\mathrm{ext}}$ was assumed to be constant, but depends on the status of the subjects, i.e., diabetic patients have higher plasma glucose than healthy subjects. The change in urinary glucose is determined via the following differential equation:

$$\frac{d\ glc_{urine}}{dt} = GLCEX$$

The cumulative amount of glucose in the urine, i.e., the UGE, is calculated from the amount of glucose in the urine via:

$$\mathrm{UGE} = \frac{\mathrm{glc}_{\mathrm{urine}} \cdot M_{\mathrm{rglc}}}{\mathrm{cf}_{\mathrm{mg/g}}}$$

3.3 Parameter fitting

After the PBPK/PD model structure for dapagliflozin and its main metabolite, dapagliflozin-3-O-glucuronide, have been established, a subset of model parameters were optimized using a subset of the available data. In a first step parameters of the pharmacokinetic model were optimized (Tab. 3), subsequently parameters of the pharmacodynamic model (Tab. 4).
The results of the parameter adjustment, including the cost reduction over the optimization steps and the goodness of fit, are shown in Fig. 10a and Fig. 10b for the parameters of the pharmacokinetic model.

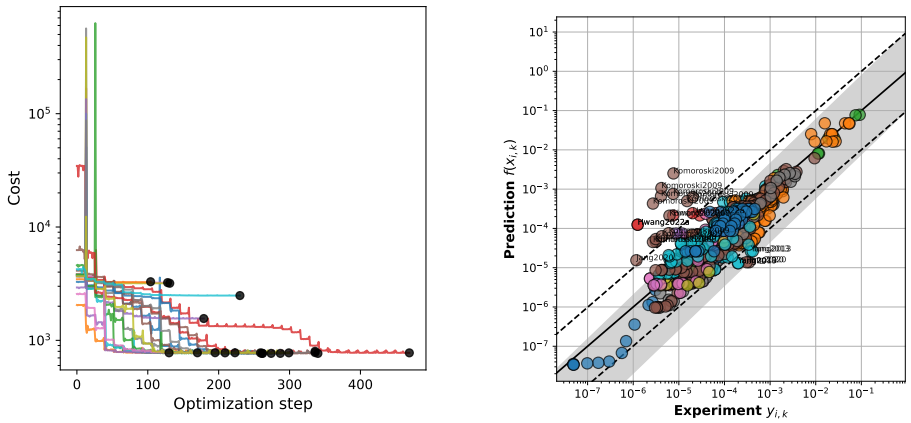

(a) Error convergence (b) Goodness-of-fit

Figure 10: **Optimization Performance.** Overview of Error convergence (cost vs. optimization step) and Godness-of-fit (predicted vs. experimental intravenous data) for the pharmacokinetic parameters.

Table 3: **Optimized parameters for the dapagliflozin pharmacokinetic model.**

Parameter name	Description	Value	Unit
`ftissue_dap`	Tissue blood flow rate for DAP	0.01	l/min
`Kp_dap`	Tissue-to-plasma partition coefficient	25.517	dimensionless
`DAP2D3G_Vmax`	Liver metabolism of DAP to D3G	0.01992	mmol/min/l
`KI__f_DAP2D3G`	Renal DAP2D3G activity relative to liver	10.0	-
`KI__DAPEX_k`	Renal excretion rate of DAP	0.01815	1/min
`KI__D3GEX_k`	Renal excretion rate of D3G	0.45036	1/min
`GU__Ka_dis_dap`	Dissolution rate of DAP in GI tract	0.84842	1/hr
`GU__DAPABS_k`	Absorption rate of DAP in GI tract	0.05946	1/min

The results of the parameter adjustment, including the cost reduction over the optimization steps and the goodness of fit, are shown in Fig. 11a and Fig. 11b for the parameters of the pharmacodynamic model.

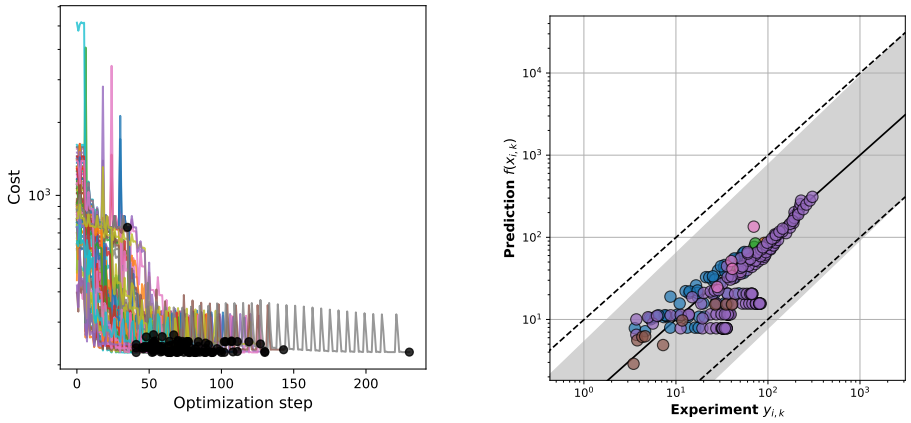

(a) Error convergence

(b) Goodness-of-fit

Figure 11: **Optimization Performance.** Overview of Error convergence (cost vs. optimization step) and Godness-of-fit (predicted vs. experimental intravenous data) for the pharmacodynamic parameters.

Table 4: **Optimized parameters for the dapagliflozin pharmacodynamic model.**

Parameter name	**Description**	**Value**	**Unit**
`KI__RTG_E50`	Half-maximal effect concentration of DAP on RTG	6.49×10^{-6}	mM
`KI__RTG_base`	Baseline renal threshold for glucose	8.00	mM
`KI__RTG_max_inhibition`	RTG maximum inhibition	0.70673	–
`KI__RTG_m_fpg`	FPG effect on RTG	1.2533	–

Parameter optimization improved the fit of the model to the data (Fig. 10a and Fig. 11a) with most optimization runs converging to similar cost, demonstrating their effectiveness in minimizing errors. The goodness of fit plots (Fig. 11b and Fig. 11b) show that the model performs well in different data sets, with many data points visually clustering closely around the identity line. Some deviations can be observed, especially in the pharmacokinetics, but overall the model is able to reproduce the data very well.

3.4 Model application

The developed PBPK/PD model of dapagliflozin was then applied to study the effect of dapagliflozin dose (Sec. 3.4.1), hepatic functional impairment (Sec. 3.4.3), renal functional impairment (Sec. 3.4.4), and the effect of food (Sec. 3.4.5) on the pharmacokinetics and pharmacodynamics of dapagliflozin.
For all four studies, the same subplots were created. To illustrate the pharmacokinetic response, eight plots were created, each showing representative simulations. These plots depict the concentrations of dapagliflozin (DAP), its metabolite dapagliflozin-3-O-glucuronide and total dapagliflozin (DAP + D3G) measured in plasma, urine and feces over time. To illustrate the pharmacodynamic response, six different diagrams were presented. The first three diagrams show the time course of the glucose concentration, the renal glucose threshold (RTG) and the urinary glucose excretion (UGE). The other three diagrams show the relationship between RTG, total glucose excretion and UGE and the plasma concentration of dapagliflozin.

3.4.1 Dose dependency

The pharmacokinetic response to different doses of dapagliflozin is shown in Fig. 12. These simulations were conducted using the most commonly administered doses of dapagliflozin identified in the literature research, ranging from 0 to 100 mg. With increasing doses, plasma concentrations of dapagliflozin, dapagliflozin-3-O-glucuronide and total dapagliflozin increase, as do amounts excreted in urine and feces. The pharmacokinetics of dapagliflozin reach their maximum faster than those of dapagliflozin-3-O-glucuronide, with plasma levels of dapagliflozin returning to baseline approximately 10 hours after administration. Dapagliflozin and dapagliflozin-3-O-glucuronide are excreted in the urine, and the unabsorbed portion of dapagliflozin is excreted in the feces.
The corresponding dose-dependency of the pharmacodynamics response is shown in Fig. 13.
At a normal fasting blood glucose level of 5 mM, the RTG without taking dapagliflozin is about 8 mM, a physiological value typical for healthy people (Tab. 4). With increasing doses of dapagliflozin, the RTG decreases due to the increased inhibition of the SGLT2 transporter. This decrease in threshold leads to greater UGE, resulting in a dose-dependent increase in UGE. This dose-dependent relationship between dapagliflozin exposure, RTG reduction, and UGE is consistent with the pharmacodynamic mechanism described by DeFronzo et al. [11], in which treatment with SGLT2 inhibitors reduces the maximum renal glucose reabsorptive capacity (T_{mG}) and increases the splay. These two effects promote glucosuria by lowering the threshold at which glucose appears in the urine. The model captures these dynamics, as illustrated by the nonlinear relationship between dapagliflozin plasma concentrations and UGE.
Simulations were then performed for all curated studies, enabling a direct comparison between the simulated results and the corresponding reference data. The dose-dependent increase of dapagliflozin and dapagliflozin-3-O-glucuronide concentrations in plasma and urine is illustrated for both single and multiple dosing (Fig. 14 and Fig. 15). In addition, the data show that the plasma and urine concentrations of both dapagliflozin and dapagliflozin-3-O-glucuronide remained similar between single and multiple dosing, with minimal accumulation of dapagliflozin after repeated administration.

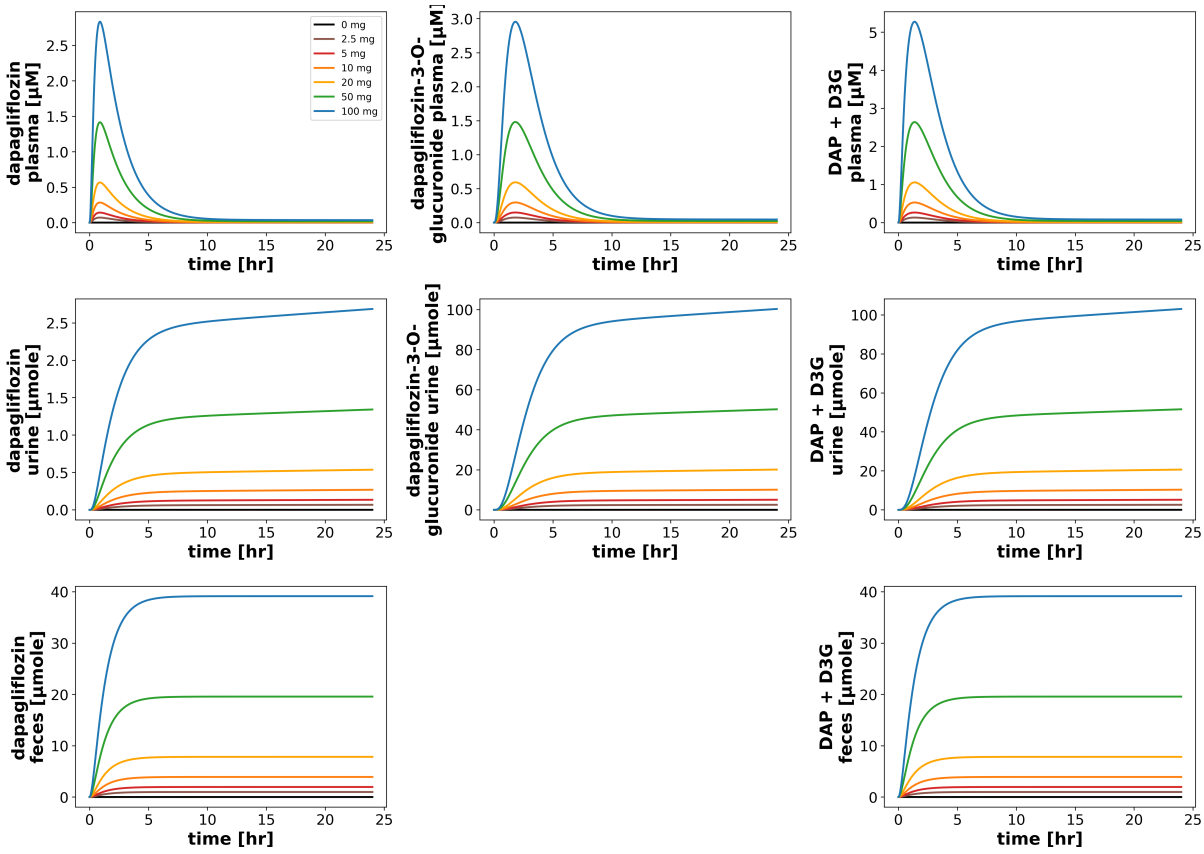

Figure 12: **Dose-dependency of dapagliflozin pharmacokinetics.** Concentrations of dapagliflozin (DAP), dapagliflozin-3-O-glucuronide (D3G) and dapagliflozin total (DAP+D3G) in plasma, urine and feces over time were simulated for dapagliflozin doses ranging from 0 to 100 mg.

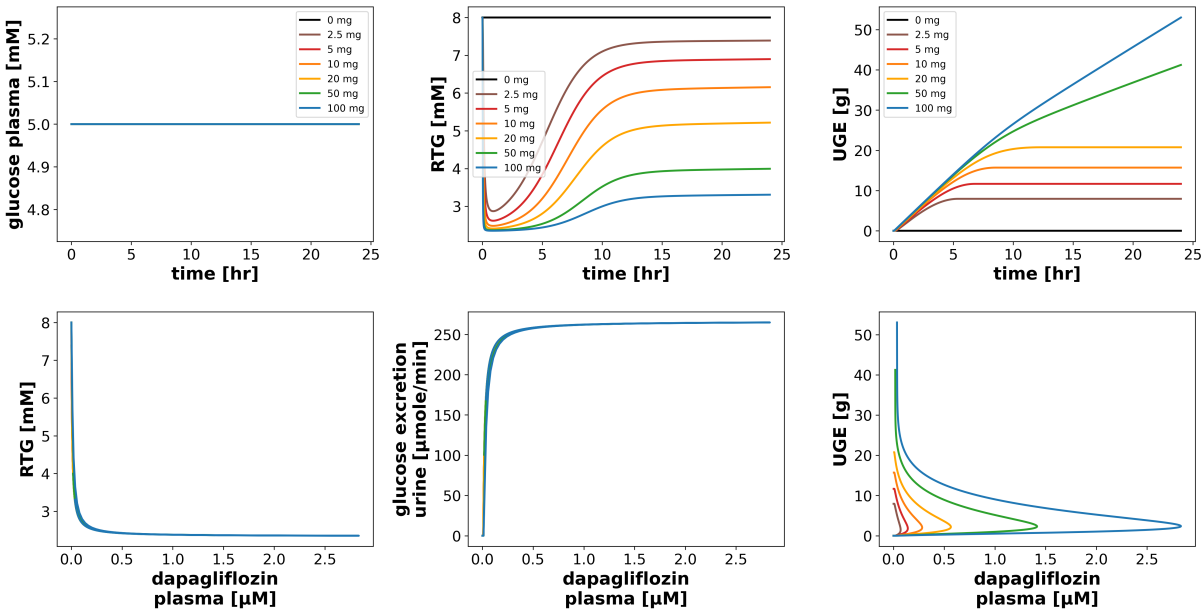

Figure 13: **Dose-dependency of dapagliflozin pharmacodynamics.** Simulated glucose plasma concentration, renal threshold for glucose (RTG), urinary glucose excretion (UGE) over time, alongside the relationship between RTG, glucose excretion in urine, and UGE with dapagliflozin plasma concentration. Simulations were conducted using dapagliflozin doses ranging from 0 to 100 mg.

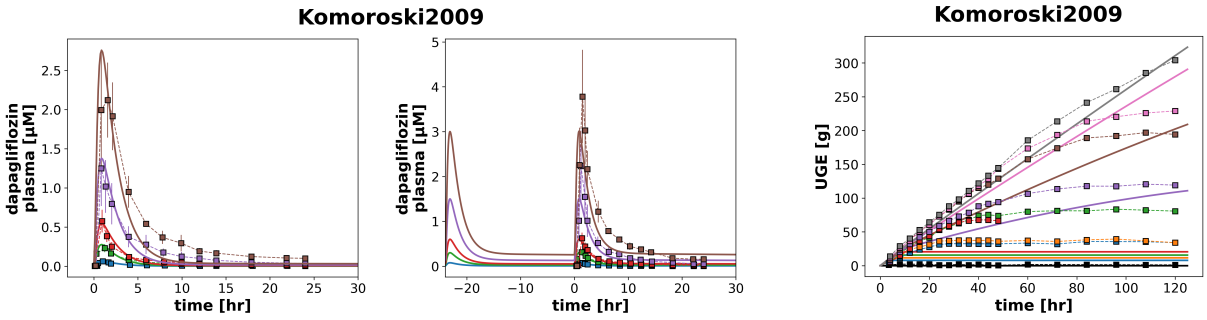

Figure 14: **Plasma concentrations of dapagliflozin and urinary glucose excretion.** Plasma concentrations of dapagliflozin after repeated daily doses of 2.5 mg, 10 mg, 20 mg, 50 mg, and 100 mg, on Day 1 and Day 14 and urinary glucose excretion following single doses of 0 mg, 2.5 mg, 5 mg, 10 mg, 20 mg, 50 mg, 100 mg, 250 mg, and 500 mg. Data from Komoroski et al. [41].

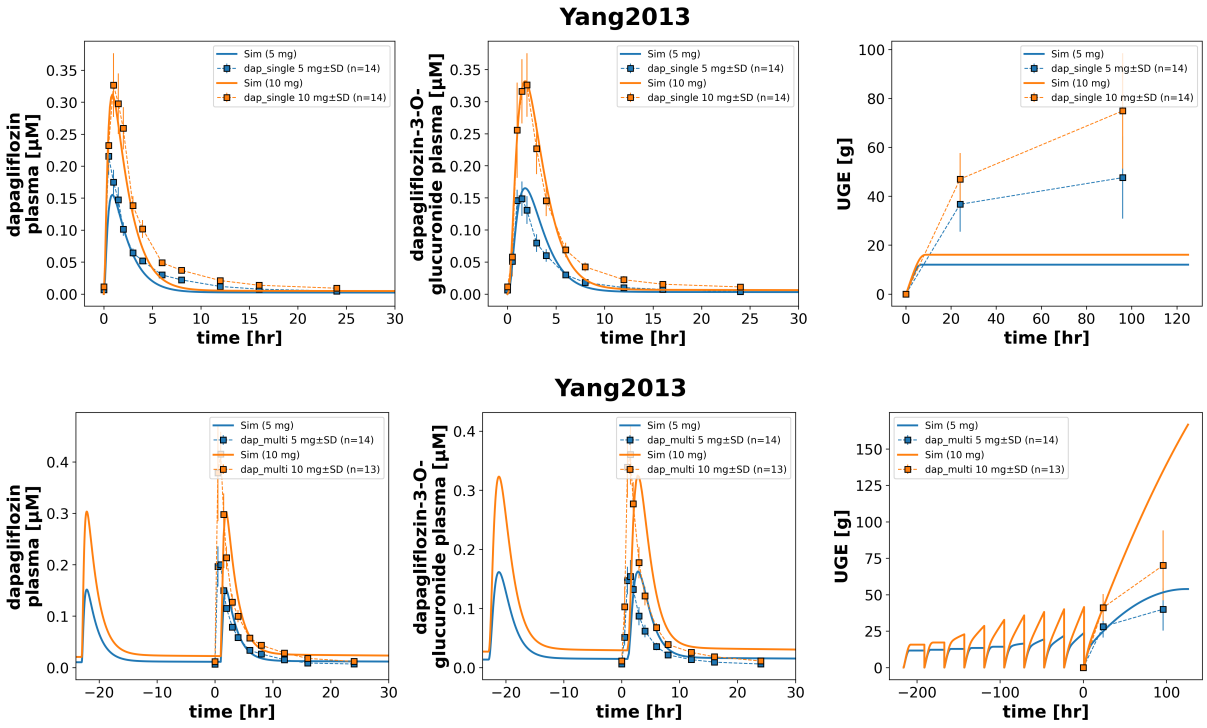

Figure 15: **Pharmacokinetics and pharmacodynamics of dapagliflozin after single and multiple dosing.** Plasma concentrations of dapagliflozin and dapagliflozin-3-O-glucuronide, along with urinary glucose excretion (UGE), after single and repeated daily doses on day 10 with 5 mg and 10 mg. Data from Yang et al. [73].

3.4.2 Glucose dependency

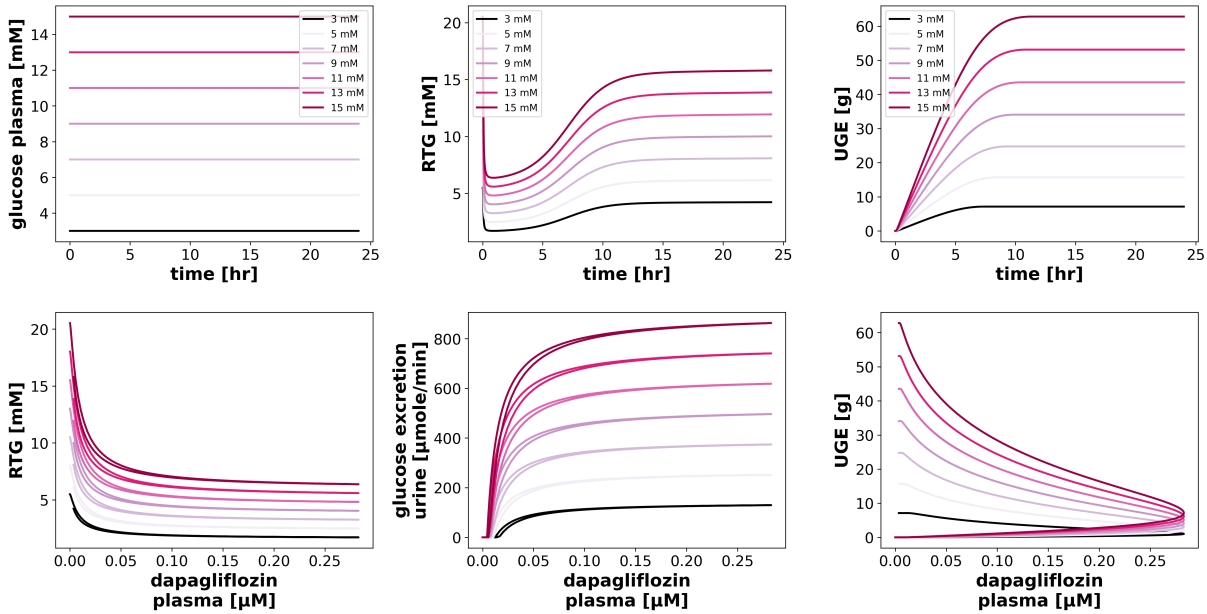

Figure 16: **Pharmacodynamic simulations of dapagliflozin under varying plasma glucose concentrations.** Glucose plasma concentration, RTG, and UGE over time, alongside the relationship between RTG, glucose excretion in urine, and UGE with dapagliflozin plasma concentration. Simulations were conducted using glucose doses ranging from 3 to 15 mM.

The simulations of glucose-dependent pharmacokinetics, with a fixed dapagliflozin dose of 10 mg, indicate that the absorption, distribution, metabolism, and excretion (ADME) of dapagliflozin are independent of blood glucose levels, which were varied between 3 and 15 mM (see Fig. 64). Pharmacodynamic responses at varying plasma glucose concentrations ranging from 3 to 15 mM in increments of 2 mM are shown in Fig. 16.

In contrast to its pharmacokinetics, the pharmacodynamic response to dapagliflozin is highly dependent on plasma glucose concentration. As glucose concentrations increase, the RTG also rises, resulting in a concentration-dependent increase in UGE. This model prediction is consistent with clinical observations, where significantly higher UGE is observed in untreated diabetes with severe hyperglycemia compared to treated diabetes.

3.4.3 Hepatic functional impairment

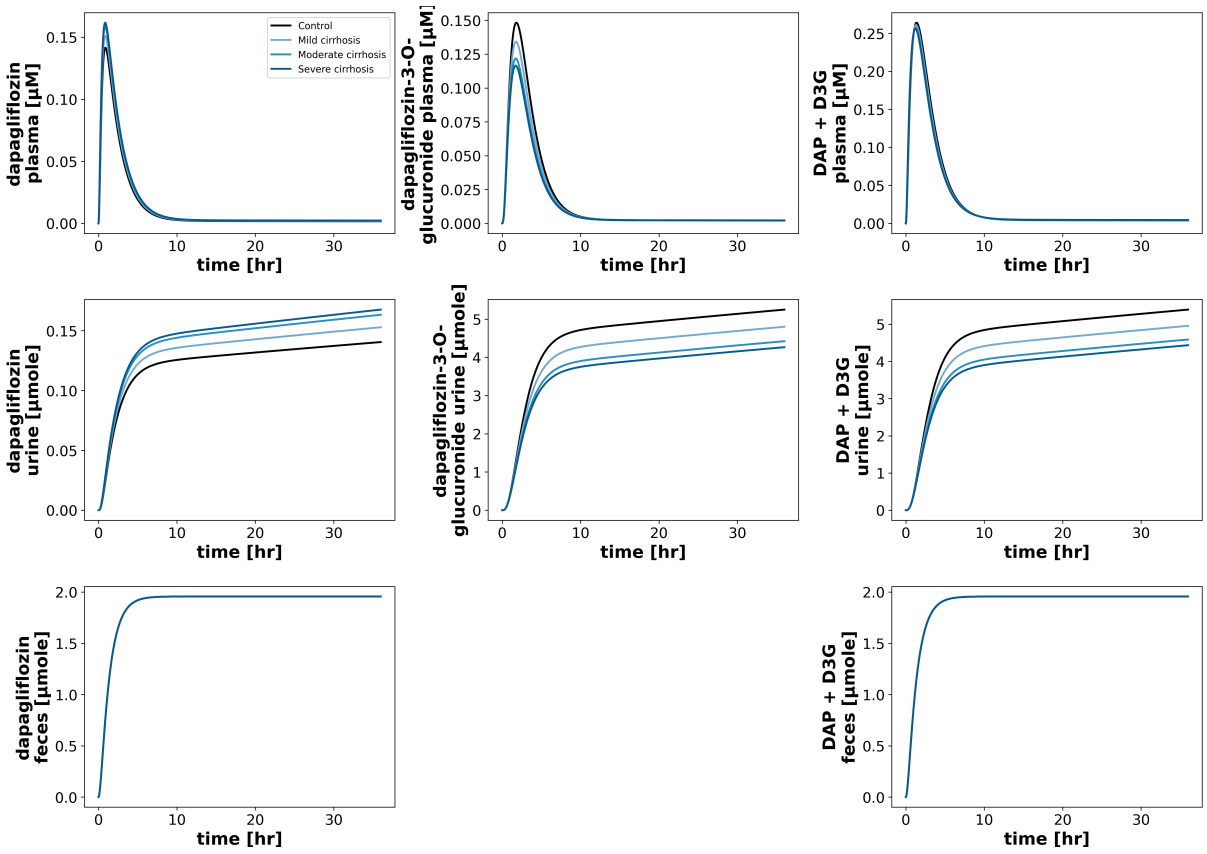

Figure 17: **Pharmacokinetic simulations of dapagliflozin in different degrees of hepatic impairment.** Concentrations of dapagliflozin, dapagliflozin-3-O-glucuronide and dapagliflozin total (DAP+D3G) in plasma, urine and feces over time. Shown for normal liver function (control), mild, moderate, and severe cirrhosis.

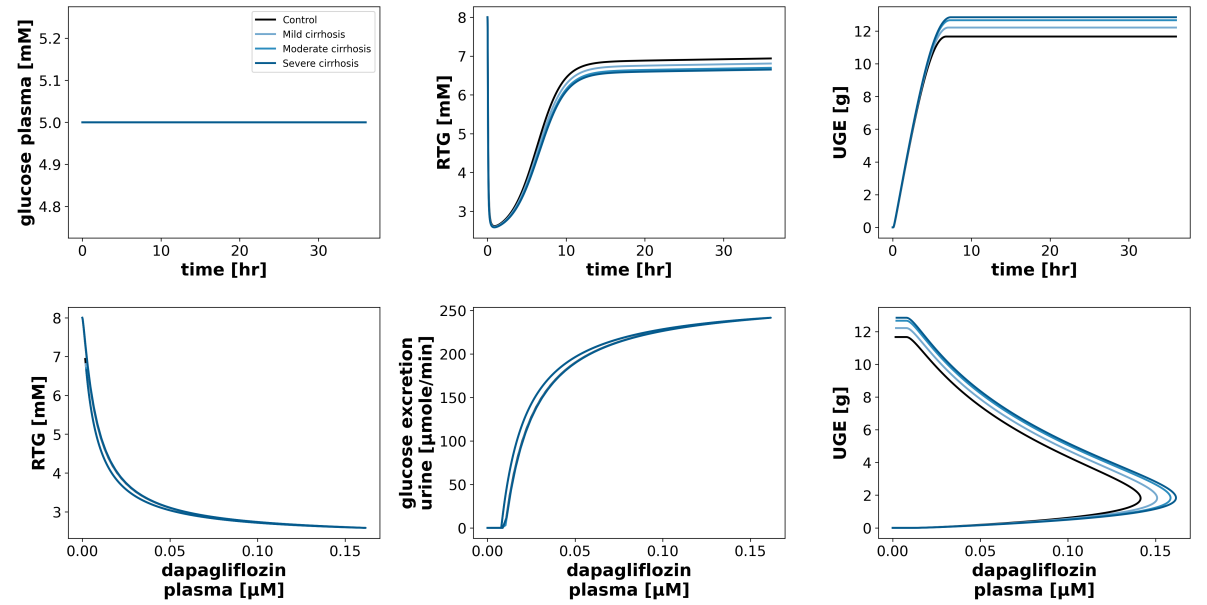

Figure 18: **Pharmacodynamic simulations of dapagliflozin in different degrees of hepatic impairment.** Time courses of glucose plasma concentration, renal threshold for glucose (RTG), and urinary glucose excretion (UGE), as well as RTG, glucose excretion in urine, and UGE versus dapagliflozin plasma concentration. Shown for subjects with normal liver function (control), mild, moderate and severe cirrhosis.

The effect of hepatic impairment on dapagliflozin pharmacokinetics and pharmacodynamics was evaluated by simulating different degrees of cirrhosis according to the Child-Turcotte-Pugh (CTP) classification: mild (Child-Pugh class A), moderate (Child-Pugh class B) and severe (Child-Pugh class C) cirrhosis, as well as a control group representing healthy individuals.
The simulations indicate that as the severity of cirrhosis increases, there is a corresponding rise in C_{max} for dapagliflozin and a decrease for dapagliflozin-3-O-glucuronide (see Fig. 17). However, the overall magnitude of this effect remains small for both compounds. A more detailed analysis of the pharmacokinetics are illustrated in Fig. 19. It shows an increase in C_{max} and AUC in advanced stages of cirrhosis for dapagliflozin and an decrease for dapagliflozin-3-O-glucuronide. Furthermore, with increasing cirrhosis severity, the elimination rate constant (kel) decreased and the half-life increased for both dapagliflozin and dapagliflozin-3-O-glucuronide. This effect was more pronounced for dapagliflozin-3-O-glucuronide. Regarding pharmacodynamic effects, only minor changes are observed overall. UGE is predicted to increase slightly with the severity of hepatic impairment (see Fig. 18). Overall, the model predicts a minor effect of hepatic impairment on dapagliflozin pharmacokinetics and pharmacodynamics.

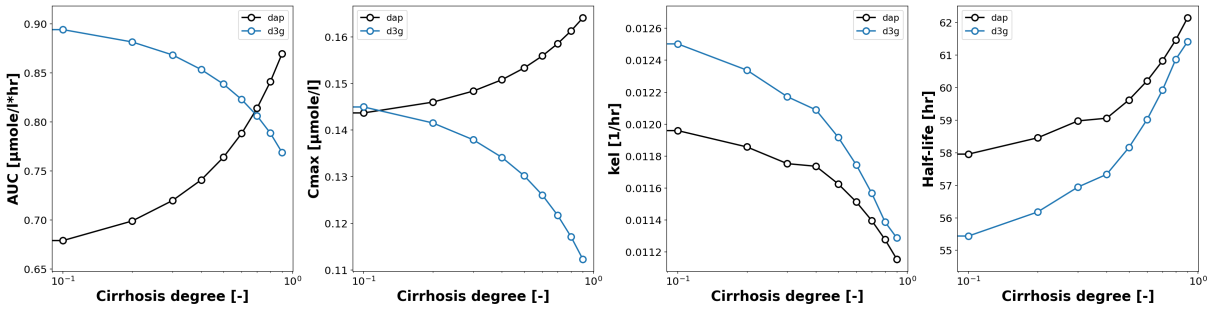

Figure 19: **Pharmacokinetic parameters of dapagliflozin and dapagliflozin-3-O-glucuronide for hepatic function assessment.** Area under the curve (AUC), maximum concentration ($C_{\max}$), elimination rate constant (k_{el}), and half-life of dapagliflozin (black) and dapagliflozin-3-O-glucuronide (blue) over cirrhosis degrees from 0.0 (healthy) to 0.9 (severe).

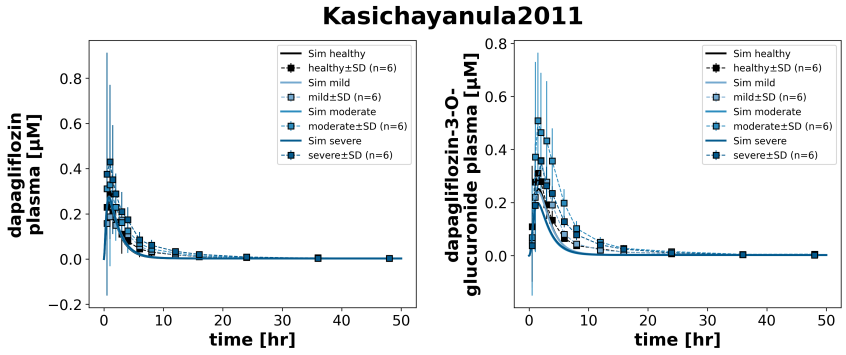

Figure 20: **Plasma concentrations of dapagliflozin and dapagliflozin-3-O-glucuronide across hepatic impairment groups.** Plasma concentrations of dapagliflozin and dapagliflozin-3-O-glucuronide shown for normal hepatic function (healthy), mild, moderate, and severe hepatic impairment. Data from Kasichayanula et al. [34].

The data from the studies confirmed that the different stages of hepatic impairment have only a minor effect on dapagliflozin in plasma, but a more pronounced effect on dapagliflozin-3-O-glucuronide (see Fig. 20). However, the simulations accurately reflect the influence of hepatic impairment only in the case of dapagliflozin. For dapagliflozin-3-O-glucuronide in plasma, the moderate stage surprisingly resulted in the highest plasma concentrations, rather than the healthy subjects, as might be expected. One possible explanation could be a compensatory metabolism by the kidneys, which, in addition to the liver, have substantial capacity to convert dapagliflozin to dapagliflozin-3-O-glucuronide [33].

3.4.4 Renal functional impairment

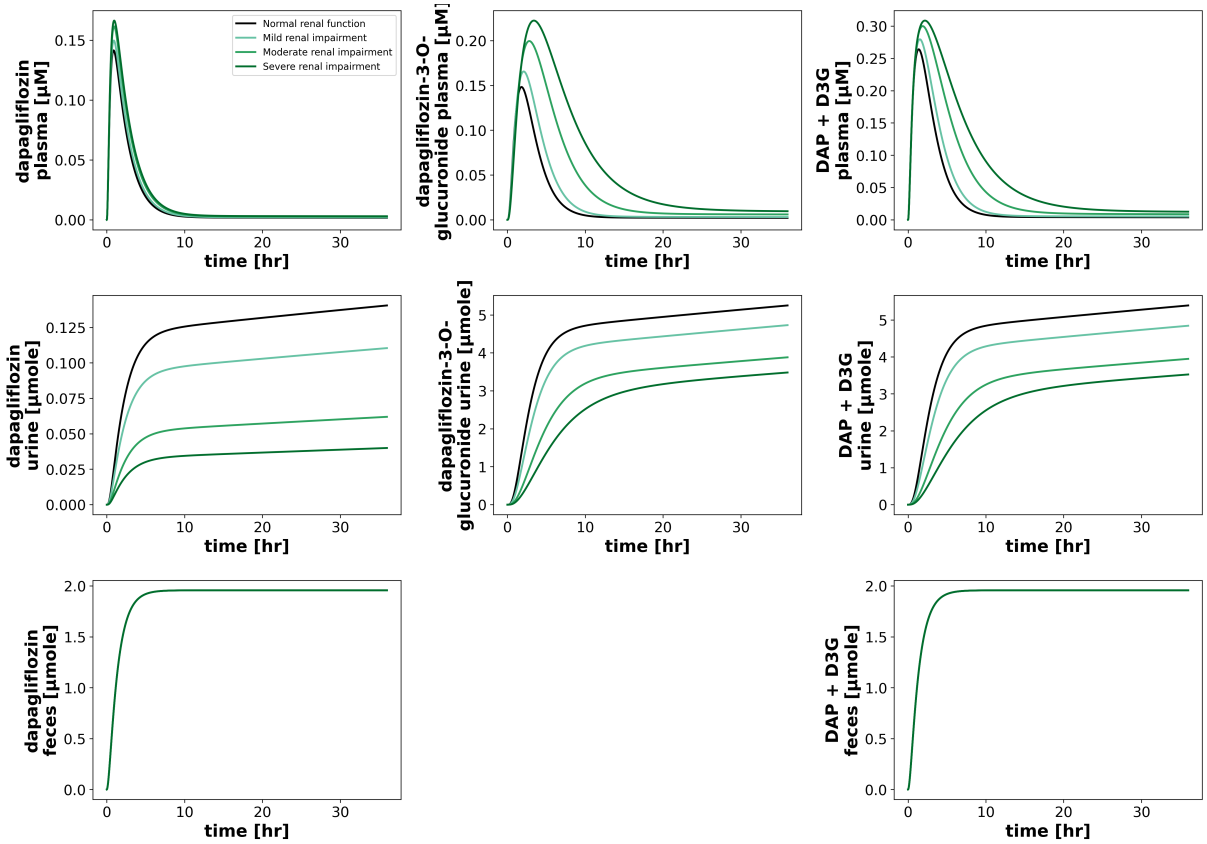

Figure 21: **Pharmacokinetics simulations of dapagliflozin in different degrees of renal impairment.** Simulated concentrations of dapagliflozin, dapagliflozin-3-O-glucuronide and dapagliflozin total (DAP+D3G) in plasma, urine and feces over time. Shown for normal renal function, mild, moderate, and severe impairment.

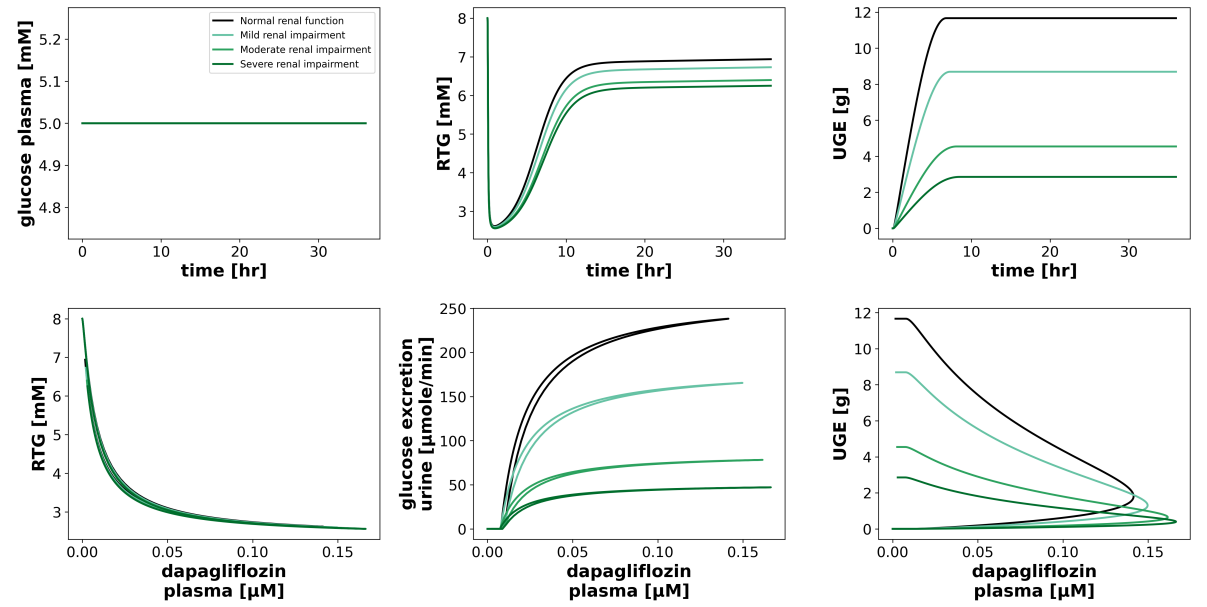

Figure 22: **Pharmacodynamic simulations of dapagliflozin in different degrees of renal impairment.** Time courses of glucose plasma concentration, renal threshold for glucose (RTG), and urinary glucose excretion (UGE), as well as RTG, glucose excretion in urine, and UGE versus dapagliflozin plasma concentration for normal renal function, mild, moderate, and severe impairment.

The model was used to investigate the effect of renal impairment on dapagliflozin. Four different degrees of renal dysfunction were simulated in each plot, representing normal, mild, moderate, and severe renal impairment.
Simulations show that plasma dapagliflozin concentrations are only slightly affected by different renal function groups, whereas dapagliflozin-3-O-glucuronide exhibits progressive increases in both C_{max} and AUC with worsening renal impairment (see Fig. 21). kel of dapagliflozin increases with improving liver function, accompanied by a decrease in half-life. In contrast, dapagliflozin-3-O-glucuronide exhibits a parabolic trend, with both parameters peaking at normal liver function. See Fig. 23. Furthermore, reduced renal function leads to decreased urinary excretion of both dapagliflozin and dapagliflozin-3-O-glucuronide, likely due to impaired glomerular filtration, while fecal excretion of dapagliflozin remains largely unchanged.
The latter effect is also reflected in the pharmacodynamics (see Fig. 22). The more severe the renal impairment, the less glucose is excreted via the urine. However, similar to liver impairment, renal dysfunction has little impact on the RTG.

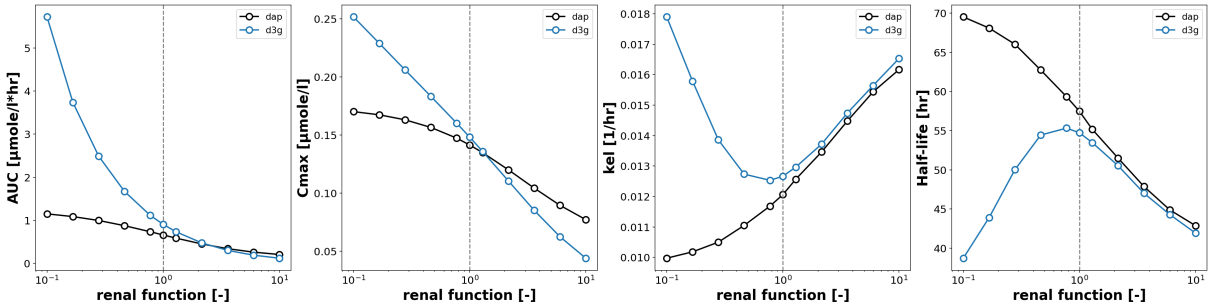

Figure 23: **Pharmacokinetic parameters of dapagliflozin and dapagliflozin-3-O-glucuronide for renal function.** Area under the curve (AUC), maximum plasma concentration (C_{max}), elimination rate constant (kel), and half-life of dapagliflozin (black) and dapagliflozin-3-O-glucuronide (blue), across renal function levels. Renal function values of 10^{-1}, 10^{0}, and 10^{1} correspond to severely impaired, normal, and highly increased renal function.

The results agree well with clinical data; see Fig. 24. With increasing kidney damage, the AUC for dapagliflozin and dapagliflozin-3-O-glucuronide in plasma increases accordingly. As with hepatic impairment, there is a clear difference between dapagliflozin and its metabolite dapagliflozin-3-O-glucuronide: While renal dysfunction has only a minor effect on the plasma and urine levels of dapagliflozin, it significantly affects the concentrations of dapagliflozin-3-O-glucuronide.

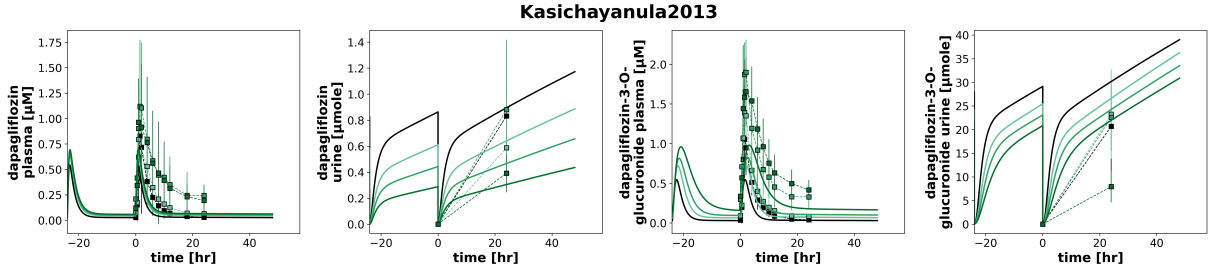

Figure 24: **Pharmacokinetics of dapagliflozin and its metabolite across renal function groups.** Plasma and urine concentration-time profiles for dapagliflozin and dapagliflozin-3-O-glucuronide across different renal impairment groups. Shown for normal renal function, mild, moderate, and severe impairment. Data from Kasichayanula et al. [33].

3.4.5 Food-drug interaction

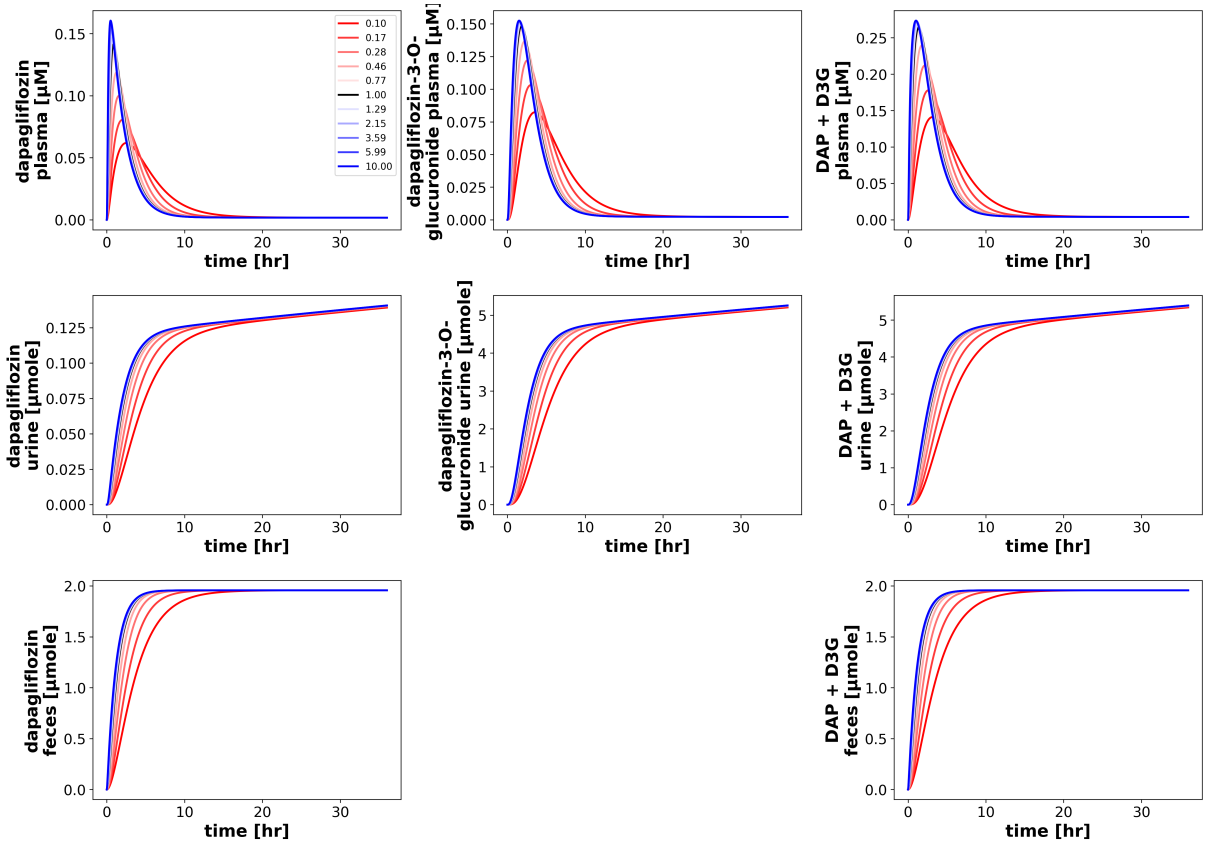

Figure 25: **Pharmacokinetic simulations of dapagliflozin under food-effect conditions.** Simulated concentrations of dapagliflozin (DAP), dapagliflozin-3-O-glucuronide (D3G) and dapagliflozin total (DAP+D3G) in plasma, urine and feces over time.

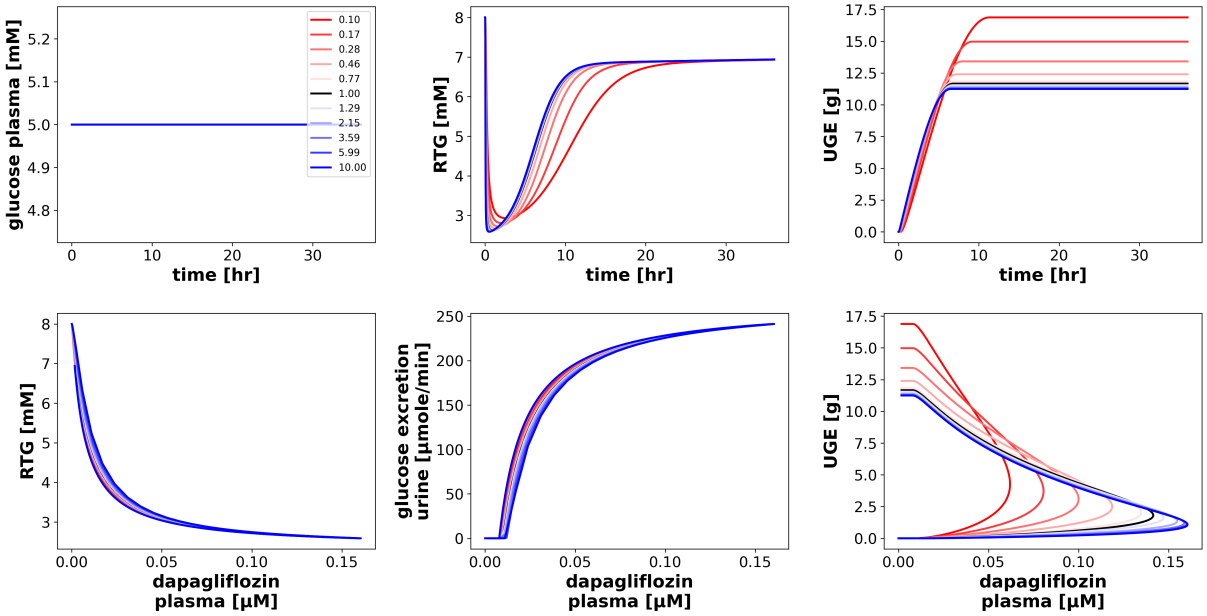

Figure 26: **Pharmacodynamic simulations of dapagliflozin under food-effect conditions.** Time course for plasma glucose, renal threshold for glucose (RTG), and urinary glucose excretion (UGE), as well as RTG, glucose excretion in urine, UGE versus dapagliflozin plasma concentration under varying absorption rates.

To investigate the influence of gastrointestinal absorption on the pharmacokinetics (see Fig. 25) and pharmacodynamics (see Fig. 26) of dapagliflozin, the focus was placed on the fractional absorption parameter. This parameter was systematically varied on a logarithmic scale from 0.1 to 10 to simulate a single 5 mg oral dose of dapagliflozin with and without food intake.
The simulations show that higher absorption rates lead to a faster and stronger increase in the plasma concentrations of dapagliflozin and dapagliflozin-3-O-glucuronide as well as to a faster and more pronounced urinary excretion of the two compounds.
From a pharmacodynamic point of view, the amount of glucose excreted in the urine is clearly dependent on the plasma concentration of dapagliflozin and thus on the absorption rate. Higher absorption leads to decreased urinary glucose excretion.
A more detailed analysis of the pharmacokinetics revealed that changes in absorption rate primarily affected the C_{max} and had minimal effect on AUC. This pattern was observed for both dapagliflozin and dapagliflozin-3-O-glucuronide, but the effect on dapagliflozin is stronger. In addition, variations in absorption also affected kel and half-life. This was significantly greater for dapagliflozin than for dapagliflozin-3-O-glucuronide, indicating a stronger interplay between absorption kinetics and elimination dynamics for the parent compound (see Fig. 27).

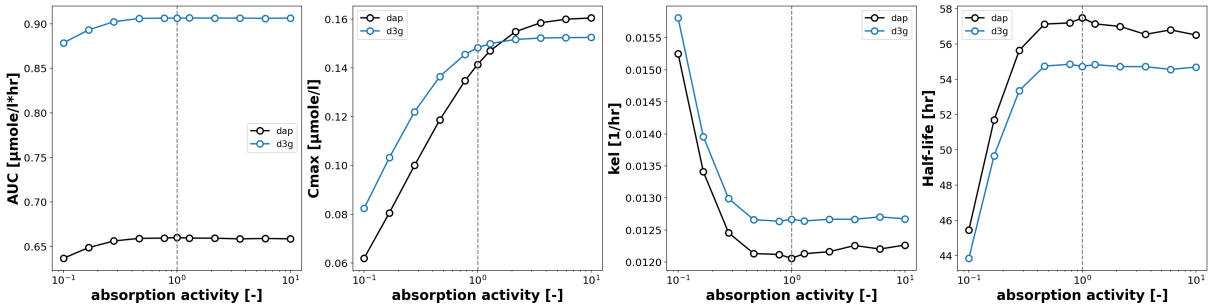

Figure 27: **Pharmacokinetic parameters of dapagliflozin and dapagliflozin-3-O-glucuronide for absorption activity scan.** AUC, C_{max}, kel and half-life for absorption activity of dapagliflozin (black) and dapagliflozin-3-O-glucuronide (blue).

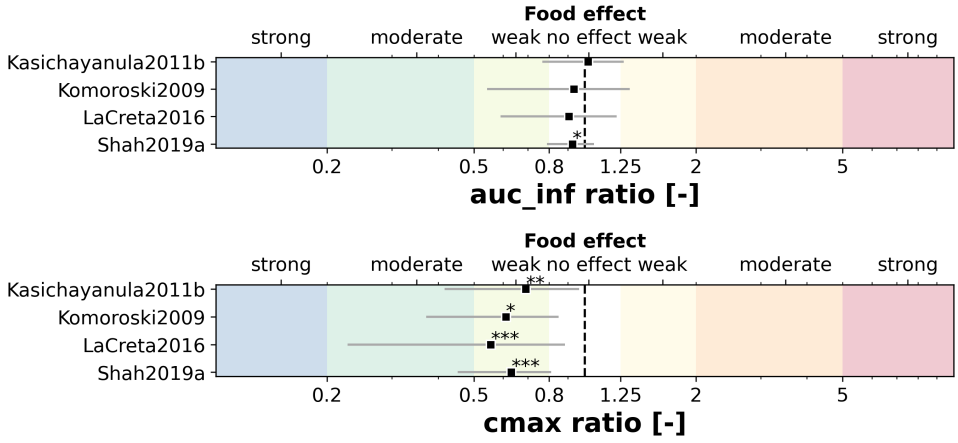

Figure 28: **Impact of food on pharmacokinetic parameters of dapagliflozin.** Shown are changes AUC_∞ and C_{max} comparing fed and fasted conditions. Significance levels are indicated by p-values: α: $p \leq 0.05$ (*), $p \leq 0.01$ (**), $p \leq 0.001$ (***). Data from Kasichayanula et al. [31], Komoroski et al. [41], LaCreta et al. [48], Shah et al. [62].

Table 5: Effect of food intake on AUC_{inf} and C_{max} of dapagliflozin. Data from Kasichayanula et al. [31], LaCreta et al. [48], Shah et al. [62].

study	intervention	dose [mg]	mean_fasted	sd_fasted	n_fasted	mean_fed	sd_fed	n_fed	ratio	ratio_sd	effect	p-value	sig	t-statistic	df	method
Kasichayanula2011b	DAP10	10 mg	497	94	14	507	81	14	1.02	0.25	no effect	0.77		-0.30	26	t-test two-sided
Komoroski2009	DAP250	250 mg	13337	3734	5	12455	3861	5	0.93	0.39	no effect	0.72		0.37	8	t-test two-sided
LaCreta2016	DAP2.5	2.5 mg	170	44	28	154	35.42	27	0.91	0.31	no effect	0.15		1.48	53	t-test two-sided
Shah2019a	DAP5, MET500	5 mg	291	29.6	24	269	28	24	0.92	0.14	no effect	0.01	*	2.63	46	t-test two-sided

(a) Effect of food on $\mathrm{AUC_{inf}}$.

study	intervention	dose [mg]	mean_fasted	sd_fasted	n_fasted	mean_fed	sd_fed	n_fed	ratio	ratio_sd	effect	p-value	sig	t-statistic	df	method
Kasichayanula2011b	DAP10	10 mg	136	29.92	14	940	31	14	0.69	0.27	weak inhibition	0.001	**	3.65	26	t-test two-sided
Komoroski2009	DAP250	250 mg	2510	778	5	1532	368	5	0.61	0.24	weak inhibition	0.03	*	2.54	8	t-test two-sided
LaCreta2016	DAP2.5	2.5 mg	45	11.7	28	25	13.25	27	0.56	0.33	weak inhibition	0	***	5.94	53	t-test two-sided
Shah2019a	DAP5, MET500	5 mg	74.6	13.4	24	47.1	10.4	24	0.63	0.18	weak inhibition	0	***	7.94	46	t-test two-sided

(b) Effect of food on C_{max}.

Clinical studies comparing fasted and fed states consistently showed that food intake delayed the time to maximum plasma concentration (t_{max}) by approximately one hour and C_{max} 30–50%, the AUC remained unaffected for dapagliflozin and dapagliflozin-3-O-glucuronide (see Fig. 29). For urinary data under fed conditions, only a single dataset was available, but the simulation results were consistent with the observed finding that more dapagliflozin is excreted in urine when administered with food.

To further assess the impact of food intake on total systemic exposure to dapagliflozin, the AUC_{inf} ratios between the fasted and fed states in the clinical trials were analysed (see Tab. 5). In all cases, the geometric mean AUC_{inf} ratios ranged between 0.91 and 1.02, even across a wide range of doses (2.5 to 250 mg) and in combination with metformin. These values fall within the standard no-effect range of 0.80–1.25 (Tab. 1), suggesting that food intake does not significantly alter total systemic exposure.

In contrast to AUC_{inf}, the C_{max} showed more pronounced differences between the fed and fasted states. Across the studies, the geometric mean ratios of C_{max_fed} to C_{max_fasted} ranged from approximately 0.49 to 0.70, indicating a 30–50% reduction in peak concentration when dapagliflozin was taken with food. This demonstrates that C_{max} is more sensitive to food intake (see Fig. 28). Although the effect is weak, it should not be ignored due to its potential implications for pharmacodynamic outcomes.

This reduction is consistent with a delayed and flattened absorption profile in the fed state. Despite these reductions, AUC remained unchanged, suggesting that the food effect primarily alters the rate, not the extent, of absorption.

Summary

In summary, in this work a comprehensive database of dapagliflozin pharmacokinetics and pharmacodynamics, which was used to establish a PBPK/PD model of dapagliflozin. The model successfully simulated the effect of dosage, glucose, hepatic functional impairment, renal functional impairment, and food intake, aligning well with clinical data from 27 studies: Fig. 30 [4], Fig. 31 [8], Fig. 32 [13], Fig. 33 [13], Fig. 34 [13], Fig. 35 [14], Fig. 36 [14], Fig. 37 [14], Fig. 38 [15], Fig. 39 [16], Fig. 40 [16], Fig. 41 [23], Fig. 42 [24], Fig. 43 [25], Fig. 20 [34], Fig. 44 [28], Fig. 45 [28], Fig. 46 [28], Fig. 28 [31], Fig. 48 [30], Fig. 49 [30], Fig. 50 [30], Fig. 51 [32], Fig. 24 [33], Fig. 52 [33], Fig. 53 [29], Fig. 54 [36], Fig. 55 [37], Fig. 56 [38], Fig. 14 [41], Fig. 14 [41], Fig. 57 [41], Fig. 28 [41], Fig. 28 [48], Fig. 58 [56], Fig. 59 [61], Fig. 60 [61], Fig. 61 [61], Fig. 28 [62], Fig. 62 [68], Fig. 63 [69], Fig. 15 [73].

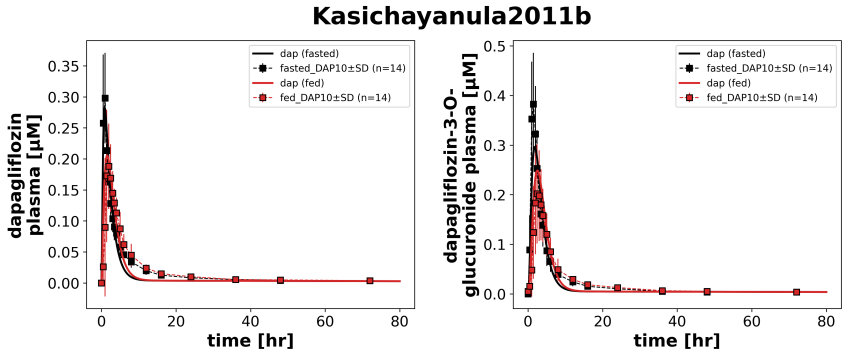

(a) Plasma concentrations of 10 mg dapagliflozin and dapagliflozin-3-O-glucuronide. Data from Kasichayanula et al. [31].

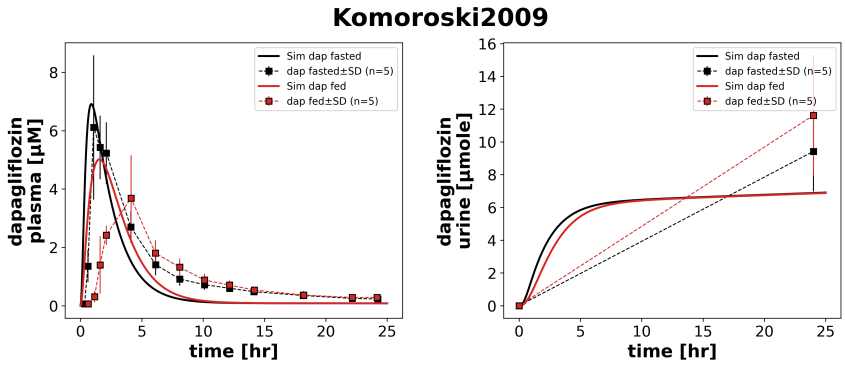

(b) Plasma and urinary concentrations of high-dose dapagliflozin (250 mg). Data from Komoroski et al. [41].

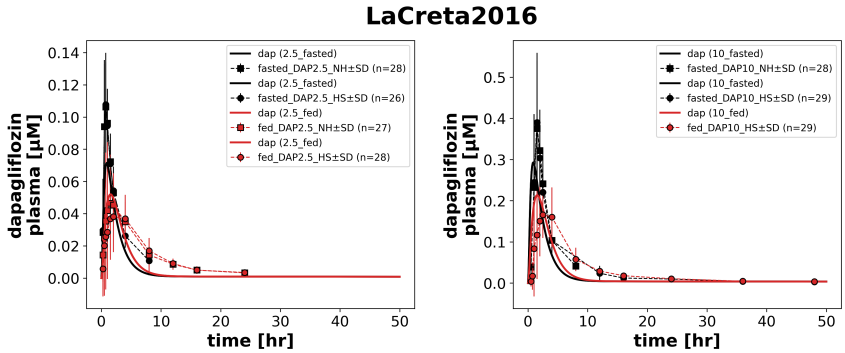

(c) Plasma concentrations of dapagliflozin (2.5 mg and 10 mg). HS = Heat-stressed; NH = non-heat-stressed. Data from LaCreta et al. [48].

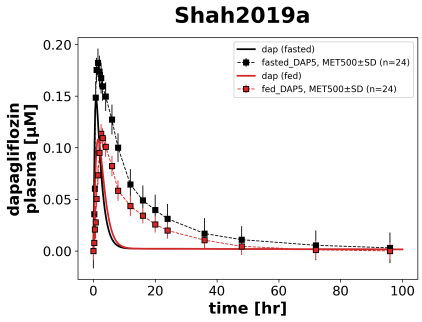

(d) Plasma concentrations of 5 mg dapagliflozin + 500 mg metformin. Data from Shah et al. [62].

Figure 29: **Pharmacokinetics of dapagliflozin under fasted and fed conditions.** Plasma concentrations of dapagliflozin and dapagliflozin-3-O-glucuronide, and urinary concentrations of dapagliflozin after single oral doses under different prandial states (fasted: black and fed: red).

4 Discussion

4.1 Data

As part of this work, a comprehensive quantitative dataset of dapagliflozin was created and used to develop a PBPK/PB model of dapagliflozin. The literature search identified 27 clinical studies that met the inclusion criteria for model development.
The quality and completeness of the data found varied from study to study. Quantitative information on excretion routes was particularly limited. Data on renal threshold for glucose (RTG), and fecal excretion were each reported only once: RTG in Sha et al. [61], and fecal excretion in FDA [15]. But data collections on kidney (Kasichayanula et al. [33], FDA [16]) and especially liver diseases (Kasichayanula et al. [34]) were also very limited.
It should be noted that weight loss, a known side effect of dapagliflozin treatment that was also observed in the studies used, may itself contribute to the improvement of metabolic function Kaku et al. [27]. These positive effects occur independently of the direct pharmacological action of the drug and may enhance its overall therapeutic effect.
Furthermore, only the known enzymes and their conversion processes could be included. Despite these limitations, the curated data set provided an adequate basis for the development of a PBPK/PD model that can characterize the pharmacokinetics and pharmacodynamics of dapagliflozin under different physiological and pathological conditions.
Although the model is based on a careful and detailed implementation of available data and mechanistic understanding, its predictions should be interpreted with caution, especially in scenarios where limited validation data are available.
Future studies addressing knowledge gaps would allow further refinement of model parameters and structure.

4.2 Model

The PBPK/PD model for dapagliflozin integrates distinct organ submodels into a comprehensive framework capable of simulating both pharmacokinetic and pharmacodynamic processes across diverse physiological conditions. By incorporating detailed representations of intestinal absorption, hepatic metabolism, and renal excretion, the model enables evaluation of dapagliflozin's pharmacokinetics and pharmacodynamics under various scenarios.
Moreover, the model's ability to simulate and directly compare pharmacokinetic and pharmacodynamic changes under renal and hepatic impairment offers a distinct advantage over traditional clinical trial data, where such comparative analyses are rarely feasible.
Parameter optimization demonstrated successful convergence for the majority of parameters, supporting the robustness and reliability of the model. Key parameters related to absorption, metabolism, and elimination were consistent with values reported in the literature on dapagliflozin pharmacokinetics and pharmacodynamics. Despite certain limitations, the model offers a physiologically sound and clinically relevant representation of dapagliflozin behavior across various patient populations and physiological conditions.

4.3 Physiological variability and functional impairments

Dose dependency
The pharmacokinetic and pharmacodynamic simulations over a dose range of 0 to 100 mg provided valuable insights into the dose-dependent behavior of dapagliflozin. As shown in Fig. 12, increasing doses led to a proportional increase in plasma concentrations of dapagliflozin and its metabolite dapagliflozin-3-O-glucuronide as well as their excretion in urine and feces. As expected, dapagliflozin reached its peak concentration faster than dapagliflozin-3-O-glucuronide and its plasma levels returned to baseline within approximately 10 hours, while dapagliflozin-3-O-glucuronide persisted longer. The pharmacodynamic response (Fig. 13) reflected these

trends: increasing the dose of dapagliflozin significantly lowered the RTG and increased UGE in a dose-dependent manner. These results emphasize the direct relationship between the dose of dapagliflozin, SGLT2 inhibition and the therapeutic effect on glucose excretion.
However, it should be noted that only a few data sets were available to evaluate the excretion in feces.

Glucose dependency
The glucose-dependent simulations performed with a fixed dose of 10 mg dapagliflozin showed that the pharmacokinetics of the drug are independent of the plasma glucose concentration in the range of 3 to 15 mM. In contrast, the pharmacodynamic response exhibited a marked dependence on glucose concentration, as shown in Fig. 16. UGE increased significantly with rising plasma glucose concentrations. This suggests that an important factor for UGE is the extent to which plasma glucose exceeds RTG. This aligns with reports of markedly higher UGE in diabetic patients, particularly when untreated. The pharmacodynamic effect of dapagliflozin across glucose levels emphasizes the central role of plasma glucose in regulating glucosuria once RTG is exceeded.

Hepatic Impairment
Model results suggest that liver impairment has only a minor impact on the pharmacokinetics of dapagliflozin. Simulations across varying degrees of cirrhosis, classified according to the Child-Turcotte-Pugh (CTP) system, indicated a slight increase in the maximum plasma concentration (C_{max}) and area under the curve (AUC) of dapagliflozin, along with a decrease in the plasma concentration of dapagliflozin-3-O-glucuronide, in more advanced stages of cirrhosis.
These findings indicate that liver dysfunction has a limited impact on systemic drug exposure, consistent with the fact that liver metabolism, primarily through Uridine 5'-diphosphoglucuronosyltransferase 1A9 (UGT1A9) mediated glucuronidation, is not the dominant clearance route for dapagliflozin, but the kidneys are also involved in conversion.
The pharmacodynamic effects of liver dysfunction were also low. Simulations showed that the efficacy of dapagliflozin, as measured by UGE, was largely preserved across all stages of liver dysfunction. A modest increase in UGE relative to dapagliflozin plasma concentrations was observed in hepatic impairment.
These findings support the hypothesis that hepatic impairment leads to altered metabolism of dapagliflozin and its metabolite. However, the overall impact on systemic exposure and pharmacodynamic effect appears to be moderate likely due compensatory mechanisms.

Renal Impairment
In contrast, renal impairment had a pronounced effect on the pharmacokinetics and pharmacodynamics of dapagliflozin. The simulations showed that while plasma concentrations of dapagliflozin itself remained relatively stable across varying levels of renal function, dapagliflozin-3-O-glucuronide exposure increased markedly in both C_{max} and AUC as renal impairment progressed. Consequently, urinary excretion patterns showed that intact renal function leads to higher urinary concentrations of dapagliflozin and dapagliflozin-3-O-glucuronide, highlighting the critical role of the kidneys in elimination.
This is consistent with the primary renal elimination of dapagliflozin-3-O-glucuronide and underscores the important role of renal clearance in its disposition, as changes in the elimination rate constant and half-life were also more pronounced for dapagliflozin-3-O-glucuronide.
From a pharmacodynamic perspective, renal dysfunction substantially reduced UGE. Despite only minor changes in plasma dapagliflozin concentrations, simulations showed a clear decline in total urinary glucose excretion with worsening renal function. This is due to reduced glomerular filtration directly affecting glucose handling, leading to a diminished therapeutic effect of dapagliflozin. This finding is clinically relevant, particularly for diabetic patients with renal impairment.

These results clearly support the hypothesis that renal impairment significantly affects the excretion of dapagliflozin and its glucuronide metabolite. The marked reduction in UGE underlines the critical role of renal clearance in both the pharmacokinetics and therapeutic efficacy of dapagliflozin.

In conclusion, the model allows a direct comparison of UGE in renal and hepatic dysfunction - an aspect that has not been adequately addressed in previous studies. The results indicate that both types of impairment reduce the clearance of dapagliflozin to its metabolite dapagliflozin-3-O-glucuronide. However, UGE is significantly diminished in renal dysfunction, while hepatic impairment has only a minor impact. This comparative analysis underlines the added value of the PBPK/PD model in the investigation of clinically relevant effects that have received little attention in the literature to date.

4.4 Food-drug interaction

The investigation of the influence of gastrointestinal absorption on the pharmacokinetics and pharmacodynamics of dapagliflozin provides deeper insights into the food effect. In contrast to previous studies that concluded the effect of food on dapagliflozin is not clinically significant, the findings suggest a different interpretation.
By systematically varying the fractional absorption parameter, we observed that faster absorption results in higher and earlier peak plasma concentrations of dapagliflozin and dapagliflozin-3-O-glucuronide, as well as increased and earlier urinary excretion of both substances. While earlier studies acknowledged a reduction in $C_{\max}$, under fed conditions, they dismissed its relevance due to the unchanged AUC [31], [62]. However, the results demonstrate that this reduction in $C_{\max}$ has pharmacodynamic implications, as the food-induced alteration in absorption rate significantly influences UGE.
Although it should be noted that limited datasets were available to evaluate pharmacodynamics under fasting conditions, the results overall suggest that the effect of food on dapagliflozin, although traditionally considered clinically insignificant due to unchanged AUC, may indeed influence therapeutic outcomes via altered pharmacodynamics. The PBPK/PD model thus reveals a potentially underappreciated aspect of food-drug interactions that warrants further clinical investigation.
These results are consistent with the hypothesis that the administration of dapagliflozin in a fed state slows absorption and consequently affects both pharmacokinetics and pharmacodynamics. Although the total systemic exposure (AUC) remains largely unchanged, the delayed and reduced peak concentrations observed under fed conditions have notable implications for the drug's pharmacodynamic effect, particularly in urinary glucose excretion.

5 Outlook

Future research should build upon the insights gained from this study and address several limitations identified during the development of the PBPK/PD model.
Particular attention should be given to urinary glucose excretion (UGE), as it directly reflects the pharmacodynamic effect of the drug. Current conclusions on UGE in the fed state and under hepatic impairment rely on a single study, and data on renal impairment are similarly limited. In addition to standardized 24-hour UGE measurements, future studies should assess glucose excretion over extended periods. This is essential to determine whether delayed or prolonged drug absorption (e.g., under fasting conditions) or altered renal function result in temporal shifts in pharmacodynamic activity [10]. Such data would help clarify whether a reduced maximum plasma concentration (C_{max}) leads to diminished total UGE or whether delayed excretion compensates over time. Understanding these dynamics is critical for characterizing the time course and persistence of therapeutic effects, thereby supporting optimized long-term treatment strategies.
Future research should also investigate the nonlinear behavior of plasma dapagliflozin-3-O-glucuronide concentrations observed in varying stages of hepatic impairment. The unexpected peak levels in moderate liver dysfunction suggest a complex interaction between preserved Uridine 5'-diphospho-glucuronosyltransferase 1A9 (UGT1A9)-mediated metabolism and impaired hepatic clearance. This mechanism could not be fully elucidated in the current model. Clinical studies quantifying UGT1A9 activity and measuring in vivo glucuronidation and clearance across the spectrum of liver disease are needed to validate this hypothesis.
To further enhance the model's physiological accuracy, better characterization of fecal excretion pathways is necessary. Only a single data set informed this elimination route, highlighting the need for targeted experimental studies to improve its representation.
In addition, incorporating drug–drug interaction (DDI) data into future PBPK/PD models will be essential to enable individualized dosing strategies and optimize therapeutic outcomes.
Looking beyond its primary glucose-lowering effect, the broader clinical benefits of dapagliflozin warrant further investigation. In addition to improving glycemic control, dapagliflozin has been associated with a reduced risk of hypoglycemia, modest weight loss, and improved cardiovascular outcomes, as reported by Scheen et al. (2014) [60]. These benefits raise the possibility of additional therapeutic value, including the management of comorbid conditions such as non-alcoholic fatty liver disease (NAFLD), where weight loss alone can significantly improve clinical outcomes [59, 63]. This is particularly relevant given the high incidence of comorbidities such as chronic kidney disease (CKD) and metabolic dysfunction-associated fatty liver disease (MAFLD) in individuals with type 2 diabetes mellitus (T2DM), as reported by Kasichayanula et al. (2011) [34]. Taken together, these multifaceted effects suggest that dapagliflozin may provide substantial benefit in these high-risk populations, offering therapeutic advantages that go well beyond glycemic control alone.

6 Supplement

Additional simulated studies

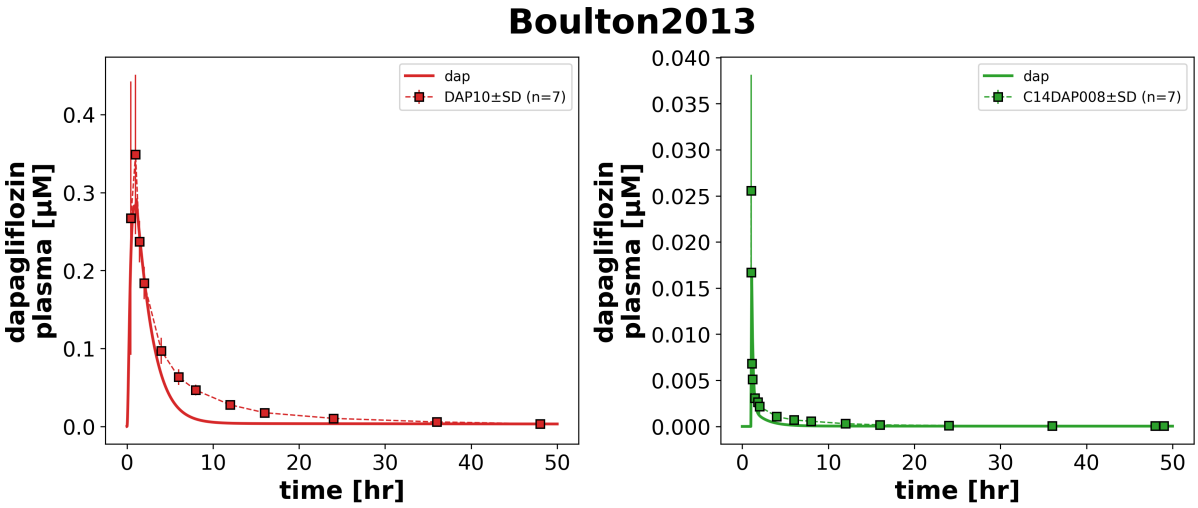

Figure 30: **Simulation of Boulton et al. [4].**

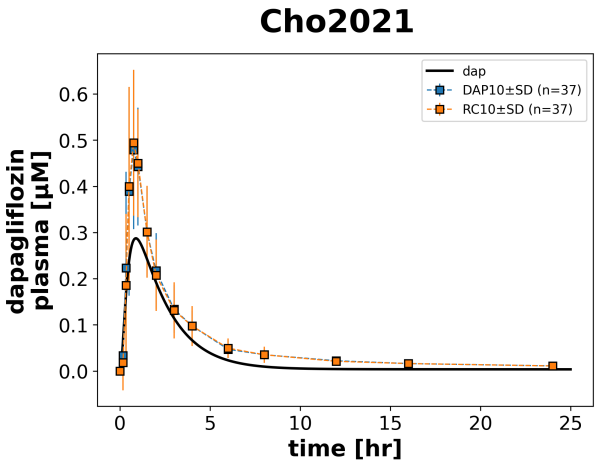

Figure 31: **Simulation of Cho et al. [8].**

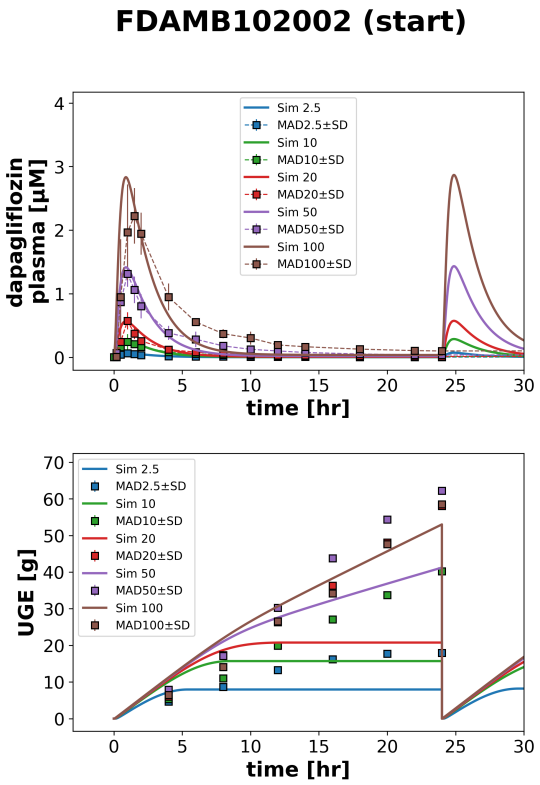

Figure 32: **Simulation of FDA [13].**

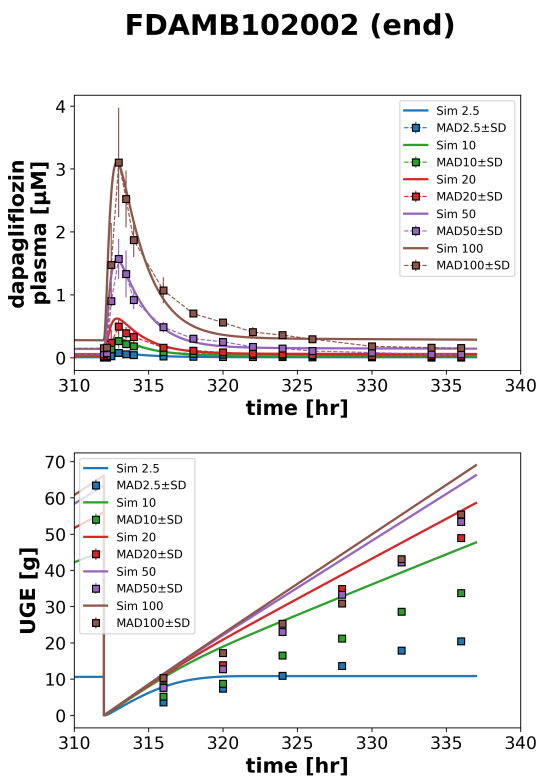

Figure 33: **Simulation of FDA [13].**

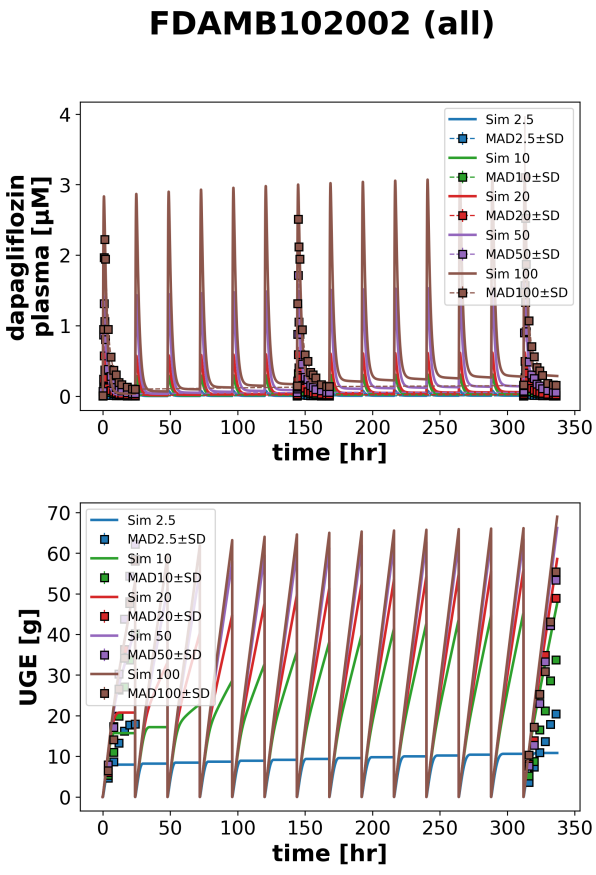

Figure 34: **Simulation of Cho et al. [8].**

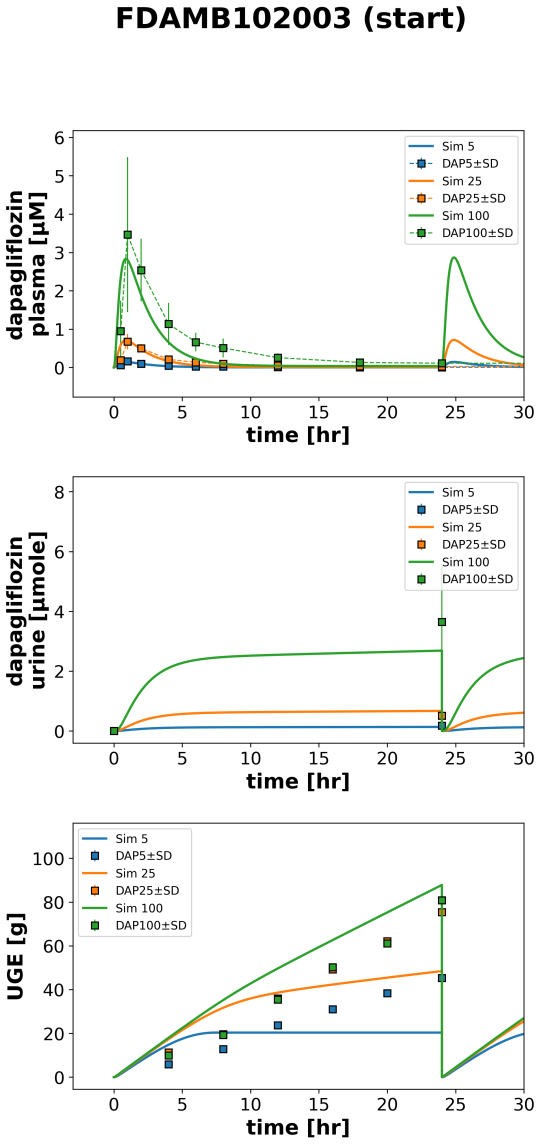

Figure 35: **Simulation of FDA [14].**

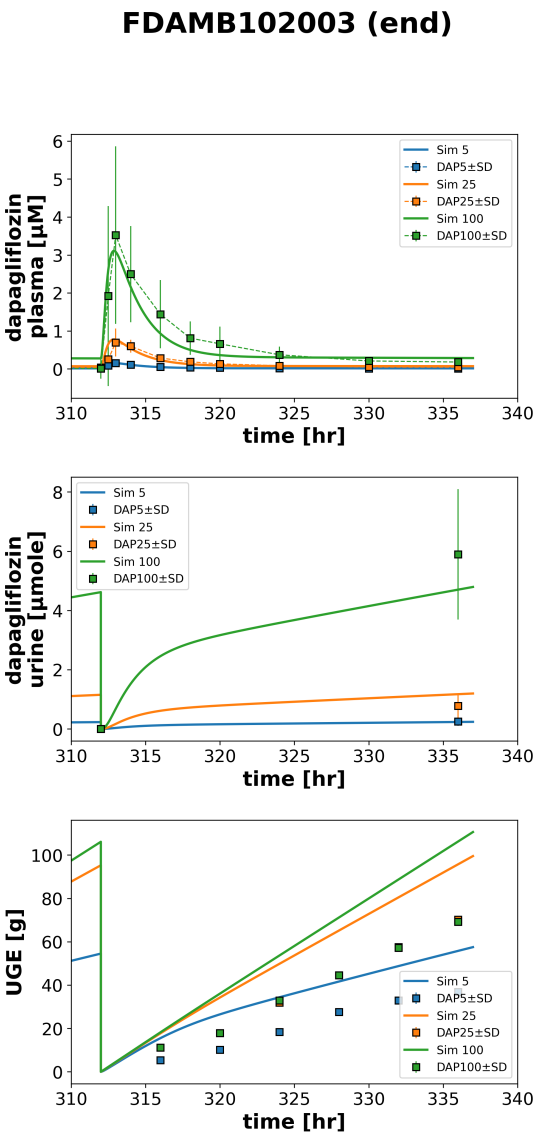

Figure 36: **Simulation of FDA [14].**

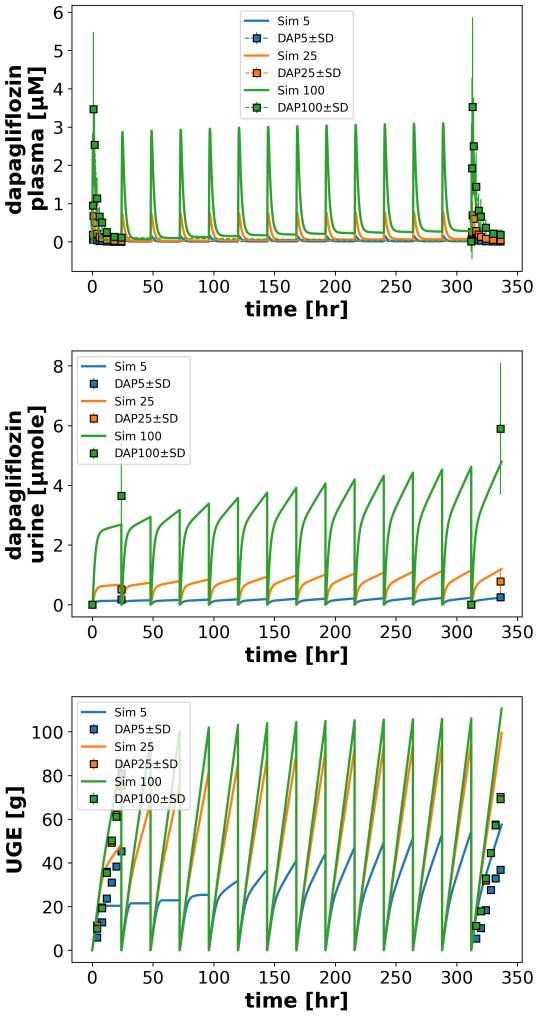

Figure 37: **Simulation of FDA [14].**

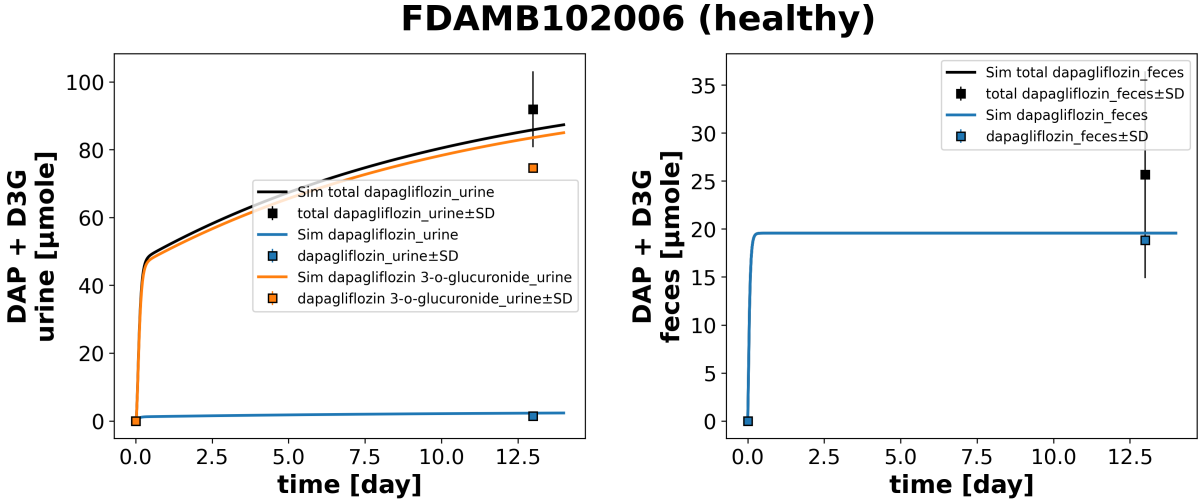

Figure 38: **Simulation of FDA [15].**

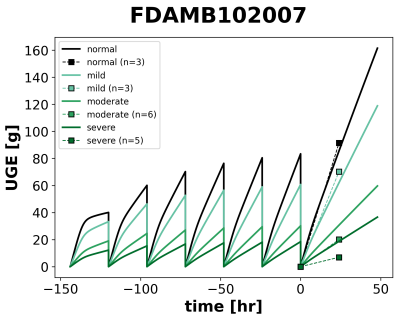

Figure 39: **Simulation of FDA [16].**

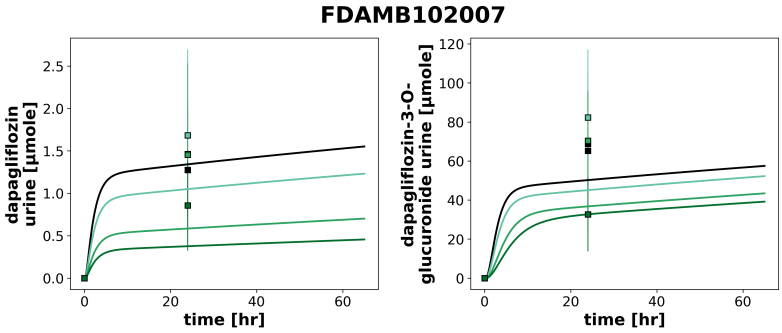

Figure 40: **Simulation of FDA [16].**

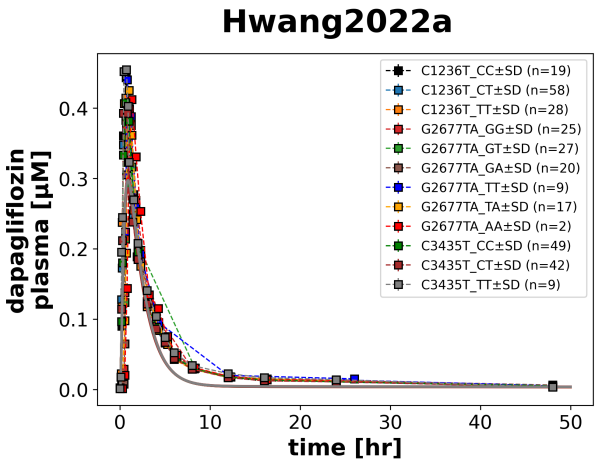

Figure 41: **Simulation of Hwang et al. [23].**

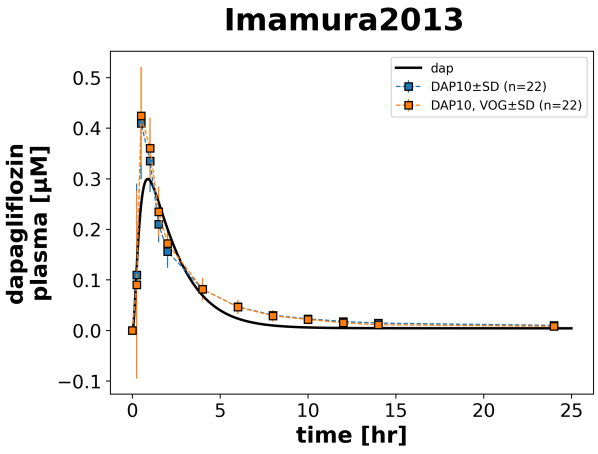

Figure 42: **Simulation of Imamura et al. [24].**

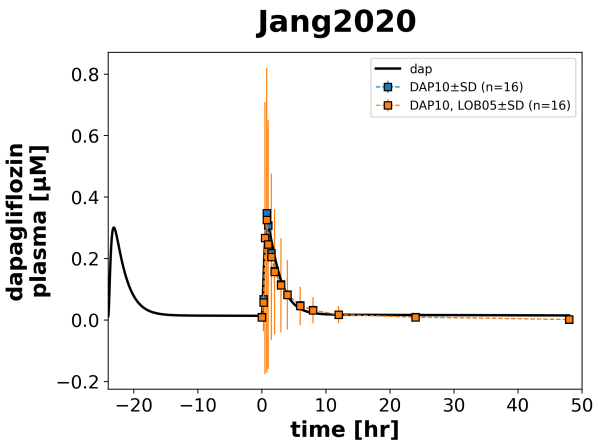

Figure 43: **Simulation of Jang et al. [25].**

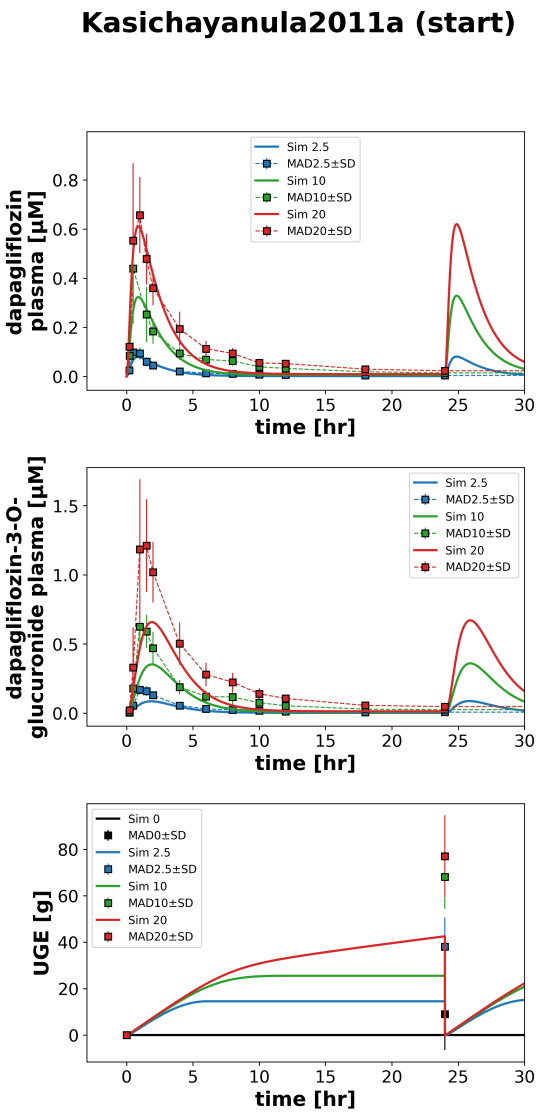

Figure 44: **Simulation of Kasichayanula et al. [28].**

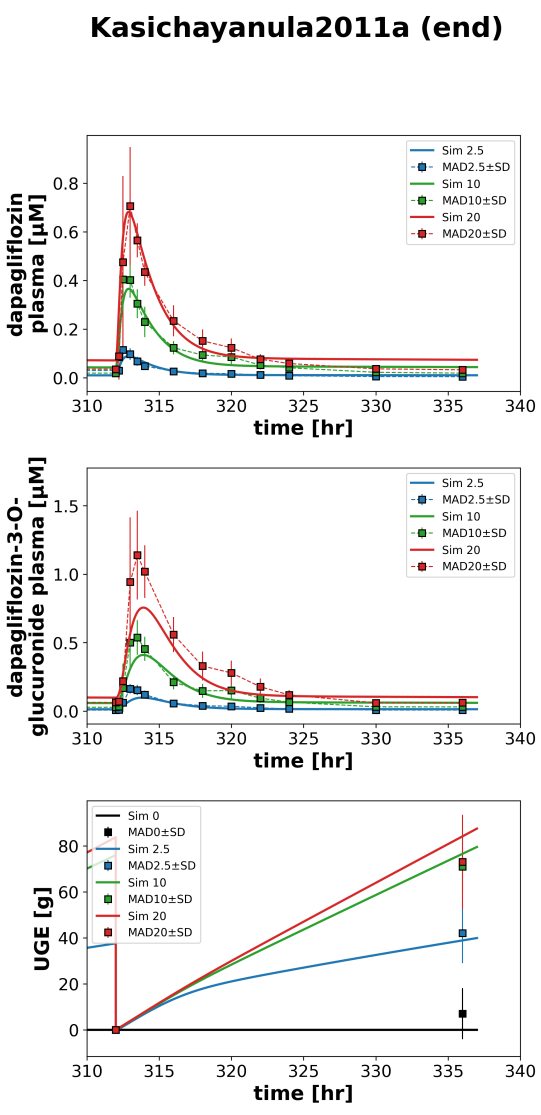

Figure 45: **Simulation of Kasichayanula et al. [28].**

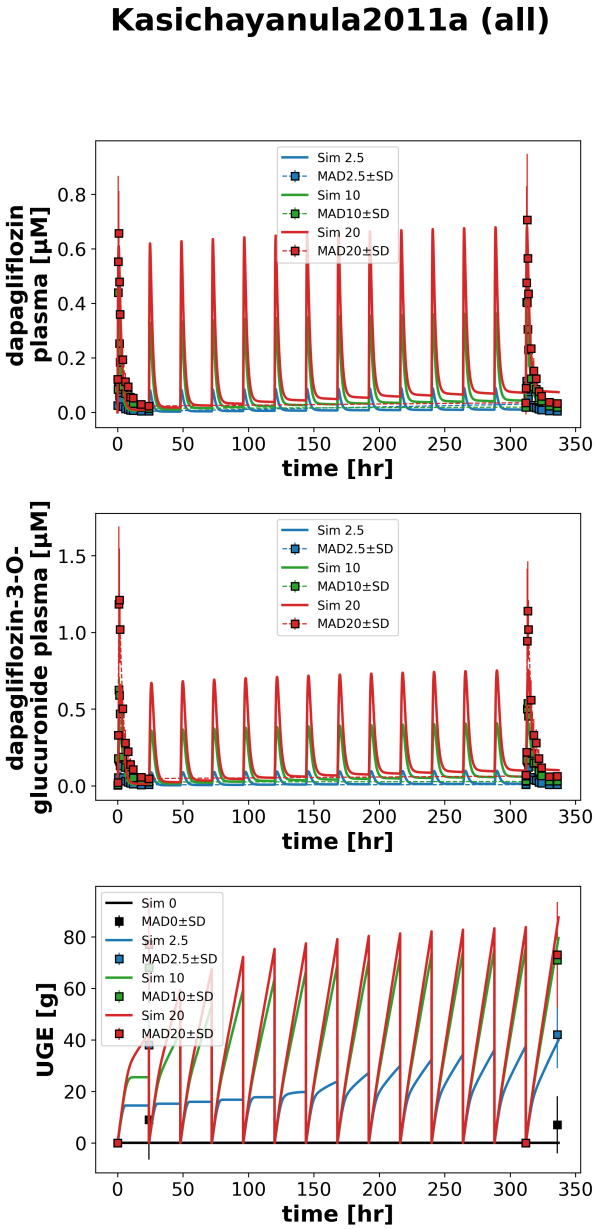

Figure 46: **Simulation of Kasichayanula et al. [28].**

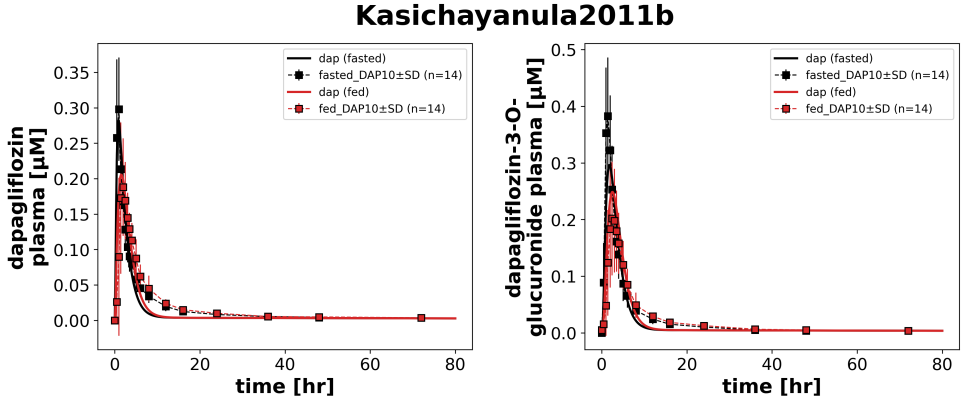

Figure 47: **Simulation of Kasichayanula et al. [31].**

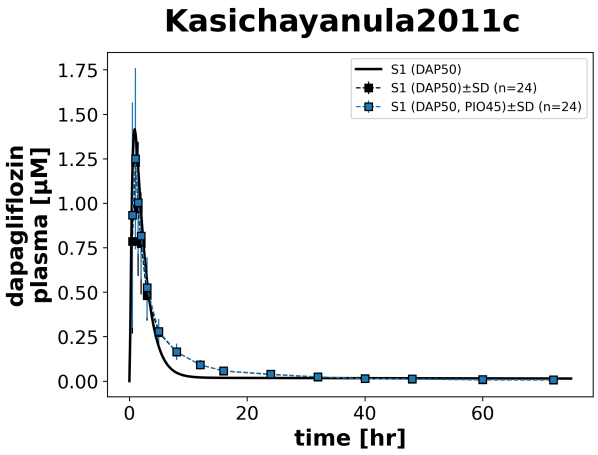

Figure 48: **Simulation of Kasichayanula et al. [30].**

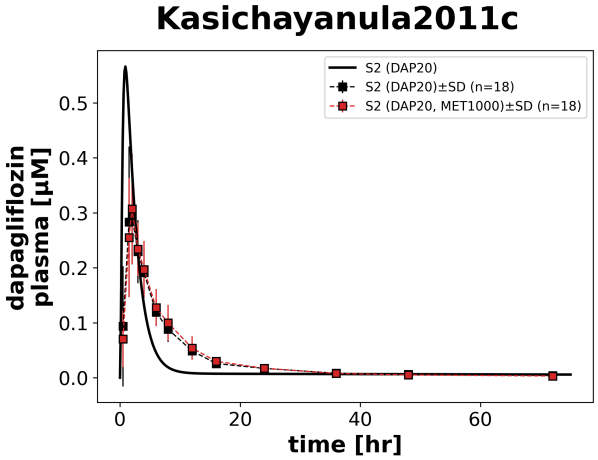

Figure 49: **Simulation of Kasichayanula et al. [30].**

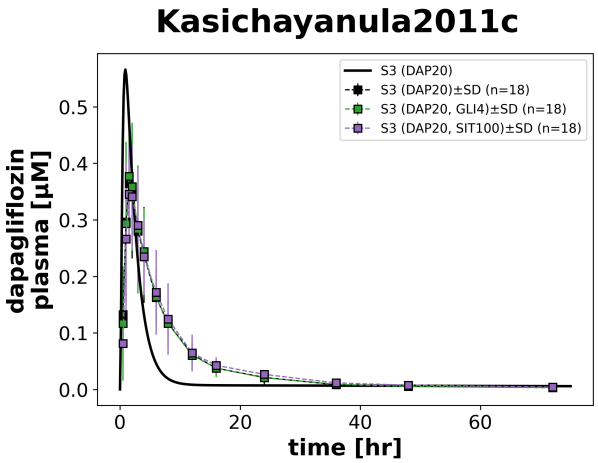

Figure 50: **Simulation of Kasichayanula et al. [30].**

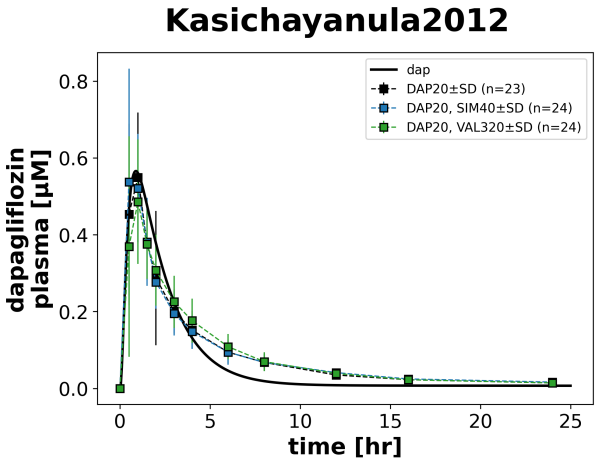

Figure 51: **Simulation of Kasichayanula et al. [32].**

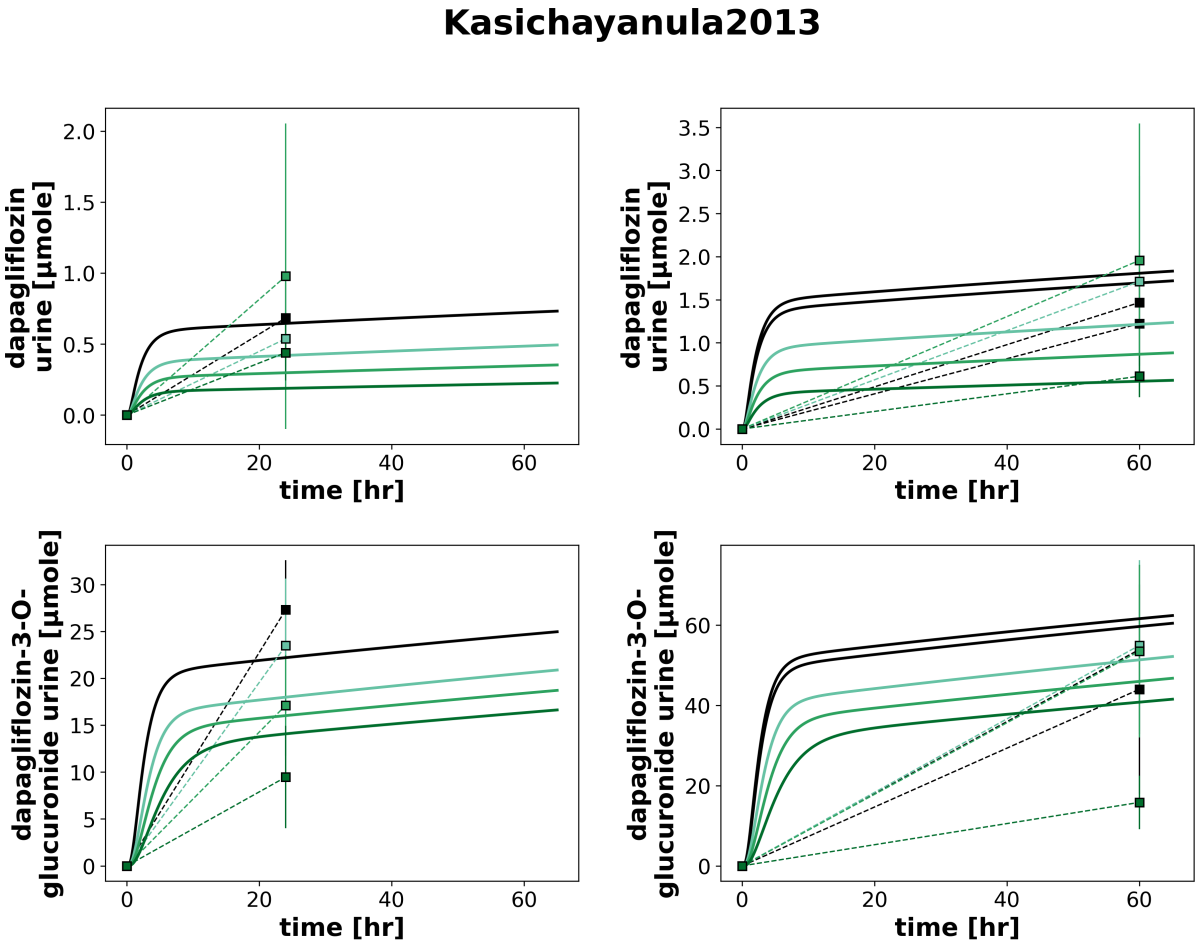

Figure 52: **Simulation of Kasichayanula et al. [33].**

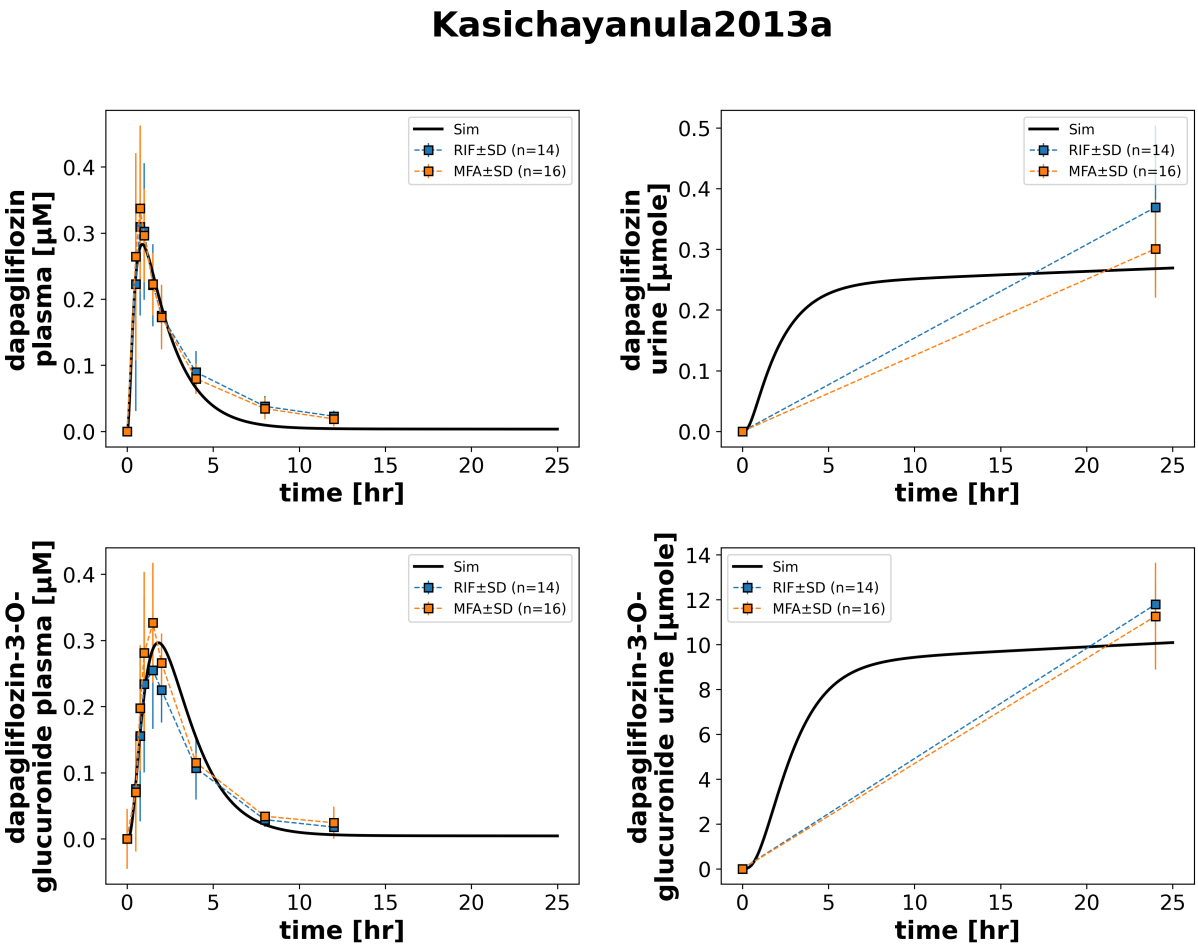

Figure 53: **Simulation of Kasichayanula et al. [29].**

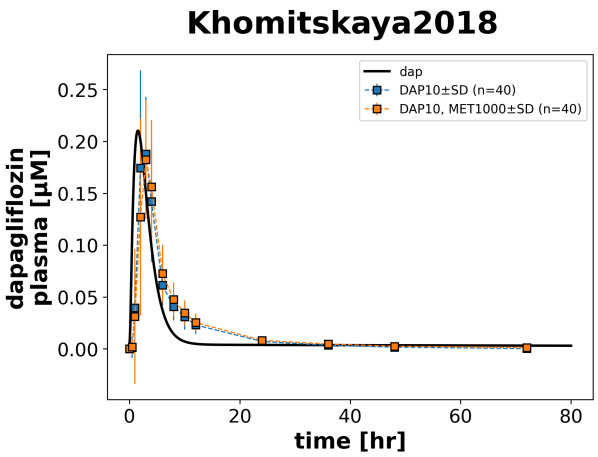

Figure 54: **Simulation of Khomitskaya et al. [36].**

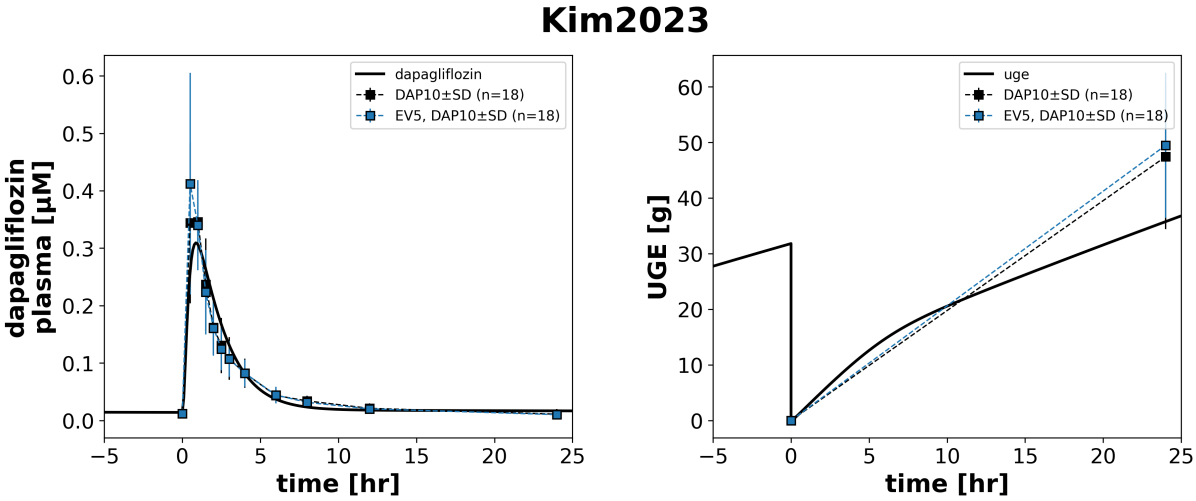

Figure 55: **Simulation of Kim et al. [37].**

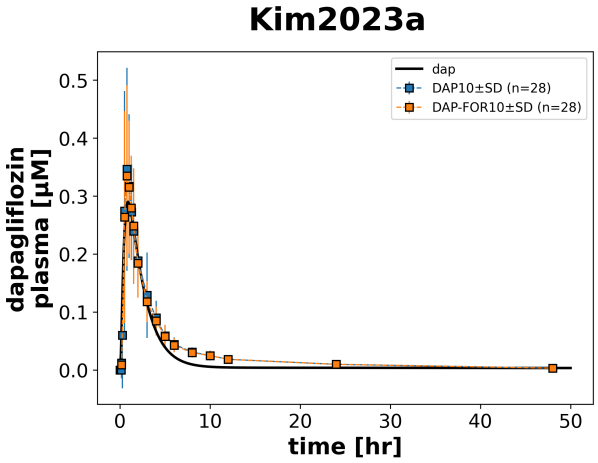

Figure 56: **Simulation of Kim et al. [38].**

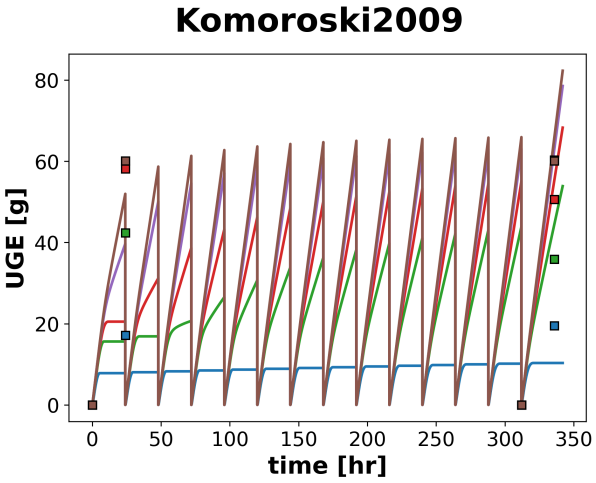

Figure 57: **Simulation of Komoroski et al. [41].**

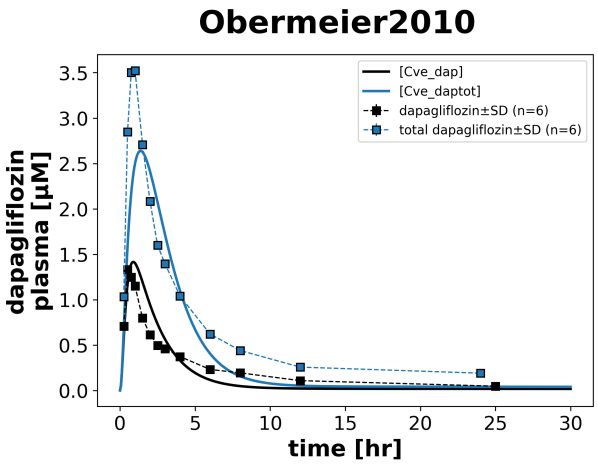

Figure 58: **Simulation of Obermeier et al. [56].**

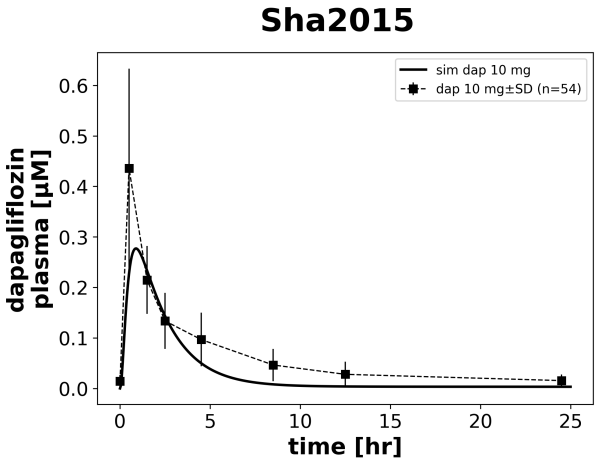

Figure 59: **Simulation of Sha et al. [61].**

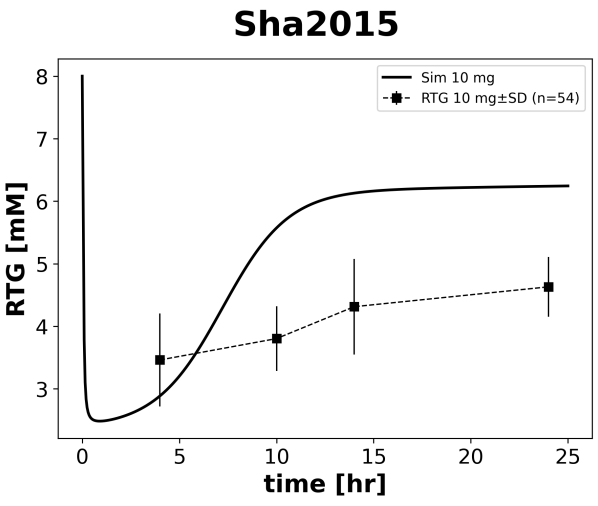

Figure 60: **Simulation of Sha et al. [61].**

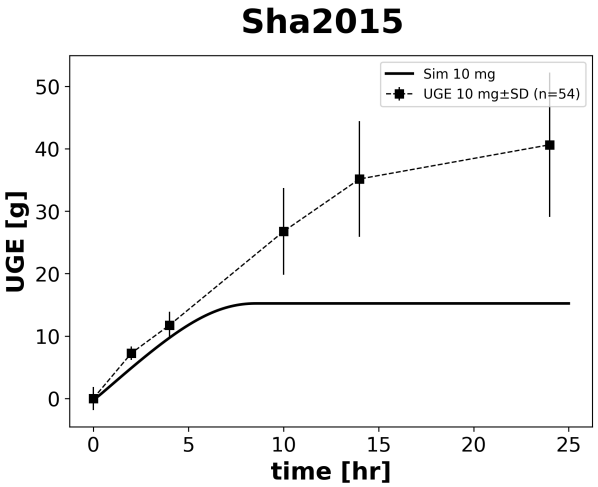

Figure 61: **Simulation of Sha et al. [61].**

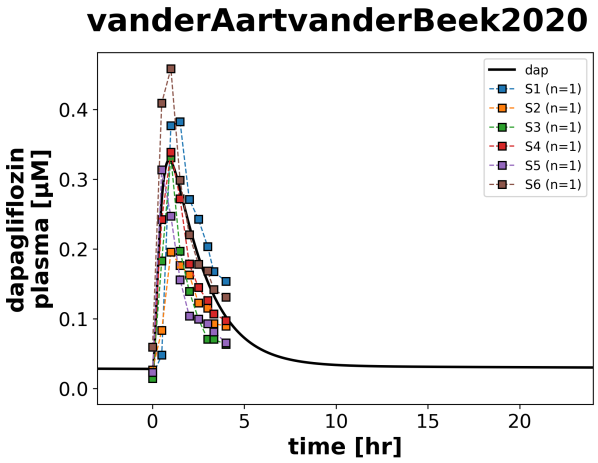

Figure 62: **Simulation of van der Aart-van der Beek et al. [68].**

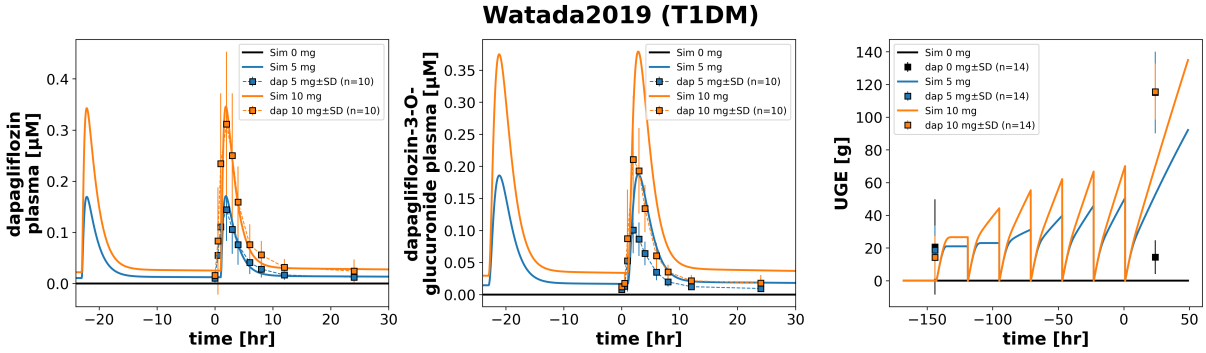

Figure 63: **Simulation of Watada et al. [69].**

Simulations

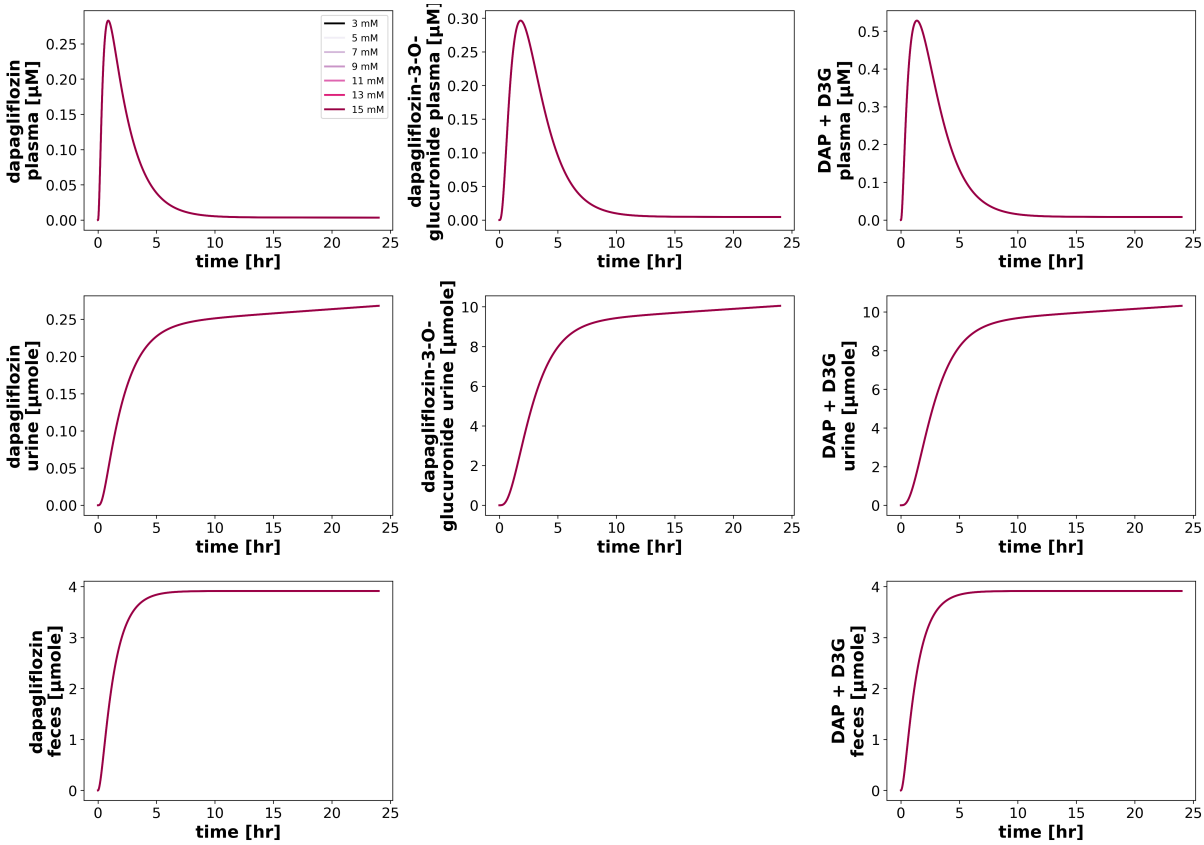

Figure 64: **Pharmacokinetic simulations of dapagliflozin under varying glucose concentrations.** Concentrations of dapagliflozin (DAP), dapagliflozin-3-O-glucuronide (D3G) and dapagliflozin total (DAP+D3G) in plasma, urine and feces were simulated under varying glucose doses ranging from 3 to 15 mM.

References

[1] Muhammad A. Abdul-Ghani, Luke Norton, and Ralph A. Defronzo. "Role of Sodium-Glucose Cotransporter 2 (SGLT 2) Inhibitors in the Treatment of Type 2 Diabetes". In: *Endocrine Reviews* 32.4 (Aug. 2011), pp. 515–531. DOI: 10.1210/er.2010-0029.

[2] American Diabetes Association Professional Practice Committee. "2. Diagnosis and Classification of Diabetes: Standards of Care in Diabetes-2024". In: *Diabetes Care* 47.Suppl 1 (Jan. 2024), S20–S42. DOI: 10.2337/dc24-S002.

[3] Pavel Balazki, Stephan Schaller, Thomas Eissing, and Thorsten Lehr. "A Quantitative Systems Pharmacology Kidney Model of Diabetes Associated Renal Hyperfiltration and the Effects of SGLT Inhibitors." In: *CPT: pharmacometrics & systems pharmacology* 7.12 (Dec. 2018), pp. 788–797. DOI: 10.1002/psp4.12359.

[4] David W. Boulton, Sreeneeranj Kasichayanula, Chi Fung Anther Keung, Mark E. Arnold, Lisa J. Christopher, Xiaohui Sophia Xu, and Frank Lacreta. "Simultaneous Oral Therapeutic and Intravenous ^{14}C-microdoses to Determine the Absolute Oral Bioavailability of Saxagliptin and Dapagliflozin." In: *British journal of clinical pharmacology* 75.3 (Mar. 2013), pp. 763–768. DOI: 10.1111/j.1365-2125.2012.04391.x.

[5] David Busse, Weifeng Tang, Markus Scheerer, Thomas Danne, Torben Biester, Viktor Sokolov, David Boulton, and Joanna Parkinson. "Comparison of Pharmacokinetics and the Exposure-Response Relationship of Dapagliflozin between Adolescent/Young Adult and Adult Patients with Type 1 Diabetes Mellitus." In: *British journal of clinical pharmacology* 85.8 (Aug. 2019), pp. 1820–1828. DOI: 10.1111/bcp.13981.

[6] Ming Chang, Xiaoni Liu, Dapeng Cui, Dan Liang, Frank LaCreta, Steven C. Griffen, Susan Lubin, Donette Quamina-Edghill, and David W. Boulton. "Bioequivalence, Food Effect, and Steady-State Assessment of Dapagliflozin/Metformin Extended-release Fixed-dose Combination Tablets Relative to Single-component Dapagliflozin and Metformin Extended-release Tablets in Healthy Subjects." In: *Clinical therapeutics* 37.7 (July 2015), pp. 1517–1528. DOI: 10.1016/j.clinthera.2015.05.004.

[7] C. G. Child and J. G. Turcotte. "Surgery and Portal Hypertension". In: *Major Problems in Clinical Surgery* 1 (1964), pp. 1–85.

[8] Sangho Cho, Jeongwook Lee, Yongwon Yoo, Minyong Cho, Seil Sohn, and Beom-Jin Lee. "Improved Manufacturability and In Vivo Comparative Pharmacokinetics of Dapagliflozin Cocrystals in Beagle Dogs and Human Volunteers." In: *Pharmaceutics* 13.1 (Jan. 2021). DOI: 10.3390/pharmaceutics13010070.

[9] Committee for Human Medicinal Products (CHMP). "Guideline on the Investigation of Drug Interactions". In: (2012).

[10] Committee for Medicinal Products for Human Use (CHMP). *Assessment Report-Forxiga*. Sept. 2012.

[11] Ralph A. DeFronzo, Marcus Hompesch, Sreeneeranj Kasichayanula, Xiaoni Liu, Ying Hong, Marc Pfister, Linda A. Morrow, Bruce R. Leslie, David W. Boulton, Agatha Ching, Frank P. LaCreta, and Steven C. Griffen. "Characterization of Renal Glucose Reabsorption in Response to Dapagliflozin in Healthy Subjects and Subjects with Type 2 Diabetes". In: *Diabetes Care* 36.10 (Oct. 2013), pp. 3169–3176. DOI: 10.2337/dc13-0387.

[12] D. Devineni, L. Morrow, M. Hompesch, D. Skee, A. Vandebosch, J. Murphy, K. Ways, and S. Schwartz. "Canagliflozin Improves Glycaemic Control over 28 Days in Subjects with Type 2 Diabetes Not Optimally Controlled on Insulin." In: *Diabetes, obesity & metabolism* 14.6 (June 2012), pp. 539–545. DOI: 10.1111/j.1463-1326.2012.01558.x.

[13] FDA. *FDA 202293Orig1s000 Review (FDAMB102002). Pharmacokinetics for Multiple-Dose Administration of Dapagliflozin in Healthy Subjects.* July 2013.

[14] FDA. *FDA 202293Orig1s000 Review (FDAMB102003). Bioequivalence Assessment during Multiple-Dose Administration of Dapagliflozin in Subjects with T2DM.* July 2013.

[15] FDA. *FDA 202293Orig1s000 Review (FDAMB102006). Urinary and Fecal Excretion Data Following a 50 mg Dose of Dapagliflozin.* July 2013.

[16] FDA. *FDA 202293Orig1s000 Review (FDAMB102007). Impact of Renal Impairment on the Pharmacokinetics and Pharmacodynamics of Dapagliflozin Was Studied in a Single (50 Mg) and Multiple Dose (20 Mg).* July 2013.

[17] FDA. *FDA 202293Orig1s000 Review. Pharmacokinetic and Pharmacodynamic Study Collection for Dapagliflozin.* July 2013.

[18] Ele Ferrannini, Silvia Jimenez Ramos, Afshin Salsali, Weihua Tang, and James F. List. "Dapagliflozin Monotherapy in Type 2 Diabetic Patients with Inadequate Glycemic Control by Diet and Exercise: A Randomized, Double-Blind, Placebo-Controlled, Phase 3 Trial". In: *Diabetes Care* 33.10 (Oct. 2010), pp. 2217–2224. DOI: 10.2337/dc10-0612.

[19] Ferran Gonzalez Hernandez, Simon J Carter, Juha Iso-Sipilä, Paul Goldsmith, Ahmed A. Almousa, Silke Gastine, Watjana Lilaonitkul, Frank Kloprogge, and Joseph F Standing. "An Automated Approach to Identify Scientific Publications Reporting Pharmacokinetic Parameters". In: *Wellcome Open Research* 6 (Apr. 2021), p. 88. DOI: 10.12688/wellcomeopenres.16718.1. (Visited on 04/24/2024).

[20] Jan Grzegorzewski, Janosch Brandhorst, Kathleen Green, Dimitra Eleftheriadou, Yannick Duport, Florian Barthorscht, Adrian Köller, Danny Yu Jia Ke, Sara De Angelis, and Matthias König. "PK-DB: Pharmacokinetics Database for Individualized and Stratified Computational Modeling". In: *Nucleic Acids Research* 49.D1 (Jan. 2021), pp. D1358–D1364. DOI: 10.1093/nar/gkaa990.

[21] Jürgen Harreiter and Michael Roden. "[Diabetes mellitus: definition, classification, diagnosis, screening and prevention (Update 2023)]". In: *Wiener Klinische Wochenschrift* 135.Suppl 1 (Jan. 2023), pp. 7–17. DOI: 10.1007/s00508-022-02122-y.

[22] Michael Hucka, Frank T. Bergmann, Claudine Chaouiya, Andreas Dräger, Stefan Hoops, Sarah M. Keating, Matthias König, Nicolas Le Novère, Chris J. Myers, Brett G. Olivier, Sven Sahle, James C. Schaff, Rahuman Sheriff, Lucian P. Smith, Dagmar Waltemath, Darren J. Wilkinson, and Fengkai Zhang. "The Systems Biology Markup Language (SBML): Language Specification for Level 3 Version 2 Core Release 2". In: *Journal of Integrative Bioinformatics* 16.2 (June 2019). DOI: 10.1515/jib-2019-0021. (Visited on 04/19/2024).

[23] Jun Gi Hwang, Sae Im Jeong, Yu Kyong Kim, Yujin Lee, Sang Chun Ji, SeungHwan Lee, and Min Kyu Park. "Common ABCB1 SNP, C3435T Could Affect Systemic Exposure of Dapagliflozin in Healthy Subject." In: *Translational and clinical pharmacology* 30.4 (Dec. 2022), pp. 212–225. DOI: 10.12793/tcp.2022.30.e23.

[24] Akira Imamura, Masahito Kusunoki, Shinya Ueda, Nobuya Hayashi, and Yasuhiko Imai. "Impact of Voglibose on the Pharmacokinetics of Dapagliflozin in Japanese Patients with Type 2 Diabetes." In: *Diabetes therapy : research, treatment and education of diabetes and related disorders* 4.1 (June 2013), pp. 41–49. DOI: 10.1007/s13300-012-0016-5.

[25] Kyungho Jang, Ji-Young Jeon, Seol Ju Moon, and Min-Gul Kim. "Evaluation of the Pharmacokinetic Interaction Between Lobeglitazone and Dapagliflozin at Steady State." In: *Clinical therapeutics* 42.2 (Feb. 2020), pp. 295–304. DOI: 10.1016/j.clinthera.2020.01.003.

[26] Hm Jones and K Rowland-Yeo. "Basic Concepts in Physiologically Based Pharmacokinetic Modeling in Drug Discovery and Development". In: *CPT: Pharmacometrics & Systems Pharmacology* 2.8 (Aug. 2013), pp. 1–12. DOI: 10.1038/psp.2013.41. (Visited on 05/25/2025).

[27] K. Kaku, S. Inoue, O. Matsuoka, A. Kiyosue, H. Azuma, N. Hayashi, T. Tokudome, A. M. Langkilde, and S. Parikh. "Efficacy and Safety of Dapagliflozin as a Monotherapy for Type 2 Diabetes Mellitus in Japanese Patients with Inadequate Glycaemic Control: A Phase II Multicentre, Randomized, Double-Blind, Placebo-Controlled Trial". In: *Diabetes, Obesity & Metabolism* 15.5 (May 2013), pp. 432–440. DOI: 10.1111/dom.12047.

[28] S. Kasichayanula, M. Chang, M. Hasegawa, X. Liu, N. Yamahira, F. P. LaCreta, Y. Imai, and D. W. Boulton. "Pharmacokinetics and Pharmacodynamics of Dapagliflozin, a Novel Selective Inhibitor of Sodium-Glucose Co-Transporter Type 2, in Japanese Subjects without and with Type 2 Diabetes Mellitus." In: *Diabetes, obesity & metabolism* 13.4 (Apr. 2011), pp. 357–365. DOI: 10.1111/j.1463-1326.2011.01359.x.

[29] S. Kasichayanula, X. Liu, S. C. Griffen, F. P. Lacreta, and D. W. Boulton. "Effects of Rifampin and Mefenamic Acid on the Pharmacokinetics and Pharmacodynamics of Dapagliflozin." In: *Diabetes, obesity & metabolism* 15.3 (Mar. 2013), pp. 280–283. DOI: 10.1111/dom.12024.

[30] S. Kasichayanula, X. Liu, W. C. Shyu, W. Zhang, M. Pfister, S. C. Griffen, T. Li, F. P. LaCreta, and D. W. Boulton. "Lack of Pharmacokinetic Interaction between Dapagliflozin, a Novel Sodium-Glucose Transporter 2 Inhibitor, and Metformin, Pioglitazone, Glimepiride or Sitagliptin in Healthy Subjects." In: *Diabetes, obesity & metabolism* 13.1 (Jan. 2011), pp. 47–54. DOI: 10.1111/j.1463-1326.2010.01314.x.

[31] S. Kasichayanula, X. Liu, W. Zhang, M. Pfister, S. B. Reele, A.-F. Aubry, F. P. LaCreta, and D. W. Boulton. "Effect of a High-Fat Meal on the Pharmacokinetics of Dapagliflozin, a Selective SGLT2 Inhibitor, in Healthy Subjects." In: *Diabetes, obesity & metabolism* 13.8 (Aug. 2011), pp. 770–773. DOI: 10.1111/j.1463-1326.2011.01397.x.

[32] Sreeneeranj Kasichayanula, Ming Chang, Xiaoni Liu, Wen-Chyi Shyu, Steven C. Griffen, Frank P. LaCreta, and David W. Boulton. "Lack of Pharmacokinetic Interactions between Dapagliflozin and Simvastatin, Valsartan, Warfarin, or Digoxin." In: *Advances in therapy* 29.2 (Feb. 2012), pp. 163–177. DOI: 10.1007/s12325-011-0098-x.

[33] Sreeneeranj Kasichayanula, Xiaoni Liu, Melanie Pe Benito, Ming Yao, Marc Pfister, Frank P. LaCreta, William Griffith Humphreys, and David W. Boulton. "The Influence of Kidney Function on Dapagliflozin Exposure, Metabolism and Pharmacodynamics in Healthy Subjects and in Patients with Type 2 Diabetes Mellitus." In: *British journal of clinical pharmacology* 76.3 (Sept. 2013), pp. 432–444. DOI: 10.1111/bcp.12056.

[34] Sreeneeranj Kasichayanula, Xiaoni Liu, Weijiang Zhang, Marc Pfister, Frank P. LaCreta, and David W. Boulton. "Influence of Hepatic Impairment on the Pharmacokinetics and Safety Profile of Dapagliflozin: An Open-Label, Parallel-Group, Single-Dose Study." In: *Clinical therapeutics* 33.11 (Nov. 2011), pp. 1798–1808. DOI: 10.1016/j.clinthera.2011.09.011.

[35] Sarah M. Keating, Dagmar Waltemath, Matthias König, Fengkai Zhang, Andreas Dräger, Claudine Chaouiya, Frank T. Bergmann, Andrew Finney, Colin S. Gillespie, Tomáš Helikar, Stefan Hoops, Rahuman S. Malik-Sheriff, Stuart L. Moodie, Ion I. Moraru, Chris J. Myers, Aurélien Naldi, Brett G. Olivier, Sven Sahle, James C. Schaff, Lucian P. Smith, Maciej J. Swat, Denis Thieffry, Leandro Watanabe, Darren J. Wilkinson, Michael L. Blinov, Kimberly Begley, James R. Faeder, Harold F. Gómez, Thomas M. Hamm, Yuichiro Inagaki, Wolfram Liebermeister, Allyson L. Lister, Daniel Lucio, Eric Mjolsness, Carole J. Proctor, Karthik Raman, Nicolas Rodriguez, Clifford A. Shaffer, Bruce E. Shapiro, Joerg Stelling,

Neil Swainston, Naoki Tanimura, John Wagner, Martin Meier-Schellersheim, Herbert M. Sauro, Bernhard Palsson, Hamid Bolouri, Hiroaki Kitano, Akira Funahashi, Henning Hermjakob, John C. Doyle, Michael Hucka, and SBML Level 3 Community members. "SBML Level 3: An Extensible Format for the Exchange and Reuse of Biological Models". In: *Molecular Systems Biology* 16.8 (Aug. 2020), e9110. DOI: 10.15252/msb.20199110.

[36] Yunona Khomitskaya, Nadezhda Tikhonova, Konstantin Gudkov, Svetlana Erofeeva, Victoria Holmes, Brian Dayton, Nigel Davies, David W. Boulton, and Weifeng Tang. "Bioequivalence of Dapagliflozin/Metformin Extended-release Fixed-combination Drug Product and Single-component Dapagliflozin and Metformin Extended-release Tablets in Healthy Russian Subjects." In: *Clinical therapeutics* 40.4 (Apr. 2018), 550–561.e3. DOI: 10.1016/j.clinthera.2018.02.006.

[37] Dasohm Kim, Minkyu Choi, Byung Hak Jin, Taegon Hong, Choon Ok Kim, Byung Won Yoo, and Min Soo Park. "Pharmacokinetic and Pharmacodynamic Drug-Drug Interactions between Evogliptin and Empagliflozin or Dapagliflozin in Healthy Male Volunteers." In: *Clinical and translational science* 16.8 (Aug. 2023), pp. 1469–1478. DOI: 10.1111/cts.13566.

[38] Hyun Chul Kim, Sangmi Lee, Siyoung Sung, Eunjin Kim, In-Jin Jang, and Jae-Yong Chung. "A Comparison of the Pharmacokinetics and Safety of Dapagliflozin Formate, an Ester Prodrug of Dapagliflozin, to Dapagliflozin Propanediol Monohydrate in Healthy Subjects." In: *Drug design, development and therapy* 17 (2023), pp. 1203–1210. DOI: 10.2147/DDDT.S404182.

[39] Adrian Köller, Jan Grzegorzewski, and Matthias König. "Physiologically Based Modeling of the Effect of Physiological and Anthropometric Variability on Indocyanine Green Based Liver Function Tests". In: *Frontiers in Physiology* 12 (Nov. 2021), p. 757293. DOI: 10.3389/fphys.2021.757293. (Visited on 04/22/2024).

[40] Adrian Köller, Jan Grzegorzewski, Hans-Michael Tautenhahn, and Matthias König. "Prediction of Survival After Partial Hepatectomy Using a Physiologically Based Pharmacokinetic Model of Indocyanine Green Liver Function Tests". In: *Frontiers in Physiology* 12 (Nov. 2021), p. 730418. DOI: 10.3389/fphys.2021.730418. (Visited on 04/22/2024).

[41] B. Komoroski, N. Vachharajani, D. Boulton, D. Kornhauser, M. Geraldes, L. Li, and M. Pfister. "Dapagliflozin, a Novel SGLT2 Inhibitor, Induces Dose-Dependent Glucosuria in Healthy Subjects." In: *Clinical pharmacology and therapeutics* 85.5 (May 2009), pp. 520–526. DOI: 10.1038/clpt.2008.251.

[42] Matthias König. *Cy3sbml - SBML for Cytoscape*. Zenodo. Mar. 2025. DOI: 10.5281/zenodo.15009089.

[43] Matthias König. *Sbmlsim: SBML Simulation Made Easy*. [object Object]. Sept. 2021. DOI: 10.5281/ZENODO.5531088. (Visited on 04/19/2024).

[44] Matthias König. *Sbmlutils: Python Utilities for SBML*. Zenodo. Aug. 2024. DOI: 10.5281/ZENODO.13325770. (Visited on 09/13/2024).

[45] Matthias König, Sascha Bulik, and Hermann-Georg Holzhütter. "Quantifying the Contribution of the Liver to Glucose Homeostasis: A Detailed Kinetic Model of Human Hepatic Glucose Metabolism". In: *PLoS computational biology* 8.6 (2012), e1002577. DOI: 10.1371/journal.pcbi.1002577.

[46] Matthias König, Andreas Dräger, and Hermann-Georg Holzhütter. "CySBML: A Cytoscape Plugin for SBML". In: *Bioinformatics* 28.18 (Sept. 2012), pp. 2402–2403. DOI: 10.1093/bioinformatics/bts432. (Visited on 04/19/2024).

[47] Mirko Koziolek, Stefano Alcaro, Patrick Augustijns, Abdul W. Basit, Michael Grimm, Bart Hens, Caroline L. Hoad, Philipp Jedamzik, Christine M. Madla, Marc Maliepaard, Luca Marciani, Annalisa Maruca, Neil Parrott, Petr Pávek, Christopher J. H. Porter, Christos Reppas, Diana van Riet-Nales, Jari Rubbens, Marina Statelova, Natalie L. Trevaskis, Kateřina Valentová, Maria Vertzoni, Dubravka Vitali Čepo, and Maura Corsetti. "The Mechanisms of Pharmacokinetic Food-Drug Interactions - A Perspective from the UNGAP Group". In: *European Journal of Pharmaceutical Sciences: Official Journal of the European Federation for Pharmaceutical Sciences* 134 (June 2019), pp. 31–59. DOI: 10.1016/j.ejps.2019.04.003.

[48] Frank LaCreta, Steven C. Griffen, Xiaoni Liu, Charles Smith, Carey Hines, Kevin Volk, Ravindra Tejwani, and David W. Boulton. "Bioequivalence and Food Effect of Heat-Stressed and Non-Heat-Stressed Dapagliflozin 2.5- and 10-Mg Tablets." In: *International journal of pharmaceutics* 511.1 (Sept. 2016), pp. 288–295. DOI: 10.1016/j.ijpharm.2016.07.017.

[49] H. Lennernäs and G. Fager. "Pharmacodynamics and Pharmacokinetics of the HMG-CoA Reductase Inhibitors. Similarities and Differences". In: *Clinical Pharmacokinetics* 32.5 (May 1997), pp. 403–425. DOI: 10.2165/00003088-199732050-00005.

[50] Andrew S. Levey, Silvia M. Titan, Neil R. Powe, Josef Coresh, and Lesley A. Inker. "Kidney Disease, Race, and GFR Estimation". In: *Clinical journal of the American Society of Nephrology: CJASN* 15.8 (Aug. 2020), pp. 1203–1212. DOI: 10.2215/CJN.12791019.

[51] James F. List, Vincent Woo, Enrique Morales, Weihua Tang, and Fred T. Fiedorek. "Sodium-Glucose Cotransport Inhibition with Dapagliflozin in Type 2 Diabetes". In: *Diabetes Care* 32.4 (Apr. 2009), pp. 650–657. DOI: 10.2337/dc08-1863.

[52] Dianna J. Magliano, Edward J. Boyko, and IDF Diabetes Atlas 10th edition scientific committee. *IDF DIABETES ATLAS*. 10th. IDF Diabetes Atlas. Brussels: International Diabetes Federation, 2021. (Visited on 01/02/2025).

[53] Beatrice Stemmer Mallol, Jan Grzegorzewski, Hans-Michael Tautenhahn, and Matthias König. *Insights into Intestinal P-glycoprotein Function Using Talinolol: A PBPK Modeling Approach*. Nov. 2023. DOI: 10.1101/2023.11.21.568168. (Visited on 05/05/2024).

[54] M. Daniel Naagaard, Roy Chang, Mats Någård, Weifeng Tang, and David W. Boulton. "Common UGT1A9 Polymorphisms Do Not Have a Clinically Meaningful Impact on the Apparent Oral Clearance of Dapagliflozin in Type 2 Diabetes Mellitus." In: *British journal of clinical pharmacology* 88.4 (Feb. 2022), pp. 1942–1946. DOI: 10.1111/bcp.15117.

[55] Nike Nemitz and Matthias König. *Physiologically Based Pharmacokinetic (PBPK) Model of Dapagliflozin*. Zenodo. June 2025. DOI: 10.5281/zenodo.15634068.

[56] M. Obermeier, M. Yao, A. Khanna, B. Koplowitz, M. Zhu, W. Li, B. Komoroski, S. Kasichayanula, L. Discenza, W. Washburn, W. Meng, B. A. Ellsworth, J. M. Whaley, and W. G. Humphreys. "In Vitro Characterization and Pharmacokinetics of Dapagliflozin (BMS-512148), a Potent Sodium-Glucose Cotransporter Type II Inhibitor, in Animals and Humans." In: *Drug metabolism and disposition: the biological fate of chemicals* 38.3 (Mar. 2010), pp. 405–414. DOI: 10.1124/dmd.109.029165.

[57] R. N. Pugh, I. M. Murray-Lyon, J. L. Dawson, M. C. Pietroni, and R. Williams. "Transection of the Oesophagus for Bleeding Oesophageal Varices". In: *The British Journal of Surgery* 60.8 (Aug. 1973), pp. 646–649. DOI: 10.1002/bjs.1800600817.

[58] Ankit Rohatgi. *WebPlotDigitizer*. 2024.

[59] W. M. Said Ahmed, A. Soliman, A. E. Ahmed Amer, R. M. El Shahat, M. M. Amin, R. S. Taha, M. M. Y. Awad, A. M. Abdel Hamid, M. S. El-Sayed, E. A. Eid, M. Dmerdash, H. E. Ali, E. M. M. Fayed, S. a. M. Naeem, A. F. Elsharawy, O. M. a. M. Elzahaby, M. K. Ayoub, and D. A. Mohammed. "Effect of Dapagliflozin against NAFLD and Dyslipidemia in Type 2 Diabetic Albino Rats: Possible Underlying Mechanisms". In: *European Review for Medical and Pharmacological Sciences* 27.17 (Sept. 2023), pp. 8101–8109. DOI: 10.26355/eurrev_202309_33570.

[60] André J. Scheen. "Evaluating SGLT2 Inhibitors for Type 2 Diabetes: Pharmacokinetic and Toxicological Considerations." In: *Expert opinion on drug metabolism & toxicology* 10.5 (May 2014), pp. 647–663. DOI: 10.1517/17425255.2014.873788.

[61] S. Sha, D. Polidori, K. Farrell, A. Ghosh, J. Natarajan, N. Vaccaro, J. Pinheiro, P. Rothenberg, and L. Plum-Mörschel. "Pharmacodynamic Differences between Canagliflozin and Dapagliflozin: Results of a Randomized, Double-Blind, Crossover Study." In: *Diabetes, obesity & metabolism* 17.2 (Feb. 2015), pp. 188–197. DOI: 10.1111/dom.12418.

[62] Priyanka A. Shah, Pranav S. Shrivastav, Jaivik V. Shah, and Archana George. "Simultaneous Quantitation of Metformin and Dapagliflozin in Human Plasma by LC-MS/MS: Application to a Pharmacokinetic Study." In: *Biomedical chromatography : BMC* 33.4 (Apr. 2019), e4453. DOI: 10.1002/bmc.4453.

[63] Mengran Shi, Hao Zhang, Wei Wang, Xiao Zhang, Jiawei Liu, Qixian Wang, Yuan Wang, Chunlin Zhang, Xiaoqin Guo, Qiao Qiao, Chun Cui, Jing Xu, and Jian Wang. "Effect of Dapagliflozin on Liver and Pancreatic Fat in Patients with Type 2 Diabetes and Non-Alcoholic Fatty Liver Disease". In: *Journal of Diabetes and Its Complications* 37.10 (Oct. 2023), p. 108610. DOI: 10.1016/j.jdiacomp.2023.108610.

[64] B. N. Singh. "Effects of Food on Clinical Pharmacokinetics". In: *Clinical Pharmacokinetics* 37.3 (Sept. 1999), pp. 213–255. DOI: 10.2165/00003088-199937030-00003.

[65] Endre T. Somogyi, Jean-Marie Bouteiller, James A. Glazier, Matthias König, J. Kyle Medley, Maciej H. Swat, and Herbert M. Sauro. "libRoadRunner: A High Performance SBML Simulation and Analysis Library". In: *Bioinformatics* 31.20 (Oct. 2015), pp. 3315–3321. DOI: 10.1093/bioinformatics/btv363. (Visited on 04/19/2024).

[66] Paul E. Stevens, Sofia B. Ahmed, Juan Jesus Carrero, Bethany Foster, Anna Francis, Rasheeda K. Hall, Will G. Herrington, Guy Hill, Lesley A. Inker, Rümeyza Kazancıoğlu, Edmund Lamb, Peter Lin, Magdalena Madero, Natasha McIntyre, Kelly Morrow, Glenda Roberts, Dharshana Sabanayagam, Elke Schaeffner, Michael Shlipak, Rukshana Shroff, Navdeep Tangri, Teerawat Thanachayanont, Ifeoma Ulasi, Germaine Wong, Chih-Wei Yang, Luxia Zhang, and Adeera Levin. "KDIGO 2024 Clinical Practice Guideline for the Evaluation and Management of Chronic Kidney Disease". In: *Kidney International* 105.4 (Apr. 2024), S117–S314. DOI: 10.1016/j.kint.2023.10.018. (Visited on 04/22/2024).

[67] Andrea Tsoris and Clinton A. Marlar. "Use Of The Child Pugh Score In Liver Disease". In: *StatPearls*. Treasure Island (FL): StatPearls Publishing, 2024. (Visited on 11/11/2024).

[68] Annemarie B. van der Aart-van der Beek, A. Mireille A. Wessels, Hiddo J. L. Heerspink, and Daan J. Touw. "Simple, Fast and Robust LC-MS/MS Method for the Simultaneous Quantification of Canagliflozin, Dapagliflozin and Empagliflozin in Human Plasma and Urine." In: *Journal of chromatography. B, Analytical technologies in the biomedical and life sciences* 1152 (Sept. 2020), p. 122257. DOI: 10.1016/j.jchromb.2020.122257.

[69] Hirotaka Watada, Masanari Shiramoto, Shinya Ueda, Weifeng Tang, Michiko Asano, Fredrik Thorén, Hyosung Kim, Toshitaka Yajima, David W. Boulton, and Eiichi Araki. "Pharmacokinetics and Pharmacodynamics of Dapagliflozin in Combination with Insulin in Japanese Patients with Type 1 Diabetes." In: *Diabetes, obesity & metabolism* 21.4 (Apr. 2019), pp. 876–882. DOI: 10.1111/dom.13593.

[70] P. G. Welling. “Effects of Food on Drug Absorption”. In: *Pharmacology & Therapeutics* 43.3 (1989), pp. 425–441. DOI: 10.1016/0163-7258(89)90019-3.

[71] Ciaran Welsh, Jin Xu, Lucian Smith, Matthias König, Kiri Choi, and Herbert M Sauro. “libRoadRunner 2.0: A High Performance SBML Simulation and Analysis Library”. In: *Bioinformatics* 39.1 (Jan. 2023). Ed. by Pier Luigi Martelli, btac770. DOI: 10.1093/bioinformatics/btac770. (Visited on 04/19/2024).

[72] I. Stuart Wood and Paul Trayhurn. “Glucose Transporters (GLUT and SGLT): Expanded Families of Sugar Transport Proteins”. In: *The British Journal of Nutrition* 89.1 (Jan. 2003), pp. 3–9. DOI: 10.1079/BJN2002763.

[73] Li Yang, Haiyan Li, Hongmei Li, Anh Bui, Ming Chang, Xiaoni Liu, Sreeneeranj Kasichayanula, Steven C. Griffen, Frank P. Lacreta, and David W. Boulton. “Pharmacokinetic and Pharmacodynamic Properties of Single- and Multiple-Dose of Dapagliflozin, a Selective Inhibitor of SGLT2, in Healthy Chinese Subjects.” In: *Clinical therapeutics* 35.8 (Aug. 2013), 1211–1222.e2. DOI: 10.1016/j.clinthera.2013.06.017.

Acknowledgements

I would like to thank Matthias König, who supervised the project and served as a second data curator to ensure the coherence of the curated data and simulations.
I also acknowledge BioRENDER for making it possible to create my visuals.
This work was supervised by Matthias König (MK) https://livermetabolism.com. MK was supported by the BMBF within ATLAS by grant number 031L0304B and the German Research Foundation (DFG) within the Research Unit Program FOR 5151 QuaLiPerF by grant number 436883643 and by grant number 465194077 (Priority Programme SPP 2311, Subproject SimLivA). This work was supported by the BMBF-funded de.NBI Cloud within the German Network for Bioinformatics Infrastructure (de.NBI) (031A537B, 031A533A, 031A538A, 031A533B, 031A535A, 031A537C, 031A534A, 031A532B).
width=!,height=!,pages=-